Selective CO Adsorption Separation from CO_2 Via Cu-modified Adsorbents

Maria Abbassi

Thesis submitted to the University of Ottawa
in partial fulfillment of the requirements for the degree of
Master of Applied Science, Chemical Engineering

Department of Chemical and Biological Engineering
Faculty of Engineering
University of Ottawa

Abstract

CO_2 capture and conversion appears to be a prominent solution to mitigate greenhouse gas emissions (GHG) and global warming issue. Among different CO_2 conversion approaches, CO_2 hydrogenation via reverse water gas shift (RWGS) reaction is one of the most promising technology to convert CO_2 to CO. Subsequently, CO is transformed to value added chemicals or liquid fuels. To improve the overall CO_2 conversion for RWGS reaction, product separation and recycling is being proposed.

In this research, adsorption separation technology has been explored to selectively separate CO from CO_2 in RWGS using pressure swing adsorption (PSA) process. To investigate the adsorption capacity and selectivity of CO, different porous materials have been identified for CO separation. In this research, activated carbons, ordered mesoporous silica, and metal organic framework materials were studied. Equilibrium isotherms of CO and CO_2 were measured in a gravimetric system at a temperature of 25 $^{\circ}$C for pressures up to 20 bar. Preliminary adsorption isotherm results had shown an insufficient CO uptake and low selectivity level compared to CO_2, thus not justifying their application for CO separation. Herein, to improve the CO adsorption capacity and selectivity, Cu-based adsorbents were developed using copper (II) chloride ($CuCl_2$) as a precursor to synthesize six different adsorbents. The adsorbents were prepared using two different synthesis methods; the modified polyol method for reduction and nanoparticle deposition of Cu (I) ions, and thermal monolayer auto-dispersion method. Furthermore, different copper (II) loadings were investigated to determine the monolayer dispersion capacity of $CuCl_2$ on the support.

The modified adsorbents by copper salt exhibited significantly high CO uptake with large CO/CO_2 selectivity, reversing the results obtained before adsorbent modification. Thus, Cu-based adsorbents are promising materials for CO separation and recovery from a gaseous mixture containing CO_2.

Résumé

Le captage et la conversion de CO_2 semblent être une solution proéminente permettant d'atténuer les émissions des gaz à effet de serre (GES) et de lutter contre le réchauffement climatique. Parmi les processus de conversion de CO_2, l'hydrogénation de CO_2 par la réaction des gaz à l'eau inverse (RWGS) et l'une des technologies les plus prometteuses pour convertir le CO_2 en CO. Par la suite, le CO est transformé en produits chimiques à valeur ajouté ou bien en combustibles liquides. Afin d'améliorer la conversion globale de CO_2 pour la réaction (RWGS), la séparation et le recyclage des produits sont proposés

Dans cette étude, la technologie de séparation par adsorption a été exploité pour séparer sélectivement le CO du CO_2 dans la réaction RWGS en utilisant un processus d'adsorption modulée en pression (AMP). Afin d'étudier la sélectivité et la capacité d'adsorption du CO, différents matériaux poreux ont été identifiés pour la séparation du CO. Dans cette étude, les charbons actifs, la silice mésoporeuse ordonnée, et les charpentes métalliques-organiques (MOF) ont été étudiés. Les équilibres isothermes du CO et du CO_2 ont été mesurés dans un système gravimétrique à la température de 25 °C, et pour des pressions allant jusqu'à 20 bar. Les résultats préliminaires des isothermes d'adsorption avaient montré une absorption insuffisante de CO et un faible niveau de sélectivité par rapport au CO_2. Chose qui ne justifie pas leur application dans la séparation de CO. Par conséquence, afin d'améliorer la capacité d'adsorption et la sélectivité du CO, des adsorbants à base de Cu ont été développés en utilisant du chlorure de cuivre (II) ($CuCl_2$) comme précurseur pour synthétiser six adsorbants différents. Les adsorbants ont été préparés en utilisant deux méthodes de synthèse différentes; la méthode de polyol modifié pour la réduction et le dépôt de nanoparticules d'ions Cu (I), et la méthode d'auto-dispersion thermique monocouche. De plus, différentes chargement de cuivre (II) ont été étudiées pour déterminer la capacité de dispersion monocouche de $CuCl_2$ sur le support.

Les adsorbants modifiés par le sel de cuivre ont montré une absorption de CO significativement élevée avec une grande sélectivité CO / CO_2, inversant les résultats obtenus avant la modification de l'adsorbant. Ainsi, les adsorbants à base de Cu sont des matériaux prometteurs pour la séparation et la récupération du CO à partir d'un mélange gazeux contenant du CO_2.

Statement of Contributions of Collaborators

I hereby declare that I am Maria Abbassi the sole author of this thesis. I performed the experimental design, procedures, carried out experimental tests, and subsequent data analysis throughout the project. I have written all of the chapters contained in this thesis.

My supervisor, Dr. Handan Tezel provided continual support and guidance throughout this project. In addition, Dr. K. Zanganeh and some members of Oxy-combustion/G2 Group, CanmetENERGY- Ottawa provided guidance and helped with the experimental setup construction.

The synthesis of the adsorbents via modified Polyol process was assisted by Dr. H. Dole from CanmetENERGY.

X-ray photoelectron spectroscopy measurements were performed and analyzed by Characterization Laboratory at CanmetENERGY.

.

Acknowledgements

First and foremost, I would like to express my gratitude to my supervisor Dr. F. Handan Tezel, for her continuous support, guidance and recommendations. Dr. Tezel's support not only included the project part, she was a mentor who continuously listened and helped me and believed in my capabilities to accomplish this work.

I would also like to extend my huge thank to my colleagues at CanmetENERGY for their help and continuous support. Dr. K. Zanganeh for giving me a chance to pursue graduate studies and for his guidance throughout my research. Dr. A. Shafeen, Ashkan Beigzadeh, Carlos Salvador, Dr. H. Dole for their encouragement and help. Craig Vaillancourt, for his technical support. Thank you also go to Engineering Service Group, members of Characterization Laboratory, Ko Vivien, Yewen Tan, Guillaume Gagnon-Caya and all members of Oxy-combustion/G2 Group and many more at CanmetENERY Ottawa.

I am indebted to my parent and family, without their love and support, I would not have been able to complete this work. I cannot thank enough my parents who continue to support me in all my endeavors. A special acknowledgment goes to my beloved husband and my lovely kids.

Finally, I would like to thank CanmetENERGY Ottawa, Natural Resources Canada for the financial support and giving me the opportunity to pursue graduate studies.

Table of Contents

List of Figures

List of Tables

Chapter 1: **Introduction**

1.1 Introduction

Carbon dioxide (CO_2) is considered as one of the most significant anthropogenic greenhouse gases (GHGs). It represents about 65% of total global greenhouse gas emissions when compared with other greenhouse gases such as methane (CH_4), nitrous oxide (N_2O), and fluorinated gases [1]. Moreover, the CO_2 concentration in the atmosphere is continuously growing with an unprecedented rate according to the National Oceanic and Atmospheric Administration (NOAA). The average global CO_2 concentration in 2019 was 409.8 ppm [2], with annual average increase rate of 2 ppm/year in the last decade (IEA, 2017). Currently, amongst the main potential sources of global CO_2 emissions is energy sector, including the heat generation and electricity production produced from coal combustion which is accounted for 45% of global CO_2 emissions compared to gas (20%) and oil (34%) (IEA report 2017). This increase in CO_2 from energy sector will continue to rise due to world economic growth and development.

The total primary energy supply (TPES) increased by almost 150% between 1971 and 2015 (IEA report 2017), It is expected that the energy consumption will increase by 57 % by 2030 according to the Energy Information Administration (EIA).

To mitigate GHG emissions and climate change, Paris Agreement was signed in 2015 to substantially reduce the GHG emissions and limit the global temperature rise well below 2 degree Celsius in comparison to the pre-industrial levels (UNFCCC, 2015). To achieve these goals, several approaches have been considered and adopted. Among them is to find alternative sources of energy e.g. renewable energy to replace the existing coal and natural gas combustion for energy production, efficient use of energy to reduce energy intensity and the third option is the development of carbon capture and storage (CCS) technologies. However, among these options, CCS is considered as a short-term transitional technology solution for GHG mitigation until the technologies get matured and become economically feasible. With respect to the CCS, carbon capture from large point source emissions is the most promising and economically viable technology option. In this approach, CO_2 is captured from the main emitters such as fossil fuel combustion systems and industrial processes using one of the three options: pre-combustion, post-

combustion or oxy-fuel combustion. The CO_2 captured is then transported through pipelines and subsequently stored in underground saline aquifer or depleted oil and gas fields. Although this technology is very promising, the CO_2 storage is only feasible where storage sites and sufficient capacity are available beside geological structures that permit safe sequestration of CO_2. Unfortunately, this is not always a feasible solution as many places in the world are not suitable for CO_2 storage due to geological reasons or the storage capacity is very limited. This led to find other alternative solutions where CO_2 storage is replaced with other technologies. Over the past few years, CO_2 conversion technologies has been extensively studied and developed to convert CO_2 to relevant chemicals and fuels.

Among several CO_2 conversion pathways shown in Figure 1-1, the most promising technology is CO_2 conversion into fuels and thereby reducing dependence on fossil fuel. This will ultimately reduce the overall CO_2 emission to the atmosphere and help mitigate GHG emissions.

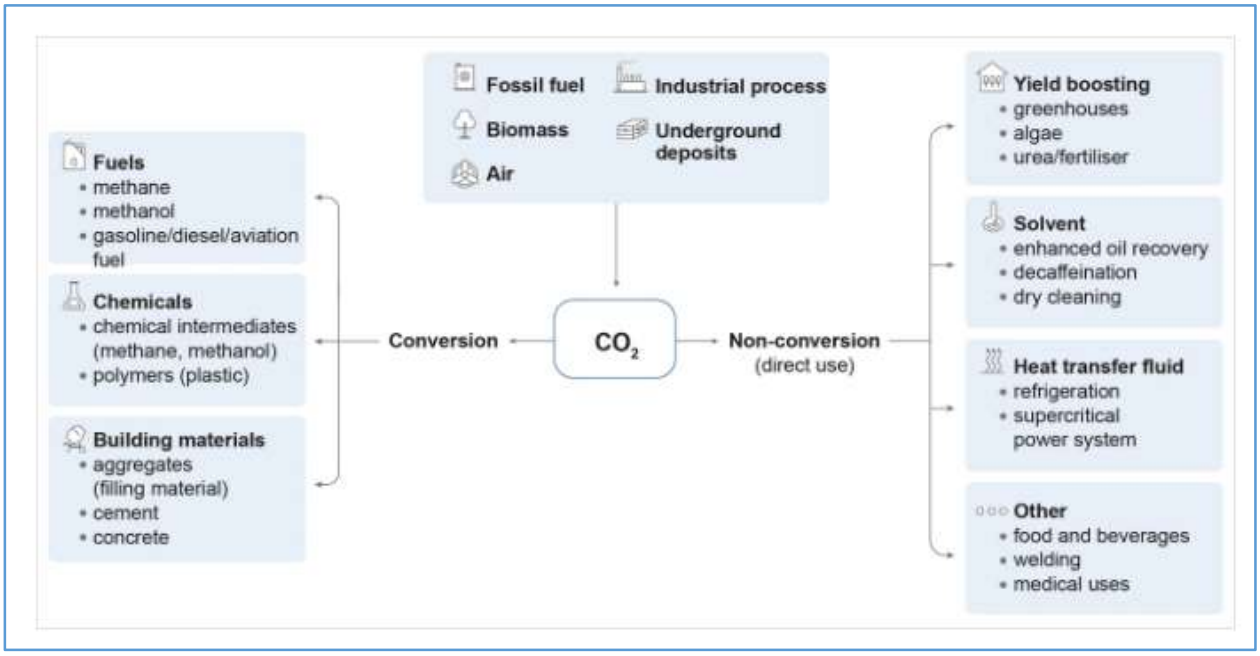

Figure 1-1. Pathways for CO_2 utilisation [3]

CO_2 conversion and utilisation has attracted great attention and supported by governments and industry groups due to its roles in mitigating CO_2 emissions permanently and for its economic value.

CO_2 utilization and conversion is divided into two different pathways. One is the non-conversion CO_2 use or direct CO_2 utilization where CO_2 can directly be used in many processes such as in enhanced oil recovery (EOR), used as solvent in injection oil reservoirs and in supercritical state in some advanced power plants, etc.

The indirect method of CO_2 utilization is through CO_2 reaction and transformation to other chemicals such as urea synthesis and its derivatives, salicylic acid, and carbonates [4]. The CO_2 hydrogenation through catalytic reactions includes various reactions to produce hydrocarbons, methanol, methane, etc. However, The CO_2 activation is a challenging operation as CO_2 is thermodynamically and kinetically stable, so high energy is required to split CO_2 molecules. To make this process more feasible, the selection of suitable catalyst and operating conditions is required. Hydrogen is the main element used in all CO_2 hydrogenation reactions and it needs to be produced from carbon free sources using renewable energy such as solar and wind energy. For instance, at low energy demand, the electricity produced from solar panels or wind turbines could be used to power water electrolysers to split water and generate hydrogen. Thus this seasonal energy is stored in hydrogen which is in turn used in different applications.

In this thesis, the focus will be on direct hydrogenation of CO_2 through Reverse Water Gas Shift (RWGS) reaction (eq. 1.1) to produce carbon monoxide (CO) and water (H_2O). Subsequently, hydrogenation of CO can be carried out through Fisher Tropsch synthesis (eq. 1.2) to produce methanol as well as long chain hydrocarbons as a final product.

$$CO_2 + H_2 \leftrightarrow CO + H_2O \tag{1.1}$$

$$(2n+1)H_2 + nCO \rightarrow C_nH_{2n+2} + nH_2O \tag{1.2}$$

As RWGS is a reversible equilibrium reaction, the unreacted CO_2 and H_2 need to be recycled back to the RWGS reactor in order to increase the overall conversion of the reaction. To recycle CO_2, a separation process is necessary to separate the product CO from unreacted CO_2 and H_2.

The proven technologies for CO separation from CO_2 and H_2 such as cryogenic distillation and liquid absorption are energy intensive [5] with high operating costs. The interest on adsorption separation including pressure swing adsorption (PSA) and temperature swing adsorption (TSA) continue to grow due to the process simplicity, low operating cost and low energy consumption.

Many porous materials have been used for CO separation, among them activated carbons, zeolites and metal organic frameworks [6]. However, their adsorption capacity and selectivity toward CO is not high for CO purification. Furthermore, the selectivity toward CO_2 is higher. To improve the adsorbents' uptake of CO, copper based adsorbents were developed to selectively adsorb CO through π complexation between Cu (I) ions and CO.

1.2 Adsorption separation

Adsorption separation process has been widely employed in many industrial applications, such as pollution control, heat storage, catalytic reactions, and gas separation and purification. The process is based on spontaneous interaction between gas or liquid molecules to the surface of a solid called the adsorbent. This interaction depends on the force field existing at the adsorbent surface. Depending on the nature of these forces, the adsorption process is classified to two different mechanisms, physisorption and chemisorption. In physisorption or physical adsorption, the interaction between the adsorbate and the adsorbent is based on Van Der Waals forces where the gas molecules maintain their electronic structure. The binding force is generally weak and depend on the polarizability and on the number of atoms involved. The process is reversible, to remove the adsorbate from the adsorbent surface, simple change in pressure or temperature is sufficient for adsorbent regeneration. On the other hand, chemisorption or chemical adsorption is a process in which a chemical interaction between the adsorbent and the adsorbate happens. The chemical bonds formed, may be covalent or ionic, involving higher energy of activation (80-240 kJ/mol). Contrary to physisorption, the chemisorption is a less reversible process, unless extreme change in operating conditions are applied.

1.2.1 Adsorption isotherms

Adsorption isotherm represents the equilibrium concentration of adsorbed gas into the surface in mmol/g as a function of partial pressure of the adsorbate at constant temperature. The plot is obtained through experimental data collected from a gravimetric or volumetric system. At constant temperature, and while varying the system pressure, the change in mass of the adsorbent is recorded indicating the amount of gas adsorbed at given pressure. Figure 1-2 represents the six types of adsorption isotherms according to the International Union of Pure and Applied Chemistry (IUPAC) classification for gas adsorption on the surface [7]. The shape of the isotherms depends

on the pore size of the adsorbent and type of interaction with the adsorbate. Microporous materials led to type I isotherms with uni-molecular adsorption. Type II isotherms correspond to non porous materials, type III, convex and undesirable, representing a weak interaction between adsorbent and adsorbate. Mesoporous materials yield to type IV isotherms, with a hysteresis loop usually associated with capillary condensation. Type V isotherms are similar to type III representing a weak interaction between the adsorbate and the adsorbent, with a hysteresis in a multi-molecular adsorption region. Type VI isotherms represent adsorption on homogeneous, nonporous material where the monolayer capacity corresponds to the step height.

In the adsorption process, the adsorbent is regenerated through two different processes, pressure swing adsorption (PSA) or temperature swing adsorption (TSA) depending on which operating parameter has been changed.

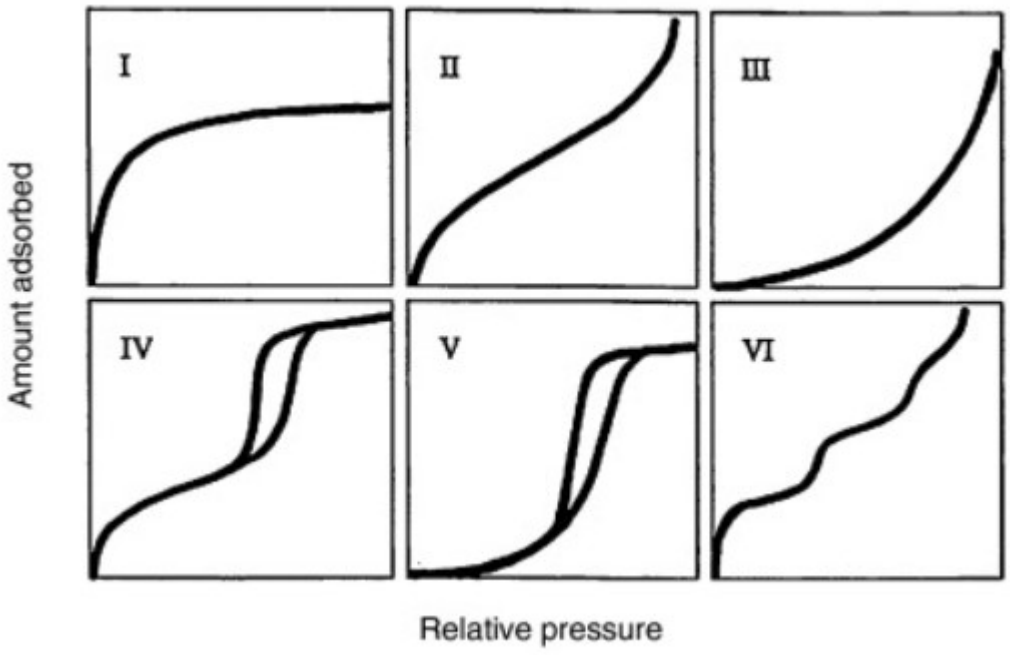

Figure 1-2. Classification of adsorption isotherms according to IUPAC [7]

1.2.2 Pressure swing adsorption

Pressure swing adsorption (PSA) is a common process used in industry for bulk gas mixture separation. The technology was invented by Skarstrom in 1959 for separation of oxygen from air. PSA process is based on reducing the operating pressure to regenerate the adsorbents. The process is mainly done in three different steps. At the first step, the adsorption happens under pressure to selectively adsorb the components from the gas feed. In next step, the adsorber is subject to expansion through pressure reduction to desorb the components previously adsorbed. In the last step, the pressure is increased back to adsorption pressure and the cycle is repeated. To enhance adsorbents regeneration, a purging gas is usually used at the end of step 2 to sweep out the desorbed components. PSA is associated to low energy cost penalty [8].

1.2.3 Temperature swing adsorption

In TSA, adsorption takes place usually at ambient temperature, while the regeneration is achieved by increasing the temperature while keeping the pressure constant. This process is usually used when the adsorbed species cannot be removed from the adsorbent by pressure swing.

In industrial applications, TSA is usually followed by purging with hot gas to sweep out the desorbed species. Some of the applications include trace impurity removal from air, gas or air drying, solvent recovery, etc. TSA is a slower process and more energy intense compared to PSA thus it is not as attractive as PSA from an economical and productivity perspective.

1.3 Research Objectives

The work presented in this thesis has been carried out to investigate the adsorption of carbon monoxide (CO) in different porous materials including activated carbons, ordered mesoporous silica and metal organic framework (MOF) materials. The focus is to develop novel adsorbents that are more selective to CO with low affinity towards CO_2. A supported metal solid adsorbent via π-complexation between metal ions and CO molecules was developed through two types of copper introduction into the porous materials:

- The thermal monolayer dispersion method using hydrous copper chloride ($CuCl_2.2H_2O$).
- Impregnation with copper chloride ($CuCl_2$) using modified polyol method.

The experimental results were compared to conclude the best methodology for adsorbents' modification.

1.4 Thesis outline

This thesis is organized in the following order:

Chapter 1 describes the introduction, and research objectives.

Chapter 2 provides the process simulation and model development details including process description and steady state model validation for RWGS reaction.

Chapter 3 presents the literature review of the latest results obtained in CO adsorption and separation technologies.

Chapter 5 presents the results obtained from experimental data carried out in different porous materials, including the modified adsorbent with copper chloride salt.

Chapter 6 provides the conclusions of this research work and recommendations for further studies.

1.5 Nomenclature

EIA	Energy Information Administration
GHG	Greenhouse gas
IUPAC	International Union of Pure and Applied Chemistry
NOAA	National Oceanic and Atmospheric Administration
PSA	pressure swing adsorption
TPES	total primary energy supply
TSA	temperature swing adsorption

1.6 References

[1] V. D. G. *et al.*, “Introductory Chapter. In: Climate Change 2014: Mitigation of Climate Change. Contribution of Working Group III to the Fifth Assessment Report of the Intergovernmental Panel on Climate Change,” 2014. [Online]. Available: https://www.ipcc.ch/site/assets/uploads/2018/02/ipcc_wg3_ar5_chapter1.pdf.

[2] R. Lindsey, “Climate Change: Atmospheric Carbon Dioxide.” https://www.climate.gov/news-features/understanding-climate/climate-change-atmospheric-carbon-dioxide (accessed Nov. 20, 2020).

[3] “Putting CO2 to Use,” Paris, 2019. [Online]. Available: https://www.iea.org/reports/putting-co2-to-use.

[4] S. Saeidi, N. A. S. Amin, and M. R. Rahimpour, “Hydrogenation of CO2 to value-added products - A review and potential future developments,” *J. CO2 Util.*, vol. 5, pp. 66–81, 2014, doi: 10.1016/j.jcou.2013.12.005.

[5] S. J. Bhadra and S. Farooq, “Separation of methane-nitrogen mixture by pressure swing adsorption for natural gas upgrading,” *Ind. Eng. Chem. Res.*, vol. 50, no. 24, pp. 14030–14045, 2011, doi: 10.1021/ie201237x.

[6] A. Evans, R. Luebke, and C. Petit, “The use of metal-organic frameworks for CO purification,” *J. Mater. Chem. A*, vol. 6, no. 23, pp. 10570–10594, 2018, doi: 10.1039/c8ta02059k.

[7] R. Kecili and Chaudhery Mustansar Hussain, “Mechanism of Adsorption on Nanomaterials,” pp. 89–115, 2018.

[8] C. A. Grande, “Advances in Pressure Swing Adsorption for Gas Separation,” *Int. Sch. Res. Netw.*, vol. 2012, pp. 100–102, 2012, doi: 10.5402/2012/982934.

Chapter 2: **Process Simulation of Reverse Water Gas Shift Reaction**

2.1 Abstract

The catalytic hydrogenation reaction of carbon dioxide (CO_2) to produce carbon monoxide (CO) via reverse water gas shift reaction (RWGS) is a viable pathway to convert CO_2 captured from different emitting sources such as power plants and industrial processes to CO. CO can be converted into value added products such as chemicals and liquid fuels through CO hydrogenation reaction. RWGS is one of the most prominent technologies with high technology readiness level for CO_2 utilization beside other technologies such as syngas synthesis from methane dry reforming and direct CO_2 hydrogenation [1]. This chapter focuses on the operation and thermodynamic properties of RWGS. A process simulation studies using Aspen HYSYS software is conducted to study the effect of different parameters such as temperature, pressure, feed flow concentration, recycle ratio on the reaction conversion and product selectivity. Sensitivity analysis is conducted to define optimal operating conditions to maximize CO_2 conversion and CO selectivity.

2.2 Introduction

Carbon dioxide is the main greenhouse gas emitted into the atmosphere. Its concentration continues to rise and currently surpassed 410 ppm according to National Oceanic and Atmospheric Administration (NOAA). Therefore, the impact on the environment is alarming. To mitigate greenhouse gas emissions, significant efforts are being implemented. The first approach is to reduce the amount of CO_2 produced from major emitters such as conventional fossil fuel combustion plants for electricity production and replace them with low carbon energy sources such as renewable and nuclear energy. The second approach is to reduce the carbon emissions by the implementation of carbon capture and storage technologies (CCS). In the latter approach, CO_2 from large emitting sources such as coal fired power plants and industrial processes is captured, transported through pipelines and securely stored underground. The CCS is a readily deployable technology; however, its implementation is facing several challenges. The main challenge is related to large capital investments. The other obstacle is related to the storage sites. In some cases the storage capacity is limited or not available thus this technology may not be always feasible.

The alternative solution for CO_2 mitigation is the utilization of CO_2 captured and its conversion to value added products such as fuels and chemicals. Currently, there is a growing effort to develop technologies to use CO_2 from industrial flue gas as a feedstock and convert it to liquid fuels and chemicals. To convert CO_2, three different pathways can be applied [2]: thermochemical conversion, photoelectrocatalysis reaction and CO_2 hydrogenation reactions. In this paper we will focus on CO_2 hydrogenation through RWGS reaction where captured CO_2 and H_2, which is obtained from a renewable source are converted to carbon monoxide and water. Subsequently, the CO produced is converted to different synthetic fuels such as gasoline, diesel oil and petrochemicals through Fisher Tropsch (FT) synthesis[3]–[5] or other CO hydrogenation processes. A schematic diagram of the overall process is shown in Figure 2-1

RWGS is also a promising reaction in space exploration since CO_2 is available at high concentration (about 95%) in Mars and H_2 is either brought from earth or produced from water electrolysis needed to produce oxygen [6]–[8].

To make CO_2 conversion more feasible, a carbon free energy source should be applied such as renewable (e.g. solar and wind) and nuclear energy. Effective reaction conditions, reactor design and the choice of active catalyst are also parameters to consider lowering the process energy demand and increase the product selectivity and CO_2 conversion.

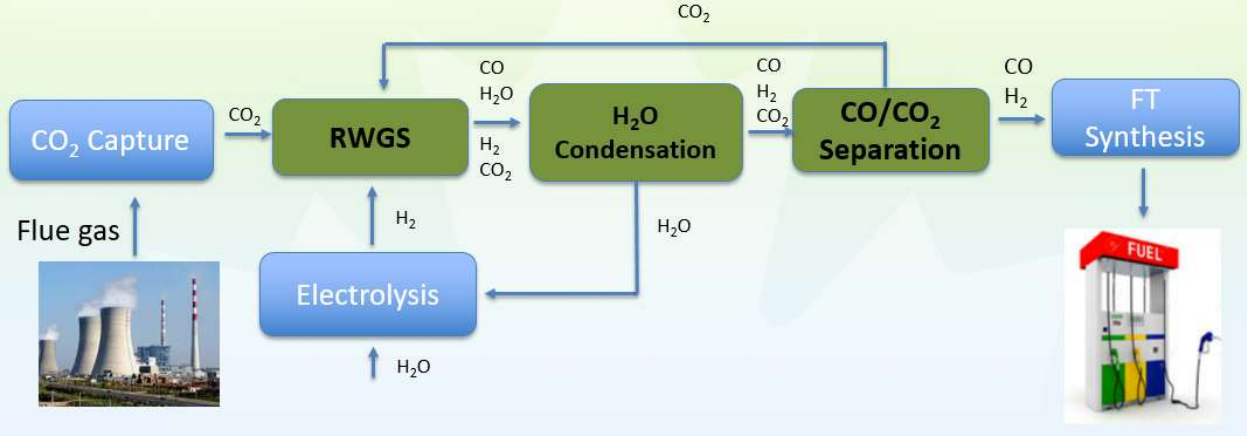

Figure 2-1. Schematic diagram of liquid fuel production from CO_2 through RWGS and FT process.

RWGS reaction has been known in chemistry since the 1800's [9]. For the last two decades, many experimental studies were carried out to demonstrate its effectiveness and the performance of different catalysts. In this study, a process simulation tool using Aspen HYSYS platform is applied to investigate the thermodynamic equilibrium data of RWGS reaction and effects of different parameters on reaction conversion and products' selectivity.

2.3 Thermodynamics of RWGS

RWGS is a reversible reaction in which CO_2 reacts with H_2 to produce CO and H_2O. The reaction stoichiometry is shown in equation (2.1):

$$CO_2 + H_2 \rightarrow CO + H_2O \qquad \Delta H = \frac{42.2kJ}{mol} \tag{2.1}$$

Since RWGS is an endothermic reaction ($\Delta H > 0$), according to Le Chatelier principle, the reaction is thermodynamically favoured at high temperatures. Furthermore, CO_2 is a very stable molecule with high Gibbs free energy of formation (ΔG = -394KJ/mole), therefore its transformation to other compounds requires an intensive amount of energy.

Figure 2-2 [10] shows the Gibbs free energy of CO_2 and some other compounds. The addition of higher Gibbs free energy reactants such as H_2 will make the CO_2 transformation thermodynamically easier with less energy requirements.

In parallel to RWGS reaction, few side reactions may also be present [11], including:

Sabatier reaction:

$$CO_2 + 4H_2 \rightarrow CH_4 + 2H_2O \quad \Delta H = \frac{-16 \ kJ}{mol} \tag{2.2}$$

CO methanation reaction:

$$CO + 3H_2 \rightarrow CH_4 + H_2O \quad \Delta H = \frac{-206 \ kJ}{mol} \tag{2.3}$$

Boudouard reaction:

$$CO + CO \rightarrow C(s) + CO_2 \quad \Delta H = \frac{-142 \ kJ}{mol} \tag{2.4}$$

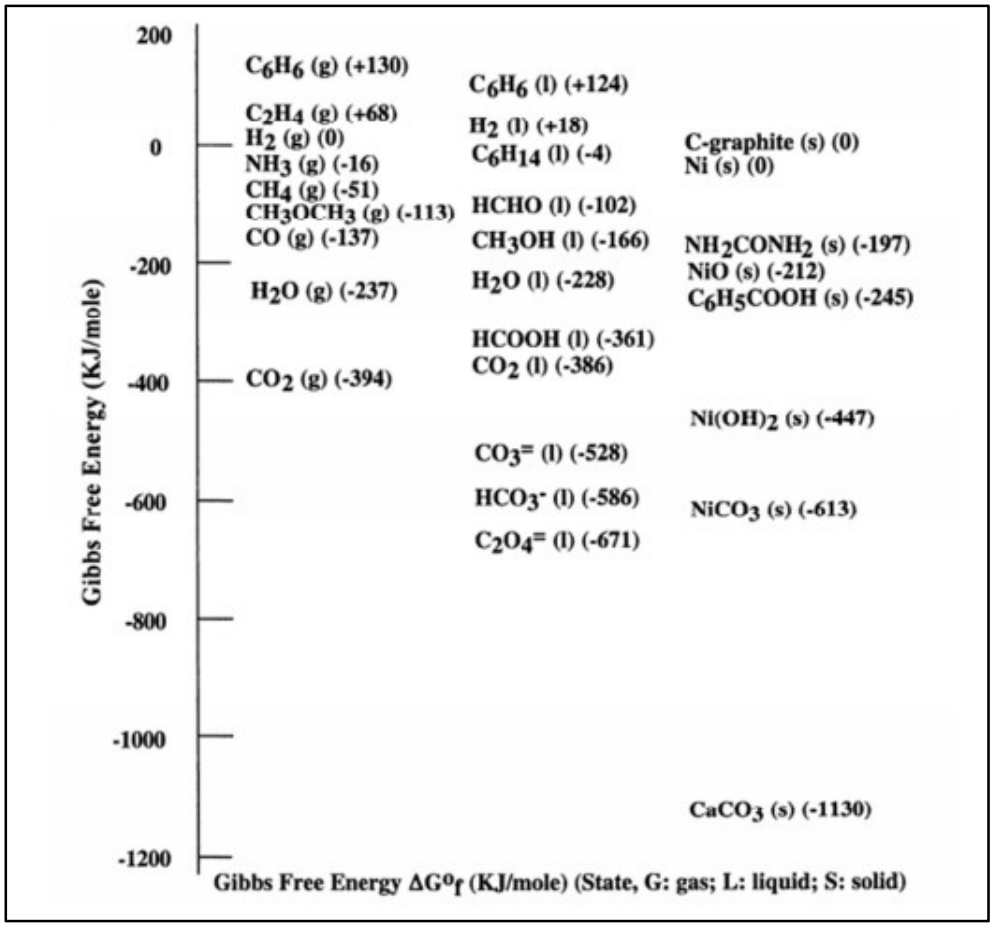

Figure 2-2. Gibbs free energy of CO_2 and some other compounds [10].

2.3.1 Equilibrium constant

To find the equilibrium composition of RWGS, the equilibrium constant K_p needs to be calculated. K_p is defined as the ratio of the partial pressures or concentration of the reactants and products at equilibrium at a certain temperature. Equation (2.5) shows the equilibrium constant equation.

$$K_P = \left(\frac{P_{CO}P_{H_2O}}{PCO_2P_{H_2}}\right)_{eq} = e^{\left[-\frac{\Delta G}{RT}\right]} \tag{2.5}$$

For RWGS, the equilibrium constant was calculated using equations (2.6) and (2.7) [12]

$$K_P = \exp\left(Z(Z(0.63508 - 0.29353Z) + 4.1778) + 0.31688\right) \tag{2.6}$$

$$Z = \left(\frac{1000}{T}\right) - 1 \quad Tin\ Kelvin \tag{2.7}$$

Since RWGS is an endothermic reaction, the equilibrium constant will increase as temperature increases and high conversions are favoured at high temperatures. The K_p calculation results are illustrated in Figure 2-3.

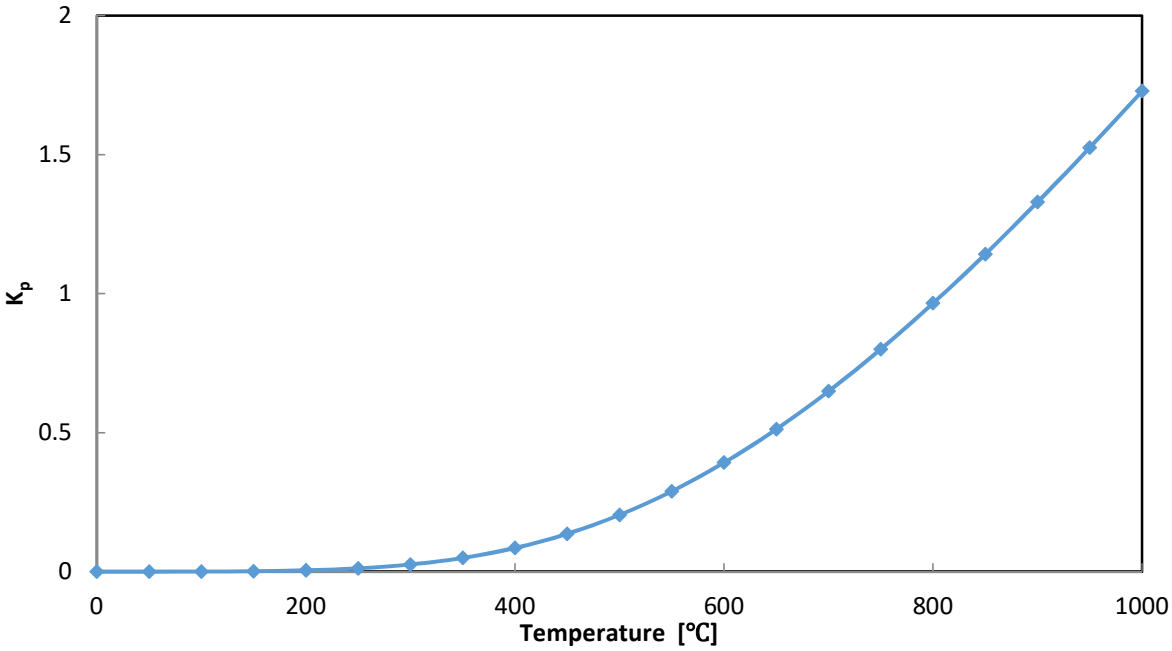

Figure 2-3. RWGS equilibrium constant K_p at different temperatures.

The equilibrium conversion of CO_2 ($X_{CO2,eq}$) can be calculated from the equilibrium constant K_p as a function of temperature. For an equimolar feed of CO_2 and H_2, the equilibrium constant is expressed in equation (2.8). Figure 2-4 illustrates how the calculated equilibrium conversion increases with increasing temperature as expected for endothermic reactions.

$$X_{CO2,eq} = \frac{\sqrt{K_P}}{1} + \sqrt{K_P} \tag{2.8}$$

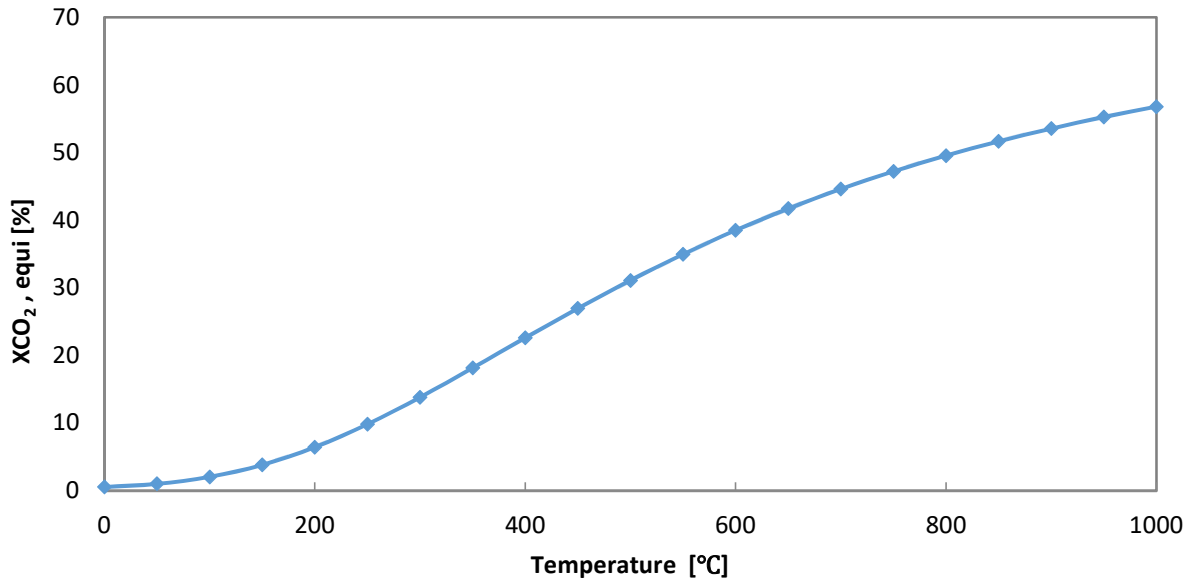

Figure 2-4. Equilibrium conversion of CO_2 as a function of temperature for the RWGS reaction.

2.3.2 CO_2 conversion and yield of CO and CH_4

The CO_2 conversion, CO and CH_4 yield are calculated using equations 2.9, 2.10 and 2.11 consecutively, with CO and CH_4 are the only detectable products gas from CO_2 hydrogenation, considering all the side reactions happening in parallel to RWGS.

$$\mathbf{CO_2\ conversion}\ (\%) = ([\mathbf{CO_2}]_{\mathbf{In}} - [\mathbf{CO_2}]_{\mathbf{Out}})/[\mathbf{CO_2}]_{\mathbf{In}}\ \boldsymbol{X}\ 100 \qquad (2.9)$$

$$\mathbf{CO\ yield}\ (\%) = [\mathbf{CO}]_{\mathbf{out}}/([\mathbf{CO}]_{\mathbf{out}} + [\mathbf{CO_2}]_{\mathbf{out}} + [\mathbf{CH_4}]_{\mathbf{out}})\ \boldsymbol{X}\ 100 \qquad (2.10)$$

$$\mathbf{CH_4\ yield}\ (\%) = [\mathbf{CH_4}]_{\mathbf{out}}/([\mathbf{CO}]_{\mathbf{out}} + [\mathbf{CO_2}]_{\mathbf{out}} + [\mathbf{CH_4}]_{\mathbf{out}})\ \boldsymbol{X}\ 100 \qquad (2.11)$$

2.4 Process simulation

2.4.1 Simulation methodology

To develop the process flow diagram shown in Figure 2-5 in HYSYS software, it is required to select the equation of state (EOS) that can correctly determine the thermodynamic property of the gas mixture such as pressure (P), temperature (T) and molar volume (V_m). Many EOS's have been developed and Peng Robinson EOS (PR-EOS) was chosen as it is widely used in gas processing and petroleum industry. It is one of the most accurate and simple equations. The PR-EOS equations is expressed as shown in equation (2.12) [13], [14].

$$P = \frac{RT}{(V_m - b)} - \frac{a}{V_m(V_m + b) + b(V_m - b)} \tag{2.12}$$

Where $a_i = \alpha_i \ 0.045724 \frac{R^2 T_{ci}^{\ 2}}{P_{ci}}$

$$b_i = 0.07780 \frac{RT_{ci}}{P_{ci}}$$

$$\alpha_i = \left[1 + m_i\left(1 - T_{ri}^{\frac{1}{2}}\right)\right]^2$$

$$m_i = 0.37464 + 1.54226\omega_i - 0.26992\omega_i^2$$

ω_i represents the acentric factor, T_{ci} P_{ci} are the critical temperature and pressure, and T_{ri} is the reduced pressure.

The following pieces of equipment are used in the process simulation:

- An equilibrium reactor (RWGS reactor) was selected to model the RWGS reaction including the possible parallel reactions such as methanation reaction. The equilibrium constant is calculated from Gibbs free energy.
- A cooler and separator, to condense and remove the water produced. Water will be recycled to an electrolyser to produce hydrogen needed for the reaction.

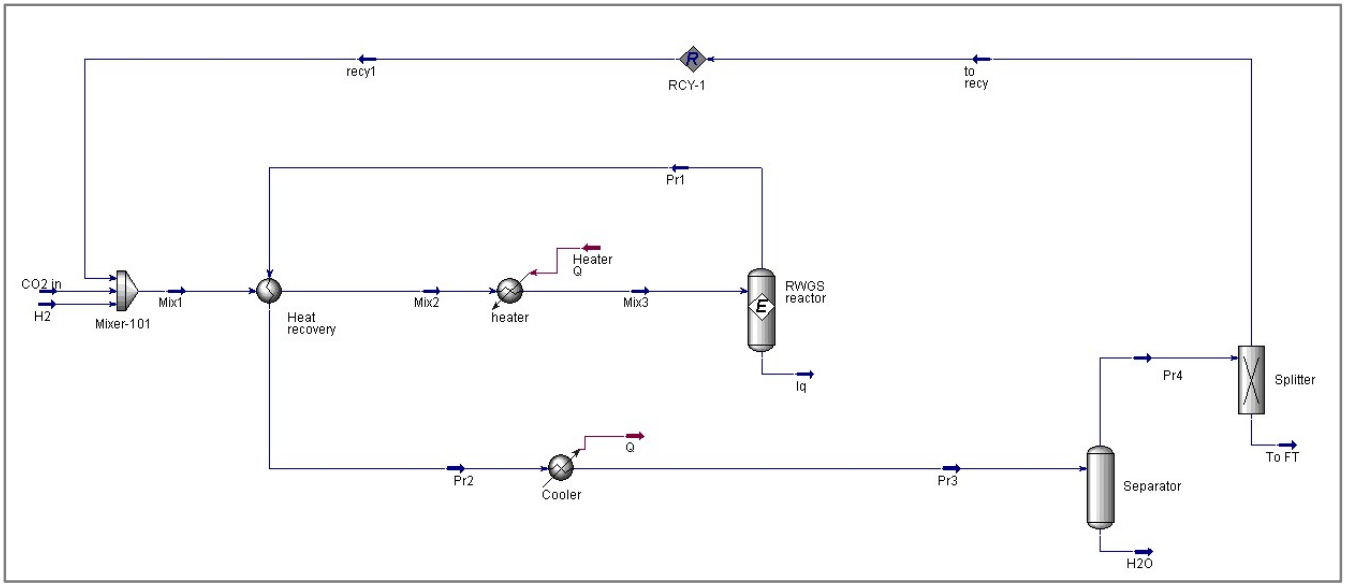

Figure 2-5. HYSYS simulation flowsheet of RWGS.

- A splitter which represents the pressure swing adsorption (PSA) or membrane separator to separate CO_2 from CO. The CO_2 or both CO_2 and H_2 are recycled back to the reactor to increase the CO_2 conversion while the produced CO is fed to the Fischer Tropsch process or another process for fuel/chemical production.
- A heater to heat the inlet reactants to a specified temperature before entering the reactor.
- A heat recovery system, which represents a heat exchanger where the hot products stream preheats the reactants stream.

2.5 Simulation results and discussion

2.5.1 Effect of temperature and pressure

RWGS is an endothermic reaction and therefore, high CO_2 conversion is favored at high temperatures. Figure 2-6 represents the equilibrium composition of RWGS with methanation reaction products at atmospheric pressure and inlet feed ratio of H_2 to CO_2 of 2 (H_2/CO_2=2). At low temperatures, the exothermic methanation reaction is thermodynamically favored. Almost all the hydrogen is used to produce methane and water with little CO formation. As the temperature increases above 700 $^{\circ}$C, the methanation reaction is supressed, and RWGS is dominant with CO and H_2O are the main products.

As we increase the reaction pressure, the CO_2 equilibrium conversion does not change for RWGS, due to the stoichiometry of the reaction (number of moles of the products are the same as the

number of moles of the reactants). This result was expected from Le Chatelier principle. However, the methane formation does increase as pressure increases as shown from the CH_4 yield calculations shown in Figure 2-7.

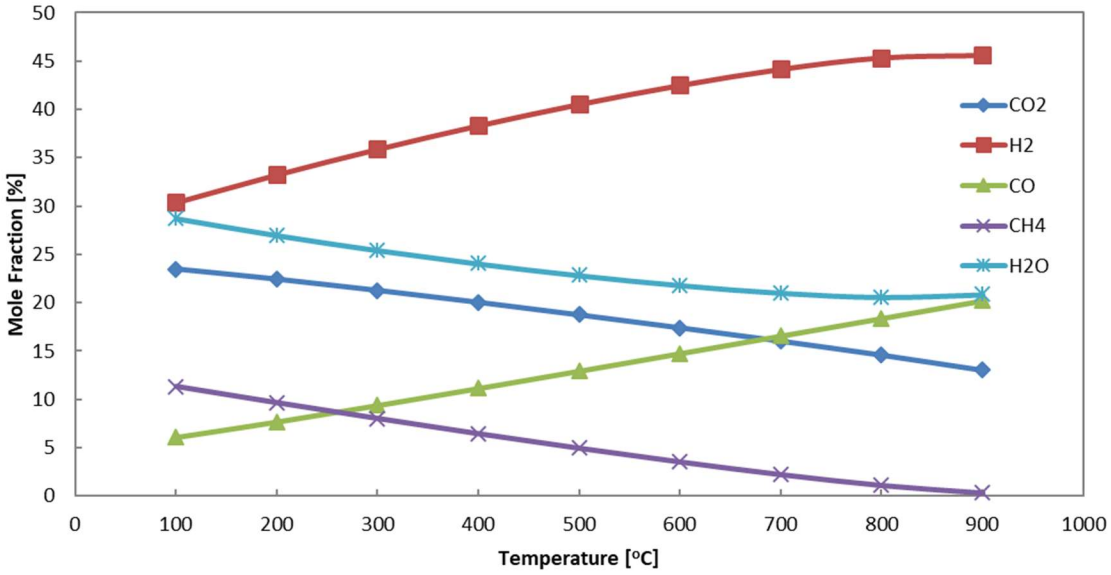

Figure 2-6. Equilibrium composition of RWGS with parallel methanation reaction at 1 atm for a feed ratio of H_2/CO_2 =2

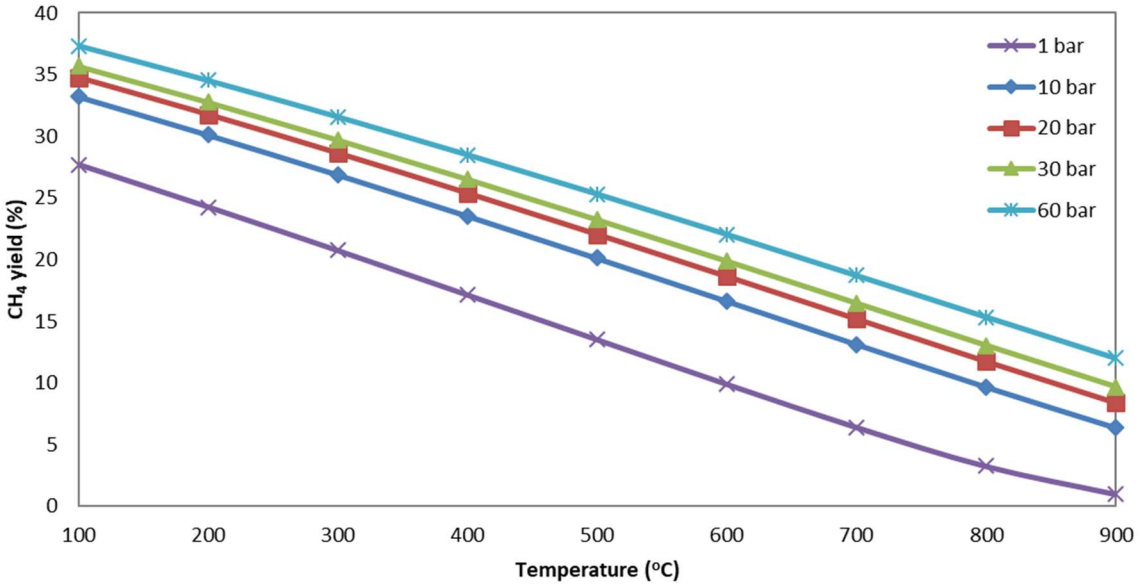

Figure 2-7. Methane yield from CO_2 methanation reaction at different pressures and temperatures with inlet feed ratio of H_2/CO_2 =2.

2.5.2 Effect of H_2/CO_2 feed ratio

The conversion of CO_2 in RWGS is not a complete conversion even at higher temperatures. At 700 °C, the CO_2 equilibrium conversion is only 34% with equimolar inlet of CO_2 and H_2. To enhance the CO_2 conversion and shift the equilibrium to the right, an excess feed ratio of H_2 to CO_2 is used [15], [16]. HYSYS simulation results shown in Figure 2-8 for H_2/CO_2 ratio varying from 1 to 6 illustrate how CO_2 conversion increases with high H_2 in the feed. The excess H_2 in the reactor led to almost complete consumption of CO_2. The unreacted H_2 can be separated and recycled back to the reactor to increase the overall conversion of the process. The drawbacks of higher H_2/CO_2 feed ratio is the occurrence of Sabatier parallel reaction, which will produce more methane at lower temperatures.

To drive the RWGS reaction to the right, Zurbrin et al.[17] suggested feeding the reactor with an excess feed of CO_2 to complete consumption of H_2, then separating and recycling the unreacted CO_2, besides excess use of H_2,. They also suggested removing water vapor from the reactor to drive the equilibrium towards the CO production.

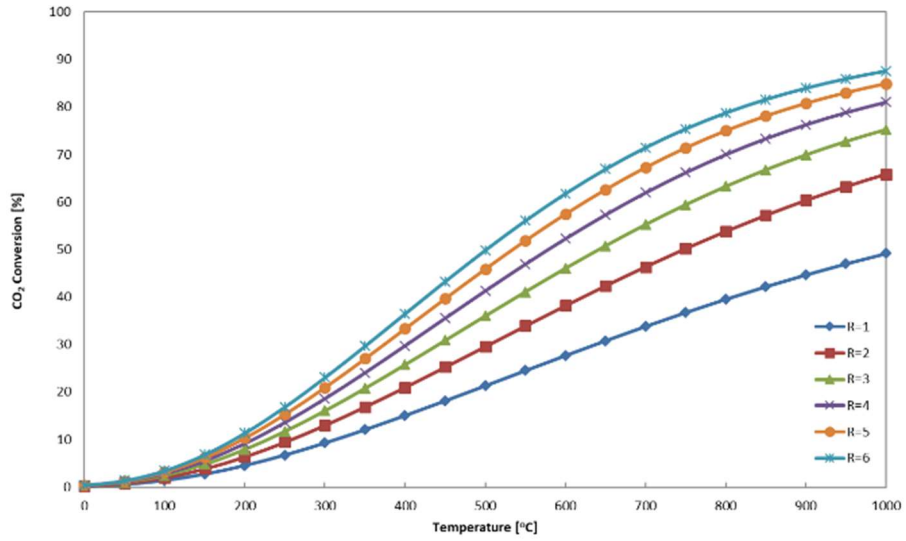

Figure 2-8. Equilibrium CO_2 conversion at 1 atm. for different temperatures and feed ratios of H_2 to CO_2 ($R=H_2/CO_2$).

2.5.3 Effect of CO_2 and H_2 recycling

To increase the CO_2 conversion, the unreacted CO_2 can be separated from CO and H_2 using one of the well-known separation processes. The pressure swing adsorption is one the most promising technology used for gas separation due to its simplicity and low energy requirements [18], [19]. The CO_2 or CO_2 and H_2 can then be recycled back to the reactor. Figure 2-9 and Figure 2-10 demonstrate the effects of recycling CO_2 and H_2 on the overall CO_2 conversion at different H_2/CO_2 feed ratios at a temperature of 700 $^{\circ}$C at atmospheric pressure. From these figures we can see that higher conversion is achieved as the recycle ratio of CO_2 or CO_2 and H_2 increases. Recycling both CO_2 and H_2 has better impact on CO_2 conversion, this result is expected since the ratio of H_2 at the inlet will increase when H_2 and CO_2 are both recycled back in comparison to only recycling CO_2. Overloading the RWGS reactor with an excess feed of H_2 or CO_2 or both will shift the reaction more to the right, thus resulting at higher CO_2 conversions as can be seen from the simulation results.

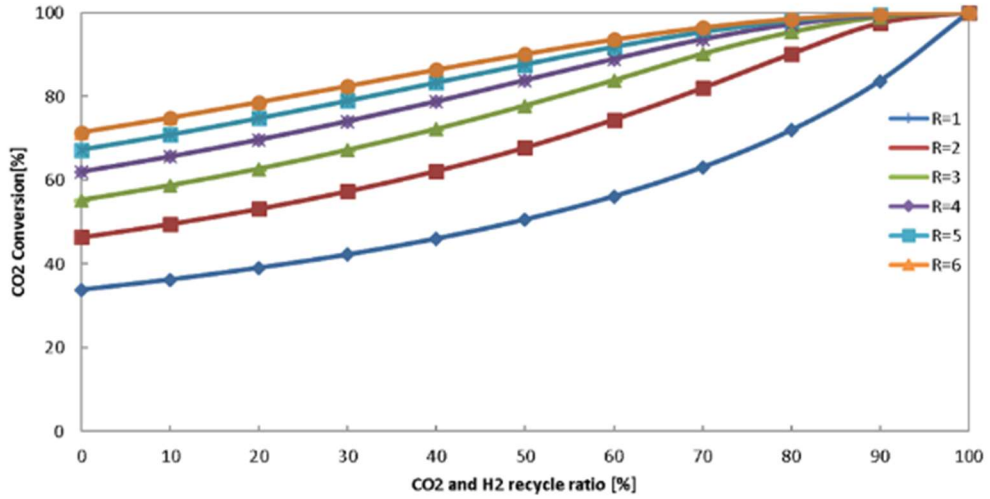

Figure 2-9. CO_2 conversion [%] at different CO_2 and H_2 recycle ratios for different inlet feed ($R=H_2/CO_2$) ratios.

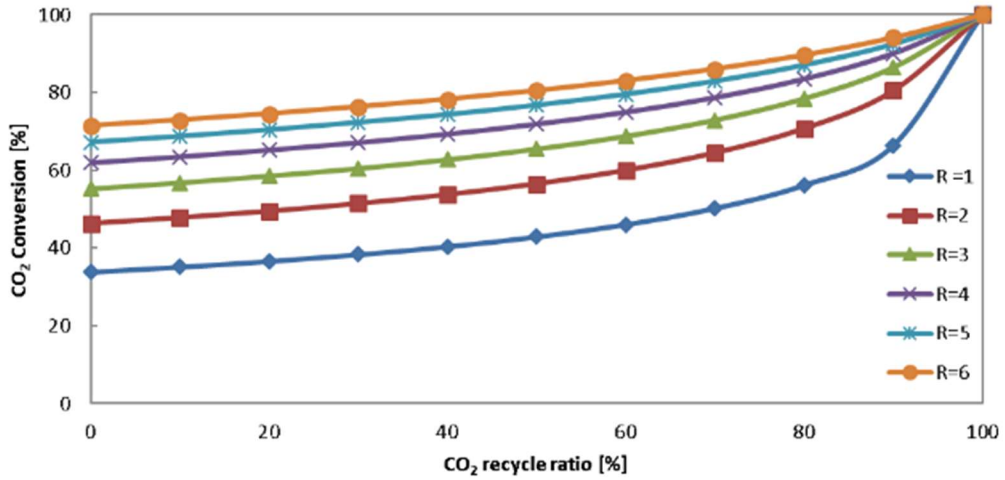

Figure 2-10. CO_2 conversion [%] at different CO_2 recycle ratios for different inlet feed ratios ($R = H_2/CO_2$).

2.6 Conclusions

HYSYS simulation results demonstrated that RWGS is favored at high temperatures, with a feed ratio of hydrogen to CO_2 higher than the stoichiometric value of 1. At 700 $^{\circ}$C, the equilibrium conversion is about 34% for a feed ratio of H_2 to CO_2 of 1. With a feed ratio of 2, the equilibrium conversion increases to 46%. Increasing the temperature has also the advantage of supressing the parallel Sabatier and methanation reactions which occur at lower temperatures. Increasing the pressure does not have any effect on RWGS as was expected, however this will favour the methane formation and would increase the cost related to compression and implementation of high-pressure equipment. To improve the overall CO_2 conversion, the unreacted CO_2 and H_2 can be recovered through a separation process and recycled back to the reactor. Pressure swing adsorption with selection of appropriate porous materials could be an efficient method for CO or CO_2 separation. Membrane separation is also a new emerging technology that can be investigated and applied in this process.

2.7 Abbreviations

CCS	Carbon capture and storage
EOS	Equation of state
HYSYS	Simulation software
FT	Fisher Tropsch
PSA	Pressure swing adsorption
NOAA	National Oceanic and Atmospheric Administration
RWGS	Reverse water gas shift

2.8 Nomenclature

CO	Carbon monoxide
CO_2	Carbone dioxide
H_2	Hydrogen
H_2O	Water

K_p	Equilibrium constant
P_c	Critical pressure
R	Universal gas constant
T_c	Critical temperature
T_r	Reduced pressure
V_m	Molar volume
ω_i	acentric factor

2.9 References

[1] Y. A. Daza and J. N. Kuhn, "CO2 conversion by reverse water gas shift catalysis: Comparison of catalysts, mechanisms and their consequences for CO2 conversion to liquid fuels," *RSC Adv.*, vol. 6, no. 55, pp. 49675–49691, 2016, doi: 10.1039/c6ra05414e.

[2] Y. A. Daza, R. A. Kent, M. M. Yung, and J. N. Kuhn, "Carbon dioxide conversion by reverse water-gas shift chemical looping on perovskite-type oxides," *Ind. Eng. Chem. Res.*, vol. 53, no. 14, pp. 5828–5837, 2014, doi: 10.1021/ie5002185.

[3] P. Kaiser, R. B. Unde, C. Kern, and A. Jess, "Production of liquid hydrocarbons with CO2 as carbon source based on reverse water-gas shift and fischer-tropsch synthesis," *Chemie-Ingenieur-Technik*, vol. 85, no. 4, pp. 489–499, 2013, doi: 10.1002/cite.201200179.

[4] F. Vidal Vázquez, P. Pfeifer, J. Lehtonen, P. Piermartini, P. Simell, and V. Alopaeus, "Catalyst Screening and Kinetic Modeling for CO Production by High Pressure and Temperature Reverse Water Gas Shift for Fischer-Tropsch Applications," *Ind. Eng. Chem. Res.*, vol. 56, no. 45, pp. 13262–13272, 2017, doi: 10.1021/acs.iecr.7b01606.

[5] Y. H. Choi *et al.*, "Carbon dioxide Fischer-Tropsch synthesis: A new path to carbon-neutral fuels," *Appl. Catal. B Environ.*, vol. 202, pp. 605–610, 2017, doi: 10.1016/j.apcatb.2016.09.072.

[6] J. E. Whitlow, "Operation, Modeling and Analysis of the Reverse Water Gas Shift Process," Feb. 2003, pp. 1116–1123, doi: 10.1063/1.1541409.

[7] S. O. Starr and A. C. Muscatello, *Mars in situ resource utilization: a review*, vol. 182. 2020.

[8] E. Muscatello, Anthony C ; Santago-Maldonado, "Mars in Situ Resource Utilization Technology Evaluation."

[9] B. F. and T. K. Robert Zubrin, Brian Frankie, Tomoko Kito, Robert Zubrin, "Mars in-situ resource utilization based on the reverse water gas shift - Experiments and mission applications," vol. AIAA 97-27, 1997.

[10] C. Song, “CO2 Conversion and Utilization: An Overview,” *ACS Symp. Ser.*, vol. 809, pp. 1–30, 2002, doi: 10.1021/bk-2002-0809.ch001.

[11] K. Stangeland, D. Kalai, H. Li, and Z. Yu, “CO2 Methanation: The Effect of Catalysts and Reaction Conditions,” in *Energy Procedia*, 2017, vol. 105, pp. 2022–2027, doi: 10.1016/j.egypro.2017.03.577.

[12] M. V. Twigg, Ed., *Catalyst Handbook*, Second Edition. London: Taylor & Francis, 1989, 1989.

[13] R. Stryjek and J. H. Vera, “PRSV: An improved peng—Robinson equation of state for pure compounds and mixtures,” *Can. J. Chem. Eng.*, vol. 64, no. 2, pp. 323–333, 1986, doi: 10.1002/cjce.5450640224.

[14] D. Peng and D. B. Robinson, “A new equation of state,” *Nature*, vol. 123, no. 3100, p. 507, 1929.

[15] J. Hu, K. P. Brooks, J. D. Holladay, D. T. Howe, and T. M. Simon, “Catalyst development for microchannel reactors for martian in situ propellant production,” *Catal. Today*, vol. 125, no. 1–2, pp. 103–110, Jul. 2007, doi: 10.1016/j.cattod.2007.01.067.

[16] K. Brooks *et al.*, “Development of a microchannel in situ propellant production system,” *AIP Conf. Proc.*, vol. 813, no. February, pp. 1111–1121, 2006, doi: 10.1063/1.2169292.

[17] T. K. Robert Zubrin, Brian Frankie, “Mars in-situ resource utilization based on the reverse water gas shift - Experiments and mission applications,” 1997.

[18] G. Férey *et al.*, “Why hybrid porous solids capture greenhouse gases?,” *Chem. Soc. Rev.*, vol. 40, no. 2, pp. 550–562, 2011, doi: 10.1039/c0cs00040j.

[19] F. Chang, Z. Wang, H. Sun, S. Gao, G. Wen, and X. Zhang, “Fei Chang,” *Chemical Communications*, vol. 2. pp. 2976–2978, 2005.

Chapter 3: **Literature Review**

3.1 Abstract

Carbon monoxide (CO) separation and purification is a significantly important process in chemical industry. The development of efficient and most economic process for its recovery is crucial for its application in industry. There has been various developed technologies implemented in large scale for CO separation from streams containing different gas mixtures. This paper provide a review of the main processes used for carbon monoxide (CO) separation from different gas mixture streams, along with their advantages and disadvantages and different CO production technologies that are mostly employed in industry. The focus of this review is on CO separation and purification by adsorption process using different common porous materials such as activated carbons, zeolites and metal organic framework materials as potential adsorbents. Moreover, surface modification of porous materials through introduction of metal salts to improve CO adsorption selectivity and capacity has been investigated. Details of π-complexing adsorbents and different methods of metal ions dispersion are discussed along with a summary of literature results on CO and CO_2 adsorption and selectivity in modified and non-modified adsorbents. Best adsorbent for CO purification are highlighted and further challenges and improvement opportunities are discussed.

3.2 Introduction

Carbon monoxide is an important building block material in C1 chemistry processes [1]. It has been used to produce a wild variety of chemicals and fuels such as formic acid, acetic acid, phosgene, esters, [2], [3]. Liquid hydrocarbon productions via CO hydrogenation in Fischer-Tropsch synthesis is another important route of CO application. CO is produced from various processes. The most common one is steam methane reforming where CO is produced together with hydrogen to form syngas. Partial oxidation of hydrocarbons and auto-thermal reforming are two other industrial processes used for syngas production. Moreover, CO is produced as off-gas from different industrial processes such as steel and metallurgical industry, carbon black manufacturing, and ceramic industry[4], [6] [7][8]. In these streams, CO is mixed with other components including CO_2, H_2O, N_2, CH_4 and other gases. Therefore, the removal of impurities and CO purification is

necessary to obtain CO with desired purity permitting its effective use in chemical industries. The CO recovery from off gas streams is another economic source of CO which can be turned into other value added chemicals while contributing to greenhouse gas mitigation given that no additional CO_2 emitted for CO production. Furthermore, the existence of trace amount of CO can poison the catalyst in hydrogen proton–exchange membrane fuel cells [9] [10], [11]. Moreover, CO is a very toxic gas for human beings and can cause serious tissue damage when breathed even at low concentrations. Therefore, selective CO capture from air where CO may exist is imperative.

There are several industrial approaches for CO separation and purification. Some processes are well developed and used at industrial scale. The most proven technologies are cryogenic distillation, absorption using liquid solvents and adsorption. The choice of suitable separation process depends on several factors. Feed gas conditions, the desired product purity, gas mixture composition, energy and operating cost are some examples. For instance, the purification of CO from a gas mixture containing high concentration of N_2 is not possible using cryogenic distillation. Both CO and N_2 have similar boiling points, hence their separation necessitate using other separation technologies than cryogenic distillation.

Adsorption separation is an emerging technology for CO purification. There has been considerable research work on development of adsorbents materials for CO purification. The most studied ones are activated carbons, zeolites and metal organic frameworks (MOFs). These porous solid adsorbents display high surface area and porosity required for high adsorption capacity. However, CO adsorption capacity is not sufficient enough for selective adsorption of CO from a gas mixture. To overcome this, adsorbents' modification with incorporation of transition metal ions had proved to improve the CO adsorption and selectivity. Active metal ions such as Cu (I), Ag (I), Pd (II) and others are dispersed on the pores of the support material to form adsorbent materials that are more selective to CO. The CO molecules bonds to the metal ions through π- complexation bonds. These bonds are known to be stronger than van Der Waals forces, thus high CO adsorption capacity and selectivity are achieved. Furthermore, the interaction between CO and metal ions can be broken by simple change in operating pressure or temperature for adsorbent regeneration.

In this review, a detailed study of recent research work on adsorbent modification using different adsorbent materials and metal dispersion methods is detailed along with a summary of adsorbent performances for CO and carbon dioxide (CO_2) separation.

3.3 CO Production

Carbon monoxide is mainly formed as a product of incomplete combustion of carbon containing compounds such as petroleum fuels and biomass. The formed mixture of CO and H_2 is called synthetic gas, which is also known as syngas. In addition, other impurities are also produced including steam, CO_2, N_2, CH_4 and others. Syngas is produced from various processes. If the carbon feedstock used is natural gas, the process is then called reforming [12] including, steam methane reforming (SMR), auto thermal reforming (ATR), partial oxidation (POX), and others. Figure 3-1 illustrates different reforming methods with purification and some CO utilization pathways [12]. The most common industrial technologies are listed in the following paragraphs.

3.3.1 Steam Methane Reforming (SMR)

Steam methane reforming is a mature technology where methane from natural gas reacts with steam to form carbon monoxide and hydrogen (reaction 3.1). The reaction is endothermic, so high operating temperature is required (up to 850 °C) for the reaction to proceed and obtain the desirable conversion [13]. Subsequently, the water-gas shift reaction (WGS) shown in equation 3.2 follows to produce more hydrogen in the presence of metal catalyst [13] inside a multi-tubular fixed-bed reactors. The two mentioned reactions are thermodynamically equilibrium limited. To overcome this limitation, research is been conducted to deploy catalytic membrane reactors [14].

$$CH_4 + H_2O \leftrightarrow CO + 3H_2 \qquad \Delta H_{298} = 206 \frac{kJ}{mol} \tag{3.1}$$

$$CO + H_2O \leftrightarrow CO_2 + H_2 \qquad \Delta H_{298} = -41 \frac{kJ}{mol} \tag{3.2}$$

$$CH_4 + 2H_2O \leftrightarrow CO_2 + 4H_2 \qquad \Delta H_{298} = 165 \frac{kJ}{mol} \tag{3.3}$$

3.3.2 Partial Oxidation (POX)

In this process, syngas is produced from hydrocarbon feedstock such as methane via partial oxidation with limited amount of oxygen (O_2) over a catalyst and mainly CO and H_2 are produced (equation 3.4). N_2 is also produced if air is used instead of pure oxygen. Similar to SMR process, the water-gas shift reaction follows to produce more H_2.

The POX is an exothermic reaction, thus it is less energy intensive compared to SMR process [15]. The methane conversion is over 90% per pass, with high selectivity to carbon monoxide [16], [17]

$$CH_4 + \frac{1}{2}\, O_2 \leftrightarrow\ CO + 2H_2 \qquad \Delta H_{298} = -36 \frac{kJ}{mol} \tag{3.4}$$

3.3.3 Auto-thermal Reforming (ATR)

This process was developed in late 1950's by Haldor Topsoe for ammonia and methanol synthesis [18]. It is a combination of steam reforming reaction and partial oxidation process in a single reactor. The heat generated from the exothermic partial oxidation is used to provide energy needed by the steam reforming reaction. Therefore, the overall process is adiabatic [19], no external input of energy is required to complete the process [20], [21].

The main advantage of ATR is in its compact design as the reactions happen in a single compact vessel reducing capital and operating cost in addition to a reduced amount of energy required when compared to the aforementioned processes.

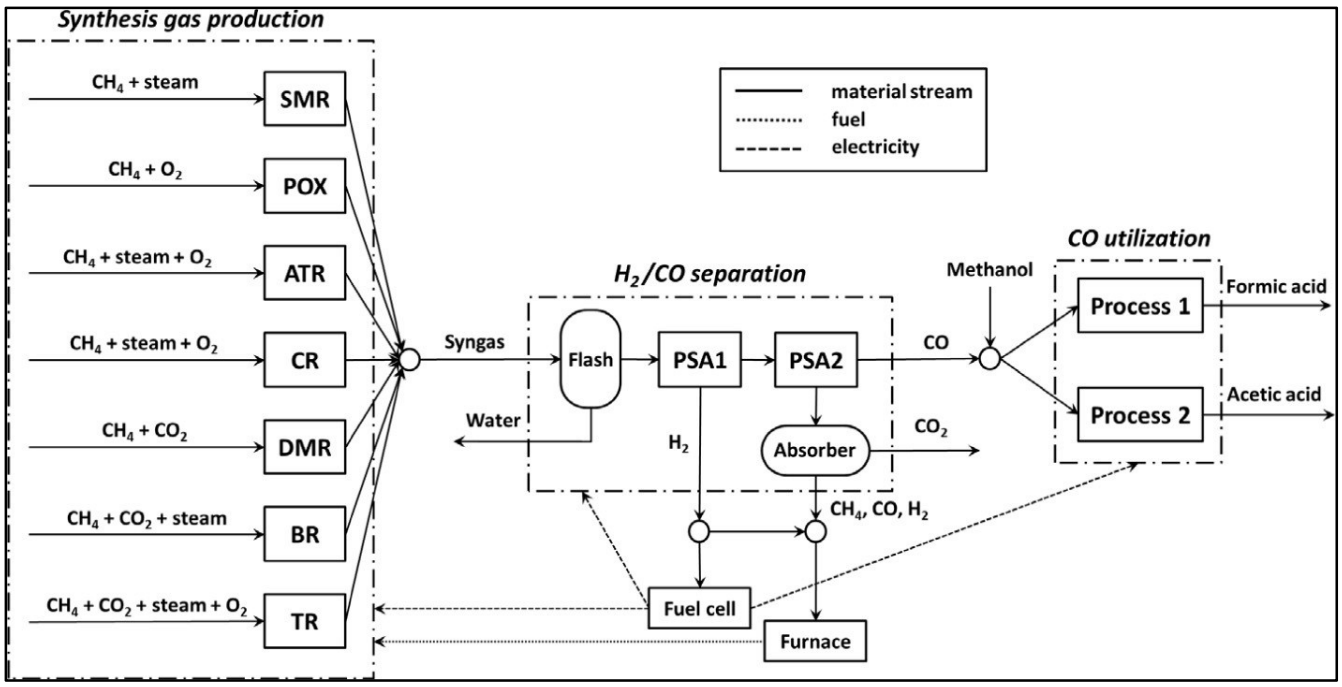

Figure 3-1. Synthesis gas production, separation and CO utilization [12]

3.4 CO gas separation

Gas separation plays an important role in industrial applications. It account for 40-60% of capital and operating cost [52]. Most chemical products go through separation and purification steps after their synthesis. Therefore, the development of an efficient and cost effective separation technology is necessary. For CO separation from gaseous mixtures, different separation processes are employed in industry. In the following sections, a review of the most commonly used technologies employed for CO purification are summarized.

3.4.1 Cryogenic distillation

Cryogenic distillation is a mature technology with widespread applications in industry. It involves cooling a gas mixture to create a phase change of different gas components, then follows with separation based on different boiling points and volatilities of the components [22]. This technology is the oldest separation method used for CO/H_2 separation in syngas [1].

To separate CO from H_2 in syngas using cryogenic distillation, two main processes are involved: partial condensation and methane wash [1]. Selecting one process among the other depends on different specifications, including the syngas quality, CO/H_2 ratio, methane concentration, purity level required and the feed gas pressure. For both processes, H_2O and CO_2 are removed first through compression and drying before applying a cryogenic temperature. In the partial condensation process, the syngas is liquefied in many cooling steps to liquefy both CO and CH_4, and obtain a high purity H_2 (98%) [1]. The CO, CH_4 and H_2 are flashed and distilled to produce high purity gas of CO. In the methane wash process, liquid methane is used to absorb CO gas producing high purity hydrogen gas. The CO and CH_4 are separated in a splitter to achieve high CO purity. The methane wash cycle is more suitable if the feed gas is at low pressure, with low H_2/CO ratio and if high H_2 gas purity is required.

Cryogenic distillation is mostly used for large scale separations. The technology drawback is the intensive energy demand with expensive operating cost [23], [24]. If N_2 exist in the gas mixture, cryogenic separation becomes less efficient and very difficult as N_2 and CO have similar boiling points which are -195.79 °C and -191.5 °C respectively.

3.4.2 COSORB Process

COSORB process was developed and commercialized by Tenneco in 1976 [25][26] to selectively recover high purity CO from a gaseous mixture. The process is based on CO complexation and de-complexation with a solvent of cuprous aluminum chloride ($CuAlCl_4$) dissolved in an aromatic hydrocarbon solvent such as toluene or benzene. CO molecules react with Cu (I) ions in Cosorb solution. The CO rich solvent is then heated in a stripper to remove the aromatic solvent and recover high purity CO. The COSORB process diagram as was developed by Kinetics Technology International (KTI) is presented in Figure 3-2. [25]

Prior to CO purification in COSORB, a pre-treatment of the feed gas is required to remove the existing H_2O, NH_3, H_2S, SO_2 and oxides as they react with $CuAlCl_4$ complex [1].

To overcome some encountered problems, KTI, the COSORB technology owner and licensor upgraded the process to COSORB II^{TM}. The process upgrading included the implementation of

more extensive pre-treatment to remove undesirable components and effective management of solid waste build up generated from the undesirable side reactions.

COPure^{SM} process was developed by R.C. Costello & Associates [27] as the latest innovation of absorption process developed to improve COSORB II, with additional gas pre-treatment and waste management.

COSORB process has the advantage of producing high purity CO (99%). In case of N_2 rich gas mixture, COSORB is more advantageous compared to the cryogenic process. The drawbacks of COSORB process is related to solvent stability and degradation, reactivity of $CuAlCl_4$ with impurities such as H_2O and H_2S [24], in addition to Cu(I) ions' instability, which reacts to form C(II) or Cu element.

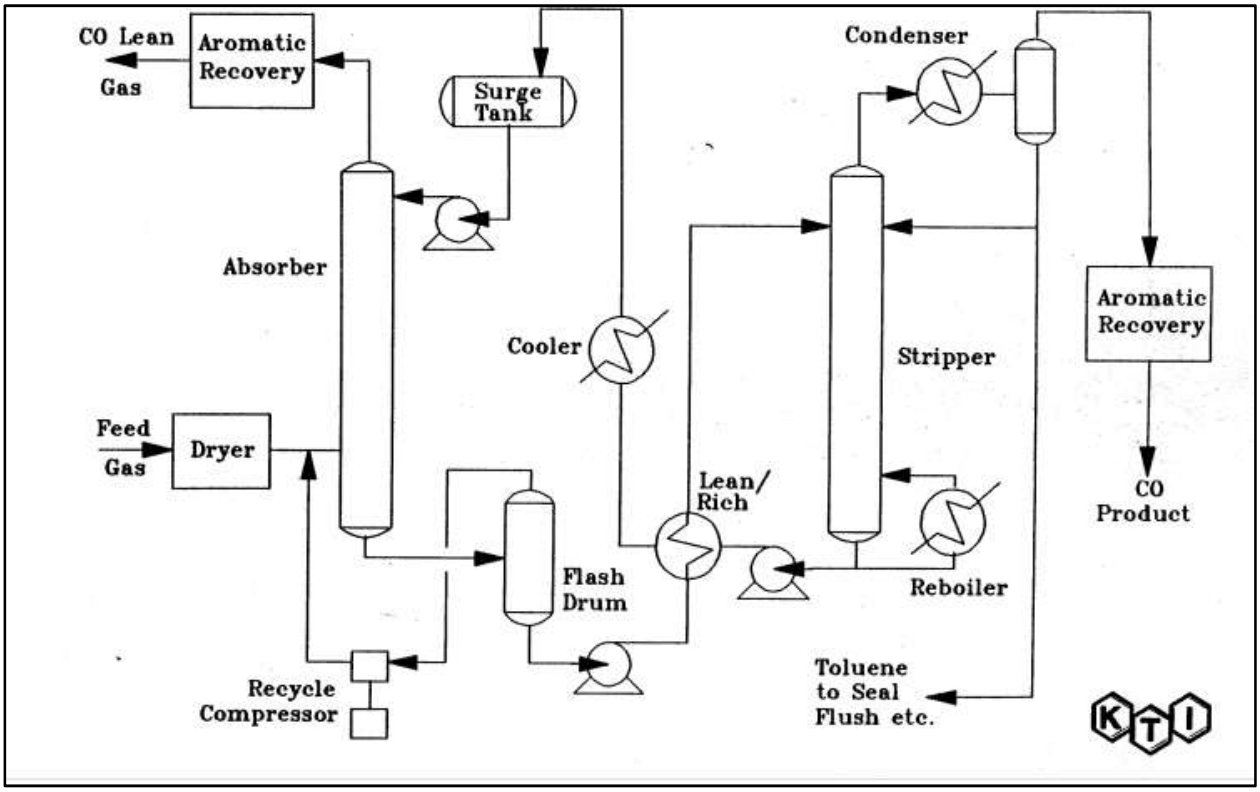

Figure 3-2. COSORB process diagram [25]

3.4.3 Ionic Liquids

The interest on ionic liquids (ILs) as solvent for CO recovery as an alternative clean solvent emerge on their physical and chemical properties. ILs are non volatile with low vapor pressure, high thermal and chemical stability, in addition to their tunable characteristic[28]. Therefore, ILs were implemented in different industrial applications [29]. e.g. electrolyte [30] and biomass processing [31]. Ionic liquid can be modified by incorporation of functional groups to the structure, thus providing better performance with specific selectivity and affinity to certain components. In the case of CO recovery, the CO ability to form π complexation with metal ions in ionic liquids make them very attractive solvents. Different Ils were investigated in literature for CO separation from gaseous mixtures. For example Zarca et al. [32] studied the mass transfer rate of CO into 1-hexyl-3-methylimidazolium chlorocuprate (I) ionic liquid. Other researches studied CO adsorption in different IL's, e.g. CO and H_2 in 1-n-butyl-3-methylimidazolium methyl sulfate ([bmim][CH_3SO_4]) [33], CO and CO_2 in 1-hexyl-3-methylimidazolium bis(trifluoromethylsulfonyl)imide ([hmim][Tf_2N]) [34], and others [35], [36].

Lower volatility, better thermal stability, less degradation, low corrosive nature and low energy and costs needed for regeneration are the advantages of ILs that make the private sector and government want further investigation into these new solvents.

3.4.4 Membrane Separation

Membrane separation is an emerging and very promising technology for CO purification. The separation is based on difference in permeability of different components of a mixture under a given driving force e.g. difference in pressure, concentration or electric potential.

The technology is advantageous over the traditional separation processes due to process simplicity and effectiveness with competitive cost [1], [37]–[39] Nevertheless, most applications involving CO separation by membrane are applied in H_2 purification from CO or for adjusting H_2/CO ratio in syngas [40] and studies on CO purification using membranes are uncommon in literature [41]. During the past decades, several papers were published regarding H_2/CO separation, including the use of polyamide composite membranes [42], [43], matrimid membranes [44], [45] and hollow

fiber membranes [46], [47]. The CO purification by membranes is still in its early stage and further research is required for material development and testing.

Supported liquid membrane [48] is an alternative approach that is been investigated for CO purification. Supported ionic liquid membranes (SILMs) where ionic liquid is immobilized within the pores of the support membrane are reported in literature for CO separation. David et al. [4] study focused on the CO adsorption on 1-hexyl-3-methyl-imidazolium chlorocuprate prepared from copper (I) chloride (CuCl) mixed with 1-hexyl-3-methylimidazolium chloride ([hmim][Cl]). It was observed that the CO adsorption capacity improved after addition of CuCl to [hmim][Cl] solvent due to π complexation between CO with Cu (I) ions. The complexation reaction mostly took place at pressure range up to to 10 bar and almost complete at 20 bar. The highest ideal separation factor for CO over N_2 was 24. Zarka et al. [49], [50] also looked at CO/N_2 separation by poly(ionic liquid)-ionic liquid composite membranes and [hmim][Cl] SILM with incorporation of copper salt. A new study by Feng et al. [51] studied 1-ethyl-3-methylimidazolium tetrafluoroborate ([emim][BF4]) SILM with $AgBF_4$ for CO/N_2 separation. $AgBF_4$ is introduced to form π complex with CO molecules and therefore improved the CO/N_2 selectivity. Similar to solid membranes, liquid membrane study results are promising but their application in higher scale is not been considered as the technology readiness is still in development stage.

3.5 Adsorption Separation

Adsorption separation process is a well-established technology for gas separation and purification. It has low energy consumption, low operating cost [52] and environmentally it is considered safer and cleaner when compared to other separation processes. The major contributor for accelerating the development of adsorption processes is the development of innovative porous materials for various applications. The selection of the appropriate material depends on the application, including gas composition, operating conditions, degree of selectivity and separation factor. For example, the separation of CO from syngas requires adsorbents that preferentially have large adsorption capacity for CO with high CO/H_2 selectivity. To maximize the adsorption capacity, the solid sorbent must have a high porosity, which is considered as the most important characteristic of the adsorbent materials [53]. It is represented by large specific surface area. Other physical characteristics of adsorbents include pore size distribution, pore volume and thermal stability. The growth of gas adsorption processes in industry resulted on development of new sustainable porous

materials for gas separation. Common materials include, activated carbons [54], zeolites [55], alumina silica and metal organic frameworks (MOFs) [56]

For CO purification, most of the commercially available adsorbent exhibit low adsorption capacity and selectivity toward CO, therefore, further chemical modification is required to improve the CO uptake and enhance the selectivity toward CO. The most prominent technique used is the incorporation of metallic salt to the adsorbent through different dispersion methods. The common metal salt is copper chloride (CuCl) where CO form a π complexation bond with Cu (I) ions. The π complexation between CO and Cu (I) ions is stronger than Van der Waals forces, but the bonds are weak, therefore a simple engineering process is used for adsorbent regeneration.

3.6 Adsorbent modification methods

π complexation adsorbents have had great attention for CO separation. The π complexation bond formed between metal ions and CO molecules is strong leading to high CO adsorption capacity and selectivity. In literature, different approaches were developed to modify the porous materials by incorporation of metallic salts into the pores of the porous support. The most common techniques include monolayer or sub-monolayer dispersion method, also called facile dispersion method and ion exchange method.

3.6.1 π-Complexation Sorbents

The interaction between the adsorbent and the adsorbate depends on the characteristics of the adsorbents and/or the adsorbates. The most known interaction include the electrostatic interaction e.g. van der Waals forces, acid-base interaction, hydrogen bonding, π- π interaction, and π complexation etc. [57]. π complexation interaction occurs between some metal cations and π electron clouds of the chemicals [58]. The d-block transition metals (27 elements) [59] and their ions from a σ bonds with a gas or solute molecule. Moreover, the d atomic orbital of the metal back-donate electron to the vacant π^* anti-bonding orbitals of the adsorbate molecule. The π complexation interaction draw more attention in adsorption/separation process compared to other interactions; the bonds formed between the adsorbent and adsorbate is stronger than Van Der Waals force thus more effective [57], with higher adsorption selectivity and higher adsorption capacity [60]. Furthermore, the binding force is not strong as in chemisorption. It is weak enough

thus a simple change in pressure or temperature can lead to adsorbent regeneration so that applying pressure swing adsorption (PSA) or temperature swing adsorption (TSA) is suitable.

π complexing adsorbents were developed using various porous materials as support, preferably the ones with large surface area, such as activated carbons, zeolites, MOFs, mesoporous materials incorporated with transition metal ions. They were successfully used in various gas separation/purification applications including olefin/paraffin separations and removal of sulfur and nitrogen compounds using different metal ions such as Cu(I), Ag(I), Pd(II) and Ni(II) [57], with Cu(I) ions are the most common one. The efficiency of π complexation sorbents depends on different factors, including the amount of the π electrons of the adsorbate and the ability of these π electrons to be donated to the vacant s-orbital of the cation, the amount of d-orbital electron of the metal ion and their capability to be donated to the adsorbate molecules and the emptiness of the outermost s- orbital of the metal cation [59]

The incorporation of metal ions into the porous support materials is performed by means of different techniques as shown in Figure 3-3. Monolayer dispersion and ion exchange are the main methods used. A brief description of each method is discussed in the following paragraphs.

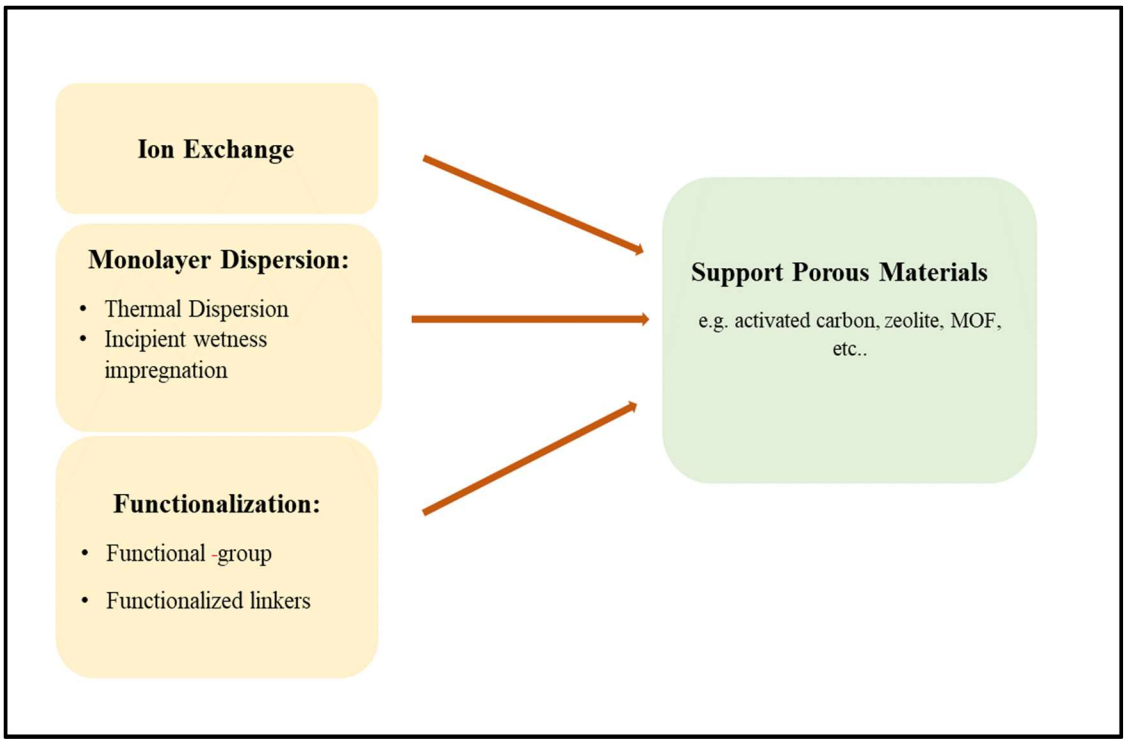

Figure 3-3. Different methods for porous material modification for π-complexing adsorbents

3.6.2 Monolayer dispersion

The principle of monolayer dispersion involves spontaneous dispersion of active components into the surface of a porous support material in a monolayer or sub-monolayer form. The method has been used for the preparation and design of heterogeneous catalyst [61] as well as in adsorbent modifications and material science. Monolayer dispersion has widespread application in sorbents development for separation and purification of different adsorbates. Dai and co-workers [62] studied the adsorption of dibenzothiophene (DBT) from n-octane using a modified MOF-5 material by addition of CuCl through a spontaneous monolayer dispersion. For selective olefin /paraffin separation, a number of studies used π-complexation sorbents by monolayer dispersion [63]–[65]; For CO separation, monolayer dispersion was extensively employed to improve CO adsorption capacity and selectivity over other adsorbates. Summary of some studies from literature are presented in Tables 3-1, 3-2 and 3-3 for different adsorbents.

The first evidence of monolayer dispersion was achieved by Russell and Stokes (1946) using MoO3 on γ -Al2O3 [59]. Xie and Tang [66], [67] did an extensive research on the subject, and had demonstrated the effectiveness of the methodology in various support materials including activated carbons, zeolites, silica gel and γ -Al2O3 [59]. To demonstrate the monolayer dispersion, different analytical techniques were employed, the most used one is X-Ray Powder Diffraction (XRD), and other analysis techniques include Extended X-ray absorption fine structure (EXAFS), X-ray photoelectron spectroscopy (XPS) and Transmission Electron Microscopy (TEM).

There are two approaches for the preparation of monolayer dispersion sorbents, the thermal monolayer dispersion and incipient wetness impregnation [59]. In thermal monolayer dispersion, the porous material in powder form is well mixed with a known amount of metal salt or oxide permitting monolayer surface coverage of the support material, before heating it at a temperature between Tamman temperature and melting point of the salt. The incipient wetness impregnation is the most common technique used in industry for synthesis of heterogeneous catalyst. In this method, the metal salt precursor is dissolved in an aqueous solution before adding the support substrate where the solution permeate into the pores[68]. Different solvents can be used such as hydrochloric acid, acetonitrile, toluene and water if the salt is soluble in water. The product is dried to remove the liquid solvent, calcined and further treated through activation treatments.

The thermal monolayer dispersion seems to be an easy method for π sorbents preparation, but its application is still in laboratory scale. On the other side, the incipient wetness impregnation is the most applied technique in industry.

3.6.3 Ion exchange

Ion exchange capability is an important property of most zeolites and some polymeric resins. It has been widely employed in adsorption process for tailoring the material structure to reach specific performance such as selectivity and adsorption capacity. The introduction of metal ions into zeolite and resins through ion exchange has been well studied in literature [69], [70].

For zeolites, the ion exchange occurs between the cation from the porous zeolite and the ions of aqueous solution as shown in reaction (3.5) considering a uni-univalent ion exchange [59]

$$A^{+}S + B^{+}Z \leftrightarrow A^{+}Z + B^{+}S \quad (3.5)$$

with S, Z denote the solution and zeolite, respectively. A and B are cations.

For CO adsorption, Cu(I) ions incorporation into zeolite materials through ion exchange to form π complexation bond with CO molecules were well studied in literature and had achieved much better results than other metallic ions. Cu (I) is insoluble in the water and get oxidized to cupric compounds in solution. Thus the ion exchange with Cu (I) ions is performed with Cu (II) ions followed by its reduction to Cu (I) under specific conditions. Cu (I) is either reduced under high temperature using a reducing gas such as CO or H_2 [71] or through another auto-reduction where an inert gas is employed.

3.7 Porous adsorbents

As it was mentioned above, the challenge with CO adsorption and separation is finding sorbents materials with high affinity and selectivity toward CO. To achieve that, sorbent modification through incorporation of metal site had proved to enhance the modified sorbent's affinity and reach higher adsorption capacity and selectivity toward CO. In this review, we will focus on three main adsorbents studied in literature, with a summary of each adsorbent performance presented in tables 3-1, 3-2 and 3-3 grouped by adsorbent type.

3.7.1 Activated carbons

Activated carbon is one of the oldest adsorbents widely used in industry. It is characterized by its low cost, large surface area, good stability and low energy required for regeneration. Many researches have accomplished CO purification by using either a commercialized activated carbon or a modified one by introduction of metallic salts to improve CO adsorption and selectivity. Cu (I) ions were more commonly applied compared to other metallic ions due to its low cost and abundancy [3], [72]. Ag(I) and Pd(II) are among other metallic ions used to form π complexes with the CO molecules. Cu(I) is either obtained from Cu(I) containing salts such as CuCl, CuBr, CuF and CuI or from the reduction of Cu(II) containing salts (e.g.$CuCl_2$ or a mixture of Cu(II) salts such as CuCl (II) and $Cu(HCOO)_2$. Cu(II) salt is first dispersed through auto-dispersion technique or wetness impregnation followed by reduction into Cu(I) at high temperature. The use of Cu(II) has the advantage of being more stable compared to Cu(I) which oxidize quickly when exposed to air. Furthermore, CuCl(II) salts are less expensive.

Several Cu (I) based activated carbon adsorbents are studied for CO/CO_2 separation as summarized in Table 3-1. The studies focussed on improving CO adsorption capacity and selectivity by incorporation of transition metals and studying different factor that impact it, such as type of metallic ions, ion reduction conditions, the amount of metallic ion loaded to achieve optimum loading value. Hirai et al. [68], [73]–[76] tried incorporation of three different copper (I) halides on activated carbon; CuCl, CuBr and CuI. The capacity of CO adsorbed was in the following order CuCl>CuBr>CuI. Their work also investigated different solvents for copper impregnation. The activated carbon impregnated with CuCl using aqueous hydrochloric acid solution displayed larger CO adsorption capacity compared to using water, acetonitrile, and toluene.

Xue et al. [77] also looked at CO/CO_2 separation using Cu-based activate carbon. An equimolar mixture of $CuCl_2$ and Cu $(HCOO)_2$ was used for adsorbent modification through auto-dispersion method and heating under vacuum for copper (II) reduction to copper (I). The results showed an improved CO adsorption capacity and CO/CO_2 selectivity of 2.6 for Cu-based adsorbents with optimum CO uptake of 4 mmol/g.

Overall, the results from literature showed an improved uptake and affinity of CO compared to CO_2 and other gases in a modified activated carbon. For CO adsorption kinetics, there is not much data presented in literature except very few ones. The summary of results from literature studies are presented in Table 3-1.

Table 3-1. Summary of CO and CO_2 adsorption data on activated carbon in the literature.

Adsorbents		Loading method	T	P	Adsorption capacity		CO/CO_2 selectivity	BET surface area	Refs
Metallic salt	Support		K	kPa	mmol/g			m^2/g	
					CO	CO_2			
$CuCl_2+Cu(CH_3COO)_2$	AC	Impregnation	298	100	1.6				[78]
CuCl	AC	Impregnation	298	100	2.3	2.02	1.13	652	[78]
	AC		298	100	0.2			1170	[78]
CuCl	AC	Impregnation using HCl	323		1.24				[79]
CuBr	AC	Impregnation using HCl	323	100	0.49				[79]
$PdCl_2$	AC	Impregnation using HCl	323	100	2.03				[79]
	AC		303		0.25			1784	[80]
$CuCl_2$	AC	Solid state dispersion	303	100	2.95	0.47	6.28	478	[80]
CuCl	AC	Solid-state auto dispersion	298	100	2.3			472	[81]
CuCl	AC	Impregnation using HCl	293	100	1.24			744	[76]
	AC		293	100	0.33			1044	[76]
CuBr	AC	Impregnation	293	100	0.95				[76]
CuCl	AC	Impregnation	293	100	0.17				[76]
	AC		303	100	0.72	2.05	0.35	480.8	[82]
	AC		303	100	0.45	1.98	0.2	481	[82]
	BPL 4X10		298	100	0.38	1.8	0.21	859	[83]

$CuCl_2$ +$Cu(HCOO)_2$	AC		Solid-state auto dispersion	298	100	1.8	25.2	2.6	505	[77]
	AC			298	100	0.2			1082	[77]
	D55/2 PSA	C		293	700	1.85			765.4	[11]
$CuCl_2$	AC		Solid-state dispersion	303	100	2.5	0.4			[84]
	AC			303	100	0.7	2	0.35		[82]
	AC			298	100	0.45			1400	[81]
CuCl	AC		Solid-state auto dispersion			2.3			472	[81]

3.7.2 Zeolites

Zeolite materials are commonly used as selective adsorbents by ion exchange, or as catalysts. For adsorption separation systems and gas purification, zeolites are widely used due to their large surface area, low cost, ion exchange property employed to tailor the structure and achieve desired performances. They are already used in many industrial processes such as water and wastewater treatment, as catalysts for chemical reactions such as cracking, isomerisation and hydrocarbon synthesis. For adsorption separations, zeolites have been investigated in many processes such as CO_2 separation [85], [86] and air separation [87].

For CO purification, zeolite sorbents can selectively adsorb CO from gaseous mixtures through two different approaches; the ion exchange, an intrinsic property of zeolite [88] or by incorporation of metallic salts through auto dispersion or impregnation method to improve CO uptake as described before. Sethia et al. [89] study focused on zeolite-X exchanged with alkaline earth metal ions; magnesium (Mg^{2+}), calcium (Ca^{2+}), strontium (Sr^{2+}) and barium (Ba^{2+}) cations. The results showed an increase in CO adsorption in the following order Sr_NaX.> Ca_NaX> Ba_NaX> NaX> Mg_NaX. The Mg-exchanged zeolite showed lower CO adsorption due to Mg^{2+} migration inside β-cages to minimize energy and therefore blocking interaction with CO molecules. The increase in CO adsorption in Ca^{2+}, Sr^{2+} and Ba^{2+} was explained by high charge density of the cations. Alkali ion metal exchanged zeolite showed also an improvement in CO adsorption compared to the original zeolite [90], [91]. Furthermore, the highest CO adsorption capacity was observed in lithium-exchanged zeolite-X due to strong electrostatic interaction between smaller Li cation and CO molecules. The CO uptake decreased moving from lithium ions toward heavier metal as the cation radius increases. Gao et al.[92] used monolayer dispersion method for $CuCl_2$ incorporation in zeolite Y with $CuCl_2$ reduction to CuCl at high temperature under CO and N_2 atmosphere. The activation under CO is more effective than that in N_2 environment due to incomplete reduction of Cu^{2+} to Cu^{+} in N_2 environment [93]. Xie et al. [66], [94] studied CO/CO_2 separation using CuCl as a precursor in zeolite with monolayer dispersion method. A summary of other studies is summarized in Table 3-2.

Table 3-2. Summary of CO and CO_2 adsorption data on zeolites in the literature.

Adsorbents		loading method	T	P	Adsoption capacity		CO/CO_2 Selectivity	BET surface area	Refs
Metallic salt	Support		K	kPa	mmol/g			m^2/g	
					CO	CO_2			
	zeolite 5A		298	100	1.2				[95]
	zeolite 13X		298	100	0.5				[95]
CuCl	NaY	monolayer dispersion	303	700	2.4	1.3	1.84		[94]
	NaY		303	700	0.5	3.27			[94]
CuCl	13X	monolayer dispersion	303	700	2.2	1.39			[94]
	13X		303	700	0.5	2.8			[94]
	13X		298	100	0.7	4	0.175	392	[83]
	Zeolite A		293	700	2.5			670	[11]
	Zeolite B		293	700	2.75			670	[11]
	KÖSTROLITH 5ABF		293	700	2.75			680	[11]
	Li-SSZ-13		298	100	0.28	2.53	0.11		[91]
	Na-SSZ-13		298	100	0.36	2.93	0.12		[91]
	K-SSZ-13		298	100	0.2	1.57	0.07		[91]
	Cs-SSZ-13		298	100	0.25	2.27	0.11		[91]

	zeolite		303	100	0.9	3.84		434	[96]
	Zeolite HY	monolayer dispersion	303	100	2.67	0.96	2.83	329	[80]
	Zeolite Y		303	100	0.23			694	[80]
	ZSM-5		303	1000	1	2.1			[97]
$CuCl_2$ + $Cu(HCOO)_2$	zeolite Y	impregnation			2.2				[78]
	Na zeolite X		303	100	1.11			721	[90]
	Li zeolite X		303	100	1.42			759	[90]
	K zeolite X		303	100	0.61			537	[90]
	Rb zeolite X		303	100	0.43			550	[90]
	Cs zeolite X		303	100	0.37			423	[90]
	Mg(70)NaX		303	100	0.8			711	[89]
	Ca(95)NaX				1.91			704	[89]
	Sr(95)NaX				1.9			622	[89]
	Ba(85)NaX				1.26			565	[89]

In general, zeolites with ion exchange or modified with metal salts exhibited larger CO uptakes compared to results obtained with activated carbon as shown from the data in Tables 3-1 and 3-2.

3.7.3 Metal Organic Frameworks

Metal organic frameworks (MOFs) have generated great interest as emerging materials for gas and vapor sorption. Since their first development, a lot have been synthesised as seen in Figure 3-4 [98].

MOFs consist of inorganic metal ions coordinated to organic linker molecules to form a repeating cage-like networked structure. In contrast to other porous materials, MOFs exhibit unique structural diversity, uniform pore structure, tunable pore size, flexibility in design, dimension and chemical functionality in addition to their very high surface area. These unique properties made these materials very promising for gas storage, separation, and purification [56], [99], [100].

MOF materials were investigated [101] for various separations, including carbon dioxide capture [102]–[105], separation of alkanes [106] and, olefin/paraffin separation [107]. They have been the subject of many research studies for CO purification from different gas mixtures. Their large surface area and tunability feature made them very promising for CO recovery.

For a number of MOFs containing unsaturated sites, it was reported that these metal sites are able to bind with CO molecules, such as in MOF-74, HKUST-1, MIL-1. MIL-100 and DUT-82 [108].

Bloch et al. [109] tested six MOF-74 coordinated to unsaturated metals (Mg, Mn, Fe, Co, Ni and Zn). The results showed CO reversibly binding to the unsaturated metal cations coated on the surface with the highest CO capacity of 6.04 mmol/h at 1.2 bar for Fe-MOF-74. Iron displays the strongest π back-bonding contribution. Another route for CO separation in MOF is via metal impregnation or ligand functionalization. For metal impregnation, similar to activated carbon material, copper (I) is introduced into the pores of the materials to enhance the interaction with CO thus improving the adsorption capacity. As an example, for CO/CO_2 separation, Kim et al.[110] used MIL-100(Fe) loaded Cu (I) ions into the pores through facile dispersion method without any external reducing agent for reduction of Cu (II) to Cu(I) ions. The presence of Fe (II) unsaturated sites attributed to Cu (II) reduction was proposed by the following mechanism:

$$\text{Fe (II)} + \text{Cu (II)Cl} \rightarrow \text{Fe (III)-Cl} + \text{Cu(I)Cl} \qquad 3.6$$

Peng et al. [111] tested similar MOF material for CO/N_2 gas mixture separation. For copper (II) introduction, samples were prepared by wetness impregnation followed by reduction of Cu(II) to Cu(I) under vacuum at elevated temperature. CO uptake and CO/N_2 selectivity improved 112 times in Cu(I) @MIL-100(Fe) compared to the parent material which is mainly ascribed to strong π complexation interaction between the adsorbent and the CO molecules. The other approach employed for improving CO adsorption is through ligand modification. Regufe et al. [112] used this technique in MIL-125 for syngas purification. The organic ligand was functionalized with amino group. The CO_2 recovery had improved in PSA system which makes this more suitable for syngas purification from CO_2 gas. The summary of results from literature is provided in Table 3.3.

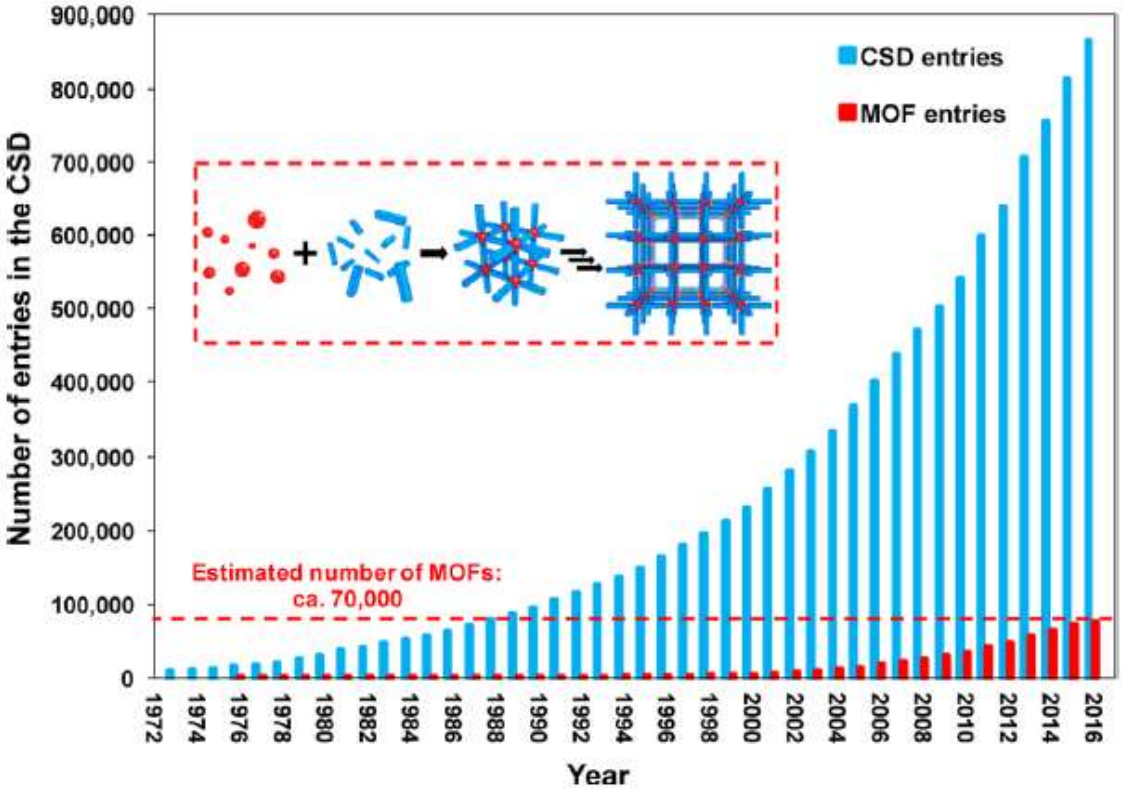

Figure 3-4. MOF Cambridge Structural Database entries since 1972 [98].

Table 3.3. The summary of CO and CO_2 adsorption data on MOF materials from literature.

Adsorbents		Loading method	T	P	Adsorption capacity		CO/CO_2 Selectivity	BET surface area	Refs
Metallic salt/solvent	Support		K	kPa	mmol/g			m^2/g	
					CO	CO_2			
$CuCl_2$ and $Cu(HCO_2)_2$)	Ni-MOF-74	Impregnation	298	100	3.5		3	1047	[108]
$CuCl_2$ and $Cu(HCO_2)_2$)	MIL-100(Fe)	wetness impregnation	298	100	2.78			762	[111]
	MIL-100(Fe)		298	100	0.38			2042	[111]
	MOF-74-Mg		298	120	4.58				[109]
	MOF-74-Mn		298	120	3.24				[109]
	MOF-74-Fe			120	6.04				[109]
	MOF-74-Co			120	5.95				[109]
	MOF-74-Ni			120	5.79				[109]
	MOF-74-Zn			120	1.95				[109]
	MOF-5		298	100	0.15			2449	[95]
	MOF-177		298	100	0.03			3275	[95]
	MIL-101(Cr)(powder)		288	113	1.13	3.8	0.30		[113]
	MIL-101(Cr)(granule)		288	113	0.66	2.6	0.25		[113]
	DUT-82		298	100	2.11			780	[114]
	Cu-BTC (or HKUST-1)		295	100	1.45	26		1663	[115]

	Cr-BDC (or MIL-101)		295	100	0.9	32		2674	[115]
	MIL-101-Cr		298	100	1.01			3788.3	[116]
Cosorb solution($CuAlCl_4$)	MIL-101-Cr	Impregnation	298	100	2.26			2390.7	[116]
	Cu-BTC (or HKUST-1)		298	100	1.2	4.5	0.27		[117]
	UTSA-16 extrudates		298	100	0.23	3.3		805	[118]
	MOF-5		298	100	0.17	0.76	0.22		[119]
NO_2-$(OC_3H_5)2(OC_7H_7)_2$	MOF-5	Incorporation of functional group	298	100	0.21	1.6	0.13		[119]
$CuCl_2$ and $Cu(HCO_2)_2$)	MIL-100(Fe)	wetness impregnation	303	100	3.52	0.49	7.2	898	[120]
	MIL-53(Al)		303	100	0.18	26.2	0.13	1235	[121]
	La(BTN)DMF		273	100	0.15	1.3	0.12		[122]
	Fe-BTTri		298	30	2.9	1.8	1.61	1630	[123]
	ZIF-100		298	100	0.12	0.88	0.06		[124]
	ZIF-95		298	100	0.12	0.8	0.09		[124]
	MAMS-1		113	100	0.6				[125]

MOFs have great potential for CO purification and gas separation in general due to their structural design, tunability, and extraordinary large surface area. However, there are some barriers that still need investigation and improvement. Material stability; the main shortcoming of MOF materials is their chemical and physical stability [126]. Material scale-up is another limitation. Most MOFs are synthesised and tested in laboratory scale. They must be tested in larger scales before commercialization.

3.8 Conclusions and Outlook

Carbon monoxide is produced through various processes, the application of one against the other depends on many factors and technology readiness for large scale applications. Cryogenic distillation is a mature technology with potential applications in large scale processes. The partial condensation cryogenic process is more suitable for syngas with high ratio of CO/H_2, high inlet pressure and lower H_2 product purity. However COSORB process has been more applicable to obtain high CO purity and in the absence of gases that may react with the COSORB solvent such as H_2O, NH_3, H_2S. Membrane separation is an emerging technology with a lot of potential in the future when it is fully developed. On the other hand, adsorption separation is an alternative proven technology for CO separation and purification. Various porous materials has been developed and studied for CO recovery, including activated carbon, zeolite and metal organic frameworks material. However, studies showed that these materials exhibit low selectivity to CO and low adsorption capacity compared to other components such as CO_2. Therefore these adsorbents' modification with incorporation of metallic salts such as copper (I) chloride has been successfully applied. The ion exchange capability in zeolite with metal ions appears to provide better results than the Cu-based activated carbon. MOF materials are the most promising adsorbents for CO purification ascribed to their tunability and modularity resulting in a wide variety of MOFs. The highest CO uptake in MOF-74 was 6.04 mmol/g at 1.2 bar and 298 K in which CO coordinate to the divalent metal cations Fe^{2+}. Furthermore, the choice of suitable material for CO separation depend on gas mixture composition, purity required, etc. For instance, for the CO separation from CO_2 gas mixture, Cu-based boehmite composites provided the highest CO/CO_2 selectivity of 12.4 mmol/g at 100 kPa and 293 K [127].

Adsorption studies of CO separations using various sorbents had showed promising results. However, further investigation and testing of these materials to understand the kinetics, material

stability, behaviour in the presence of gaseous mixtures and possibility of upscaling will be the next step before taking the adsorption technology for CO purification to larger scale applications.

3.9 Nomenclature

AC Activated carbon

BET Brunauer–Emmett–Teller

DUT Dresden University of Technology

EXAFS Extended X-ray absorption fine structure

HKUST Hong Kong University of Science and Technology

MIL Matériaux de l′Institut Lavoisier

MOF Metal Organic Frameworks

POX Partial Oxidation

SILM Supported ionic liquid membranes

SMR Steam Methane Reforming

TEM Transmission Electron Microscopy

UTSA University of Texas at San Antonio

XPS X-ray photoelectron spectroscopy

XRD X-Ray Powder Diffraction

ZIF Zeolitic imidazolate frameworks

3.10 References

[1] N. N. Dutta and G. S. Patil, "Developments in CO separation," *Gas Sep. Purif.*, vol. 9, no. 4, pp. 277–283, 1995, doi: 10.1016/0950-4214(95)00011-Y.

[2] Y. Xie *et al.*, "Zeolite Modified by CuCl for Separating CO from Gas Mixtures Containing CO2," *Adsorpt. J. Int. Adsorpt. Soc.*, vol. 32, pp. 27–32, 1996.

[3] J. W. Yoon *et al.*, "Highly selective adsorption of CO over CO2 in a Cu(I)-chelated porous organic polymer," *J. Hazard. Mater.*, vol. 341, pp. 321–327, 2018, doi: 10.1016/j.jhazmat.2017.07.065.

[4] O. C. David, G. Zarca, D. Gorri, A. Urtiaga, and I. Ortiz, "On the improved absorption of carbon monoxide in the ionic liquid 1-hexyl-3-methylimidazolium chlorocuprate," *Sep. Purif. Technol.*, vol. 97, pp. 65–72, 2012, doi: 10.1016/j.seppur.2012.02.015.

[5] J. Hu, K. P. Brooks, J. D. Holladay, D. T. Howe, and T. M. Simon, "Catalyst development for microchannel reactors for martian in situ propellant production," *Catal. Today*, vol. 125, no. 1–2, pp. 103–110, Jul. 2007, doi: 10.1016/j.cattod.2007.01.067.

[6] T. Harlacher, M. Scholz, T. Melin, and M. Wessling, "Optimizing argon recovery: Membrane separation of carbon monoxide at high concentrations via the water gas shift," *Ind. Eng. Chem. Res.*, vol. 51, no. 38, pp. 12463–12470, 2012, doi: 10.1021/ie301485q.

[7] T. Harlacher, T. Melin, and M. Wessling, "Techno-economic Analysis of Membrane-Based Argon Recovery in a Silicon Carbide Process," pp. 1–7, 2013, doi: 10.1021/ie303330b.

[8] H. Oh *et al.*, "Experiment and Modeling of Adsorption of CO from Blast Furnace Gas onto CuCl/Boehmite," *Ind. Eng. Chem. Res.*, vol. 59, no. 26, pp. 12176–12185, 2020, doi: 10.1021/acs.iecr.0c01752.

[9] B. Singh, A. Saxena, A. K. Srivastava, and R. Vijayaraghavan, "Impregnated carbon based catalyst for protection against carbon monoxide gas," *Appl. Catal. B Environ.*, vol. 88, no. 3–4, pp. 257–262, 2009, doi: 10.1016/j.apcatb.2008.11.016.

[10] H. Igarashi, H. Uchida, M. Suzuki, Y. Sasaki, and M. Watanabe, "Removal of carbon monoxide from hydrogen-rich fuels by selective oxidation over platinum catalyst supported on zeolite," *Appl. Catal. A Gen.*, vol. 159, no. 1–2, pp. 159–169, 1997, doi: 10.1016/S0926-860X(97)00075-6.

[11] M. Bastos-Neto, A. Moeller, R. Staudt, J. Böhm, and R. Gläser, "Dynamic bed measurements of CO adsorption on microporous adsorbents at high pressures for hydrogen purification processes," *Sep. Purif. Technol.*, vol. 77, no. 2, pp. 251–260, 2011, doi: 10.1016/j.seppur.2010.12.015.

[12] J. D. Medrano-García, R. Ruiz-Femenia, and J. A. Caballero, "Multi-objective Optimization of a Carbon Dioxide Utilization Superstructure for the Synthesis of Formic and Acetic Acid," *Comput. Aided Chem. Eng.*, vol. 43, pp. 1419–1424, 2018, doi: 10.1016/B978-0-444-64235-6.50248-5.

[13] F. Gallucci, L. Paturzo, A. Famà, and A. Basile, "Experimental Study of the Methane Steam Reforming Reaction in a Dense Pd/ Ag Membrane Reactor," *Ind. Eng. Chem. Res.*, vol. 43, no. 4, pp. 928–933, 2004, doi: 10.1021/ie030485a.

[14] T. Tsuru, K. Yamaguchi, T. Yoshioka, and M. Asaeda, "Methane steam reforming by microporous catalytic membrane reactors," *AIChE J.*, vol. 50, no. 11, pp. 2794–2805, 2004, doi: 10.1002/aic.10215.

[15] C. Alvarez-Galvan *et al.*, "Partial oxidation of methane to syngas over nickel-based catalysts: Influence of support type, addition of rhodium, and preparation method," *Front. Chem.*, vol. 7, no. MAR, pp. 1–16, 2019, doi: 10.3389/fchem.2019.00104.

[16] S. S. Voutetakis, G. J. Tjatjopoulos, and I. A. Vasalos, "Catalytic Partial Oxidation of Membrane in a Spouted Bed Reactor. Design of a Pilot Plant and Optimization of Operating Conditions," vol. 119, pp. 807–812, 1998.

[17] A. A. Lemonidou, A. E. Stambouli, and G. J. Tjatjopoulos, "Partial oxidation ofmethane to synthesis gas over unpromoted and (0.1-0.5 wt%) Ni-promoted calcium aluminate catalysts," vol. 43, pp. 235–240, 1997.

[18] J. G. Speight, Ed., *Gasification of Unconventional Feedstocks*. Gulf Professional Publishing, 2014.

[19] P. Chiesa, "15 - Advanced technologies for syngas and hydrogen (H2) production from fossil-fuel feedstocks in power plants," *Adv. Power Plant Mater. Des. Technol.*, pp. 383–411, 2010, doi: 10.1533/9781845699468.3.383.

[20] H. F. Chang, W. J. Pai, Y. J. Chen, and W. H. Lin, "Autothermal reforming of methane for producing high-purity hydrogen in a Pd/Ag membrane reactor," *Int. J. Hydrogen Energy*, vol. 35, no. 23, pp. 12986–12992, 2010, doi: 10.1016/j.ijhydene.2010.04.060.

[21] T. P. Tiemersma, T. Kolkman, J. A. M. Kuipers, and M. van Sint Annaland, "A novel autothermal reactor concept for thermal coupling of the exothermic oxidative coupling and endothermic steam reforming of methane," *Chem. Eng. J.*, vol. 203, pp. 223–230, 2012, doi: 10.1016/j.cej.2012.07.021.

[22] J. Wilcox, "Carbon capture," *Carbon Capture*, pp. 1–323, 2012, doi: 10.1007/978-1-4614-2215-0.

[23] S. J. Bhadra and S. Farooq, "Separation of methane-nitrogen mixture by pressure swing adsorption for natural gas upgrading," *Ind. Eng. Chem. Res.*, vol. 50, no. 24, pp. 14030–14045, 2011, doi: 10.1021/ie201237x.

[24] J. A. Hogendoorn, W. P. M. van Swaaij, and G. F. Versteeg, "The absorption of carbon monoxide in COSORB solutions: absorption rate and capacity," *Chem. Eng. J. Biochem. Eng. J.*, vol. 59, no. 3, pp. 243–252, 1995, doi: 10.1016/0923-0467(94)02959-8.

[25] A. Keller and R. Schendel, "The use of COSORB II to recover high purity CO gas from a feed gas," *AIChE Summer Meet.*, pp. 1–9, 1988.

[26] D. J. Haese and D. G. Walker, *The COSORB Process*, 5th ed. 1974.

[27] " https://www.rccostello.com/copure.html. accessed Feb 05, 2021.

[28] K. R. Seddon, "Ionic Liquids for Clean Technology," *J. Chem. Technol. Biotechnol.*, vol. 68, no. 4, 1999.

[29] K. R. Seddon, “Ionic liquids: a taste of the future,” *Nat. Mater.*, vol. 2, no. 6, pp. 363–365, 2003, doi: 10.1038/nmat907.

[30] M. Galiński, A. Lewandowski, and I. Stepniak, “Ionic liquids as electrolytes,” *Electrochim. Acta*, vol. 51, pp. 5567–5580, 2006.

[31] S. S. Y. Tan and D. R. Macfarlane, “Ionic liquids in biomass processing,” *Top. Curr. Chem.*, vol. 290, pp. 311–339, 2009.

[32] G. Zarca, I. Ortiz, and A. Urtiaga, “Recovery of carbon monoxide from flue gases by reactive absorption in ionic liquid imidazolium chlorocuprate(I): Mass transfer coefficients,” *Chinese J. Chem. Eng.*, vol. 23, no. 5, pp. 769–774, 2015, doi: 10.1016/j.cjche.2014.06.040.

[33] J. Kumełan, Á. Pérez-Salado Kamps, D. Tuma, and G. Maurer, “Solubility of the single gases H2 and CO in the ionic liquid [bmim][CH3SO4],” *Fluid Phase Equilib.*, vol. 260, no. 1, pp. 3–8, 2007, doi: 10.1016/j.fluid.2006.06.010.

[34] J. Kumełan, D. Tuma, and G. Maurer, “[hmim][Tf 2 N] †,” *Engineering*, pp. 966–971, 2009.

[35] J. Jacquemin, M. F. Costa Gomes, P. Husson, and V. Majer, “Solubility of carbon dioxide, ethane, methane, oxygen, nitrogen, hydrogen, argon, and carbon monoxide in 1-butyl-3-methylimidazolium tetrafluoroborate between temperatures 283 K and 343 K and at pressures close to atmospheric,” *J. Chem. Thermodyn.*, vol. 38, no. 4, pp. 490–502, 2006, doi: 10.1016/j.jct.2005.07.002.

[36] Stephen E. Repper, A. Haynes, O. Logo, E. J. Ditzelb, and G. J. Sunley, “Infrared spectroscopic study of absorption and separation of CO using copper(i)-containing ionic liquids,” *Dalt. Trans.*, vol. 46, no. 7, pp. 2821–2828, 2017.

[37] M. Khanipour, A. Mirvakili, A. Bakhtyari, M. Farniaei, and M. R. Rahimpour, “Enhancement of synthesis gas and methanol production by flare gas recovery utilizing a membrane based separation process,” *Fuel Process. Technol.*, vol. 166, pp. 186–201, 2017, doi: 10.1016/j.fuproc.2017.06.008.

[38] G. Bernardo, T. Araújo, T. da Silva Lopes, J. Sousa, and A. Mendes, "Recent advances in membrane technologies for hydrogen purification," *Int. J. Hydrogen Energy*, vol. 45, no. 12, pp. 7313–7338, 2020, doi: 10.1016/j.ijhydene.2019.06.162.

[39] P. Bernardo, E. Drioli, and G. Golemme, "Membrane gas separation: A review/state of the art," *Ind. Eng. Chem. Res.*, vol. 48, no. 10, pp. 4638–4663, 2009, doi: 10.1021/ie8019032.

[40] R. W. Baker, "Future directions of membrane gas separation technology," *Ind. Eng. Chem. Res.*, vol. 41, no. 6, pp. 1393–1411, 2002, doi: 10.1021/ie0108088.

[41] G. Zarca, I. Ortiz, and A. Urtiaga, "Copper(I)-containing supported ionic liquid membranes for carbon monoxide/nitrogen separation," *J. Memb. Sci.*, vol. 438, pp. 38–45, 2013, doi: 10.1016/j.memsci.2013.03.025.

[42] J. Poudel, J. H. Choi, and S. C. Oh, "Process design characteristics of syngas (CO/H 2) separation using composite membrane," *Sustain.*, vol. 11, no. 3, 2019, doi: 10.3390/su11030703.

[43] M. Peer, M. Mahdeyarfar, and T. Mohammadi, "Investigation of syngas ratio adjustment using a polyimide membrane," *Chem. Eng. Process. Process Intensif.*, vol. 48, no. 3, pp. 755–761, 2009, doi: 10.1016/j.cep.2008.09.006.

[44] D. Berstad, P. Nekså, and G. A. Gjøvåg, "Low-temperature syngas separation and CO2 capture for enhanced efficiency of IGCC power plants," *Energy Procedia*, vol. 4, pp. 1260–1267, 2011, doi: 10.1016/j.egypro.2011.01.182.

[45] O. C. David, D. Gorri, A. Urtiaga, and I. Ortiz, "Mixed gas separation study for the hydrogen recovery from H2/CO/N2/CO2 post combustion mixtures using a Matrimid membrane," *J. Memb. Sci.*, vol. 378, no. 1–2, pp. 359–368, 2011, doi: 10.1016/j.memsci.2011.05.029.

[46] M. Peer, S. M. Kamali, M. Mahdeyarfar, and T. Mohammadi, "Separation of hydrogen from carbon monoxide using a hollow fiber polyimide membrane: Experimental and simulation," *Chem. Eng. Technol.*, vol. 30, no. 10, pp. 1418–1425, 2007, doi: 10.1002/ceat.200700173.

[47] O. C. David, D. Gorri, K. Nijmeijer, I. Ortiz, and A. Urtiaga, "Hydrogen separation from multicomponent gas mixtures containing CO, N 2 and CO 2 using Matrimid ® asymmetric hollow

fiber membranes," *J. Memb. Sci.*, vol. 419–420, pp. 49–56, 2012, doi: 10.1016/j.memsci.2012.06.038.

[48] M. F. San Román, E. Bringas, R. Ibañez, and I. Ortiz, "Liquid membrane technology: Fundamentals and review of its applications," *J. Chem. Technol. Biotechnol.*, vol. 85, no. 1, pp. 2–10, 2010, doi: 10.1002/jctb.2252.

[49] G. Zarca, W. J. Horne, I. Ortiz, A. Urtiaga, and J. Bara, "ionic liquid)-ionic liquid composite membranes containing a copper salt," *J. Memb. Sci.*, vol. 515, 2016, doi: 10.1016/j.memsci.2016.05.045.

[50] G. Zarca, I. Ortiz, and U. Ane, "Copper(I)-containing supported ionic liquid membranes for carbon monoxide/nitrogen separation," *J. Memb. Sci.*, vol. 438, pp. 38–45, 2013.

[51] S. Feng, Y. Wu, J. Luo, and Y. Wan, "AgBF4/[emim][BF4] supported ionic liquid membrane for carbon monoxide/nitrogen separation," *J. Energy Chem.*, vol. 29, pp. 31–39, 2019, doi: 10.1016/j.jechem.2018.02.004.

[52] R. T. Y. Adsorbents, *Fundamentals and Applications*. New York: Wiley, 2003.

[53] R. T. Yang, *Gas Separation By Adsorption Processes*. Imperial College Press, 1997.

[54] C. Moreno-Castilla, "Adsorption of organic molecules from aqueous solutions on carbon materials," *Carbon N. Y.*, vol. 42, no. 1, pp. 83–94, 2004, doi: 10.1016/j.carbon.2003.09.022.

[55] S. Auerbach, K. Carrado, P. Dutta, S. Sircar, and A. Myers, *Gas Separation by Zeolites*, no. January. 2003.

[56] J. R. Li, R. J. Kuppler, and H. C. Zhou, "Selective gas adsorption and separation in metal-organic frameworks," *Chem. Soc. Rev.*, vol. 38, no. 5, pp. 1477–1504, 2009, doi: 10.1039/b802426j.

[57] N. A. Khan and S. H. Jhung, "Adsorptive removal and separation of chemicals with metal-organic frameworks: Contribution of π-complexation," *J. Hazard. Mater.*, vol. 325, pp. 198–213, 2017, doi: 10.1016/j.jhazmat.2016.11.070.

[58] D. J. Safarik and R. B. Eldridge, “Olefin/paraffin separations by reactive absorption: a review,” *Ind. Eng. Chem. Res.*, vol. 37, no. 7, pp. 2571–2581, 1998, doi: 10.1021/ie970897h.

[59] R. T. Yang, π-Complexation Sorbents and Applications. 2003.

[60] A. Luna-Triguero *et al.*, “Π-Complexation for olefin/paraffin separation using aluminosilicates,” *Chem. Eng. J.*, vol. 380, no. August 2019, 2020, doi: 10.1016/j.cej.2019.122482.

[61] Y. Xie, Y. Zhu, B. Zhao, and Y. Tang, An important principle for catalyst preparation-spontaneous monolayer dispersion of solid compounds onto surfaces of supports, vol. 118. Elsevier Masson SAS, 1998.

[62] W. Dai, J. Hu, L. Zhou, S. Li, X. Hu, and H. Huang, “Removal of dibenzothiophene with composite adsorbent MOF-5/Cu(I),” *Energy and Fuels*, vol. 27, no. 2, pp. 816–821, 2013, doi: 10.1021/ef3020662.

[63] R. T. Yang and E. S. Kikkinides, “New sorbents for olefin/paraffin separations by adsorption via π -complexation,” *AIChE J.*, vol. 41, no. 3, pp. 509–517, 1995, doi: 10.1002/aic.690410309.

[64] L. S. Cheng and R. T. Yang, “Monolayer cuprous chloride dispersed on pillared clays for olefin-paraffin separations by π-complexation,” *Adsorption*, vol. 1, no. 1, pp. 61–75, 1995, doi: 10.1007/BF00704146.

[65] S. U. Rege, J. Padin, and R. T. Yang, “Olefin/Paraffin Separations by Adsorption: π-Complexation vs. Kinetic Separation,” *AIChE J.*, vol. 44, no. 4, pp. 799–809, 1998, doi: 10.1002/aic.690440405.

[66] Y.-C. Xie and Y.-Q. Tang, “Spontaneous Monolayer Dispersion of Oxides and Salts onto Surfaces of Supports: Applications to Heterogeneous Catalysis,” *Adv. Catal.*, vol. 37, pp. 1–43, 1990.

[67] Y. Xie, X. Xu, B. Zhao, Y. Tang, and G. Wu, “Studies on the dispersion states of Fe2O3 on γ-Al2O3 by means of Mössbauer spectroscopy and XRD,” *Catal. Letters*, vol. 13, no. 3, pp. 239–245, 1992, doi: 10.1007/BF00770996.

[68] H. Hirai, K. Wada, and K. Makoto, “Active Carbon-Supported Copper(I) Chloride as Solid Adsorbent for Carbon Monoxide,” *Bull. Chem. Soc. Jpn.*, vol. 59, no. 7, pp. 2217–2223, 1986.

[69] R. P. Townsend, “Ion Exchange in Zeolites: Some Recent Developments in Theory and Practice,” in *New Developments in Zeolite Science and Technology*, Y. Murakami, A. Iijima, and J. W. Ward, Eds. Elsevier, 1986, pp. 273–282.

[70] X. Chen, B. Shen, H. Sun, and G. zhan, “Ion-exchange modified zeolites X for selective adsorption desulfurization from Claus tail gas: Experimental and computational investigations,” *Microporous Mesoporous Mater.*, vol. 261, no. September 2017, pp. 227–236, 2018, doi: 10.1016/j.micromeso.2017.11.014.

[71] laude M. Naccache and Y. Ben Taarit, “Oxidizing and acidic properties of copper-exchange Y zeolite,” *J. Catal.*, vol. 22, no. 2, pp. 171–181, 1971.

[72] W. Huang, X. Zhou, Q. Xia, J. Peng, H. Wang, and Z. Li, “Preparation and adsorption performance of GrO@Cu-BTC for separation of CO2/CH4,” *Ind. Eng. Chem. Res.*, vol. 53, no. 27, pp. 11176–11184, 2014, doi: 10.1021/ie501040s.

[73] H. Hirai, K. Wada, and M. Komiyama, “Active Carbon-Supported Copper(I) Chloride As Carbon Monoxide Solid Adsorbent,” *Chem. Lett.*, vol. 12, no. 3, pp. 361–364, 1983, doi: 10.1246/cl.1983.361.

[74] H. Hirai, M. Komiyama, and K. Wada, “ACTIVE CARBON-SUPPORTED ALUMINIUM COPPER CHLORIDE AS WATER-RESISTANT CARBON MONOXIDE ADSORBENT,” *CSJ Journals*, vol. 11, no. 7, pp. 1025–1028, 1982.

[75] H. Hirai, K. Wada, and K. Makoto, “Active Carbon-Supported Aluminium Copper(I) Chloride as Solid Carbon Monoxide Adsorbent,” *Bull. Chem. Soc. Jpn.*, vol. 59, no. 4, pp. 1043–1049, 1986.

[76] H. Hirai, K. Wada, and K. Makoto, “Carbon monoxide adsorbent composed of copper (I) chloride and polystyrene resin having amino groups.,” *Bull. Chem. Soc. Jpn.*, vol. 59, pp. 2553–2558, 1986.

[77] C. Xue, W. Hao, W. Cheng, J. Ma, and R. Li, "CO adsorption performance of CuCl/activated carbon by simultaneous reduction-dispersion of mixed Cu(II) salts," *Materials (Basel).*, vol. 12, no. 10, 2019, doi: 10.3390/ma12101605.

[78] J. Ma, L. Li, J. Ren, and R. Li, "CO adsorption on activated carbon-supported Cu-based adsorbent prepared by a facile route," *Sep. Purif. Technol.*, vol. 76, no. 1, pp. 89–93, 2010, doi: 10.1016/j.seppur.2010.09.022.

[79] H. Tamon, K. Kitamura, and M. Okazaki, "Adsorption of carbon monoxide on activated carbon impregnated with metal halide," *AIChE J.*, vol. 42, no. 2, pp. 422–430, 1996, doi: 10.1002/aic.690420212.

[80] F. Gao, Y. Wang, X. Wang, and S. Wang, "Selective CO adsorbent CuCl/AC prepared using CuCl2 as a precursor by a facile method," *RSC Adv.*, vol. 6, no. 41, pp. 34439–34446, 2016, doi: 10.1039/c6ra03116a.

[81] Y. Huang, Y. Tao, L. He, Y. Duan, J. Xiao, and Z. Li, "Preparation of CuCl@AC with high CO adsorption capacity and selectivity from CO/N2 binary mixture," *Adsorption*, vol. 21, no. 5, pp. 373–381, 2015, doi: 10.1007/s10450-015-9677-5.

[82] C. A. Grande, F. V. S. Lopes, A. M. Ribeiro, J. M. Loureiro, and A. E. Rodrigues, "Adsorption of off-gases from steam methane reforming (H2, CO2, CH4, CO and N2) on activated carbon," *Sep. Sci. Technol.*, vol. 43, no. 6, pp. 1338–1364, 2008, doi: 10.1080/01496390801940952.

[83] J. A. Delgado, V. I. Águeda, M. A. Uguina, J. L. Sotelo, P. Brea, and C. A. Grande, "Adsorption and Diffusion of H2, CO, CH4, and CO2 in BPL Activated Carbon and 13X Zeolite: Evaluation of Performance in Pressure Swing Adsorption Hydrogen Purification by Simulation," *Ind. Eng. Chem. Res.*, vol. 53, no. 40, 2014, doi: 10.1021/ie403744u.

[84] F. Gao, S. Wang, W. Wang, J. Duan, J. Dong, and G. Chen, "Adsorption separation of CO from syngas with CuCl@AC adsorbent by a VPSA process," *RSC Adv.*, vol. 8, no. 69, pp. 39362–39370, 2018, doi: 10.1039/c8ra08578a.

[85] S. E. Siporin, B. C. Mcclaine, and R. J. Davis, “Adsorption of N 2 and CO 2 on Zeolite X Exchanged with Potassium , Barium , or Lanthanum,” pp. 4707–4713, 2003, doi: 10.1021/la020971n.

[86] E. J. Garc *et al.*, “Tuning the Adsorption Properties of Zeolites as Adsorbents for CO 2 Separation : Best Compromise between the Working Capacity and Selectivity,” 2014, doi: 10.1021/ie500207s.

[87] X. Yang, F. E. Epiepang, J. Li, Y. Wei, Y. Liu, and R. T. Yang, “Sr-LSX zeolite for air separation,” *Chem. Eng. J.*, vol. 362, no. November 2018, pp. 482–486, 2019, doi: 10.1016/j.cej.2019.01.066.

[88] L. V. C. Rees, “Ion Exchange in Zeolites,” in *Annu. Rep. Prog. Chem., Sect. A. Gen. Phys and Inorg. Chem*, no. 97, 1970, pp. 191–212.

[89] G. Sethia, R. S. Somani, and H. Chand Bajaj, “Adsorption of carbon monoxide, methane and nitrogen on alkaline earth metal ion exchanged zeolite-X: Structure, cation position and adsorption relationship,” *RSC Adv.*, vol. 5, no. 17, pp. 12773–12781, 2015, doi: 10.1039/c4ra11511b.

[90] R. S. Pillai, G. Sethia, and R. V Jasra, “Sorption of CO , CH 4 , and N 2 in Alkali Metal Ion Exchanged Zeolite-X : Grand Canonical Monte Carlo Simulation and Volumetric Measurements,” pp. 5816–5825, 2010, doi: 10.1021/ie901713m.

[91] J. Feng, Y. Hu, Q. Bao, D. Liang, and Y. Xu, “Carbon monoxide and carbon dioxide adsorption on alkali metal cation-exchanged SSZ-13 zeolites,” *Micro Nano Lett.*, vol. 15, no. 8, pp. 529–534, 2020, doi: 10.1049/mnl.2020.0023.

[92] F. Gao, Y. Wang, and S. Wang, “Selective adsorption of CO on CuCl/Y adsorbent prepared using CuCl2 as precursor: Equilibrium and thermodynamics,” *Chem. Eng. J.*, vol. 290, pp. 418–427, 2016, doi: 10.1016/j.cej.2016.01.054.

[93] A. J. Herna and R. T. Yang, “Desulfurization of Commercial Liquid Fuels by Selective Adsorption via π -Complexation with Cu (I) - Y Zeolite,” no. I, pp. 3103–3110, 2003, doi: 10.1021/ie0301132.

[94] Y. Xie *et al.*, “from Gas Mixtures Containing C02,” *Adsorpt. J. Int. Adsorpt. Soc.*, vol. 32, pp. 27–32, 1996.

[95] D. Saha and S. Deng, “Adsorption equilibria and kinetics of carbon monoxide on zeolite 5A, 13X, MOF-5, and MOF-177,” *J. Chem. Eng. Data*, vol. 54, no. 8, pp. 2245–2250, 2009, doi: 10.1021/je9000087.

[96] Lf. V. S. Lopes *et al.*, “Adsorption of H2, CO2, CH4, CO, N2 and H2O in Activated Carbon and Zeolite for Hydrogen Production, Separation Science and Technology,” *Sep. Sci. Technol.*, no. 44, pp. 1045–1073, 2009, doi: 10.1080/01496390902729130.

[97] N. Heymans, B. Alban, S. Moreau, and G. De Weireld, “Experimental and theoretical study of the adsorption of pure molecules and binary systems containing methane, carbon monoxide, carbon dioxide and nitrogen. Application to the syngas generation,” *Chem. Eng. Sci.*, vol. 66, no. 17, pp. 3850–3858, 2011, doi: 10.1016/j.ces.2011.05.018.

[98] P. Z. Moghadam *et al.*, “Development of a Cambridge Structural Database Subset: A Collection of Metal-Organic Frameworks for Past, Present, and Future,” *Chem. Mater.*, vol. 29, no. 7, pp. 2618–2625, 2017, doi: 10.1021/acs.chemmater.7b00441.

[99] S. Qiu, M. Xue, and G. Zhu, “Metal-organic framework membranes: From synthesis to separation application,” *Chem. Soc. Rev.*, vol. 43, no. 16, pp. 6116–6140, 2014, doi: 10.1039/c4cs00159a.

[100] H. Li, K. Wang, Y. Sun, C. T. Lollar, J. Li, and H. C. Zhou, “Recent advances in gas storage and separation using metal–organic frameworks,” *Mater. Today*, vol. 21, no. 2, pp. 108–121, 2018, doi: 10.1016/j.mattod.2017.07.006.

[101] K. Adil *et al.*, “Gas/vapour separation using ultra-microporous metal-organic frameworks: Insights into the structure/separation relationship,” *Chem. Soc. Rev.*, vol. 46, no. 11, pp. 3402–3430, 2017, doi: 10.1039/c7cs00153c.

[102] R. Babarao *et al.*, “Does functionalisation enhance CO2 uptake in interpenetrated MOFs? An examination of the IRMOF-9 series,” *Chem. Commun.*, vol. 50, no. 24, pp. 3238–3241, 2014, doi: 10.1039/c4cc00700j.

[103] F. Martínez, R. Sanz, G. Orcajo, D. Briones, and V. Yángüez, "Amino-impregnated MOF materials for CO2 capture at post-combustion conditions," *Chem. Eng. Sci.*, vol. 142, pp. 55–61, 2016, doi: 10.1016/j.ces.2015.11.033.

[104] F. Salles, A. Ghoufi, G. Maurin, R. G. Bell, C. Mellot-Draznieks, and G. Férey, "Molecular dynamics simulations of breathing MOFs: Structural transformations of MIL-53(Cr) upon thermal activation and CO2 adsorption," *Angew. Chemie - Int. Ed.*, vol. 47, no. 44, pp. 8487–8491, 2008, doi: 10.1002/anie.200803067.

[105] S. Bourrelly, P. L. Llewellyn, C. Serre, F. Millange, T. Loiseau, and G. Férey, "Different adsorption behaviors of methane and carbon dioxide in the isotypic nanoporous metal terephthalates MIL-53 and MIL-47," *J. Am. Chem. Soc.*, vol. 127, no. 39, pp. 13519–13521, 2005, doi: 10.1021/ja054668v.

[106] B. Chen *et al.*, "A microporous metal-organic framework for gas-chromatographic separation of alkanes," *Angew. Chemie - Int. Ed.*, vol. 45, no. 9, pp. 1390–1393, 2006, doi: 10.1002/anie.200502844.

[107] A. Cadiau, K. Adil, P. M. Bhatt, Y. Belmabkhout, and M. Eddaoudi, "A metal-organic framework-based splitter for separating propylene from propane," *Science (80-.).*, vol. 353, no. 6295, pp. 137–140, 2016, doi: 10.1126/science.aaf6323.

[108] A. Evans, R. Luebke, and C. Petit, "The use of metal-organic frameworks for CO purification," *J. Mater. Chem. A*, vol. 6, no. 23, pp. 10570–10594, 2018, doi: 10.1039/c8ta02059k.

[109] E. D. Bloch *et al.*, "Reversible CO binding enables tunable CO/H2 and CO/N2 separations in metal-organic frameworks with exposed divalent metal cations," *J. Am. Chem. Soc.*, vol. 136, no. 30, pp. 10752–10761, 2014, doi: 10.1021/ja505318p.

[110] A. R. Kim, T. U. Yoon, S. I. Kim, K. Cho, S. S. Han, and Y. S. Bae, "Creating high CO/CO2 selectivity and large CO working capacity through facile loading of Cu(I) species into an iron-based mesoporous metal-organic framework," *Chem. Eng. J.*, vol. 348, no. April, pp. 135–142, 2018, doi: 10.1016/j.cej.2018.04.177.

[111] J. Peng *et al.*, "A supported Cu(I)@MIL-100(Fe) adsorbent with high CO adsorption capacity and CO/N2 selectivity," *Chem. Eng. J.*, vol. 270, pp. 282–289, 2015, doi: 10.1016/j.cej.2015.01.126.

[112] R. M. J. *et al.*, "Syngas Purification Using MIL-125(Ti)_NH2," *Energy and Fuels*, no. 29, pp. 4654–4664, 2015.

[113] K. Munusamy, G. Sethia, D. V. Patil, P. B. Somayajulu Rallapalli, R. S. Somani, and H. C. Bajaj, "Sorption of carbon dioxide, methane, nitrogen and carbon monoxide on MIL-101(Cr): Volumetric measurements and dynamic adsorption studies," *Chem. Eng. J.*, vol. 195–196, pp. 359–368, 2012, doi: 10.1016/j.cej.2012.04.071.

[114] G. Nickerl, U. Stoeck, U. Burkhardt, I. Senkovska, and S. Kaskel, "A catalytically active porous coordination polymer based on a dinuclear rhodium paddle-wheel unit," *J. Mater. Chem. A*, vol. 2, no. 1, pp. 144–148, 2014, doi: 10.1039/c3ta12795h.

[115] P. Chowdhury, S. Mekala, F. Dreisbach, and S. Gumma, "Adsorption of CO, CO 2 and CH 4 on Cu-BTC and MIL-101 metal organic frameworks: Effect of open metal sites and adsorbate polarity," *Microporous Mesoporous Mater.*, vol. 152, pp. 246–252, 2012, doi: 10.1016/j.micromeso.2011.11.022.

[116] Y. Wang *et al.*, "CuAlCl4 doped MIL-101 as a high capacity CO adsorbent with selectivity over N2," *Front. Chem. Sci. Eng.*, vol. 8, no. 3, pp. 340–345, 2014, doi: 10.1007/s11705-014-1438-6.

[117] J. R. Karra and K. S. Walton, "Molecular simulations and experimental studies of CO2, CO, and N2 adsorption in metal-organic frameworks," *J. Phys. Chem. C*, vol. 114, no. 37, pp. 15735–15740, 2010, doi: 10.1021/jp105519h.

[118] V. I. Agueda *et al.*, "Adsorption and diffusion of H2, N2, CO, CH4 and CO2 in UTSA-16 metal-organic framework extrudates," *Chem. Eng. Sci.*, vol. 124, pp. 159–169, 2015, doi: 10.1016/j.ces.2014.08.039.

[119] H. Deng, C. J. D. H. F. R. B. Ferreira, Towne, J. C. B. K. B. Wang, and O. M. Yaghi, "Multiple functional groups of varying ratios in metal-organic frameworks," *Science (80-.).*, vol. 327, pp. 846–850, 2010, doi: 10.1126/science.1181761.

[120] A. R. Kim, T. U. Yoon, S. I. Kim, K. Cho, S. S. Han, and Y. S. Bae, "Creating high CO/CO2 selectivity and large CO working capacity through facile loading of Cu(I) species into an iron-based mesoporous metal-organic framework," *Chem. Eng. J.*, vol. 348, no. I, pp. 135–142, 2018, doi: 10.1016/j.cej.2018.04.177.

[121] P. Rallapalli, K. P. Prasanth, D. Patil, R. S. Somani, R. V. Jasra, and H. C. Bajaj, "Sorption studies of CO2, CH4, N2, CO, O2 and Ar on nanoporous aluminum terephthalate [MIL-53(Al)]," *J. Porous Mater.*, vol. 18, no. 2, pp. 205–210, 2011, doi: 10.1007/s10934-010-9371-7.

[122] J. Duan *et al.*, "High CO2/N2/O2/CO separation in a chemically robust porous coordination polymer with low binding energy," *Chem. Sci.*, vol. 5, no. 2, pp. 660–666, 2014, doi: 10.1039/c3sc52177j.

[123] D. A. Reed *et al.*, "Reversible CO scavenging via adsorbate-dependent spin state transitions in an iron(II)-triazolate metal-organic framework," *J. Am. Chem. Soc.*, vol. 138, no. 17, pp. 5594–5602, 2016, doi: 10.1021/jacs.6b00248.

[124] B. Wang, A. P. Cote, H. Furukawa, M. O'Keeffe, and O. M. Yaghi, "Colossal cages in zeolitic imidazolate frameworks as selective carbon dioxide reservoirs," *Nature*, vol. 453, no. 7192, 2008.

[125] S. Ma, D. Sun, X. Sen Wang, and H. C. Zhou, "A mesh-adjustable molecular sieve for general use in gas separation," *Angew. Chemie - Int. Ed.*, vol. 46, no. 14, pp. 2458–2462, 2007, doi: 10.1002/anie.200604353.

[126] Z. Kang, L. Fan, and D. Sun, "Recent advances and challenges of metal-organic framework membranes for gas separation," *J. Mater. Chem. A*, vol. 5, no. 21, pp. 10073–10091, 2017, doi: 10.1039/c7ta01142c.

[127] K. Cho, J. Kim, H. T. Beum, T. Jung, and S. S. Han, “Synthesis of CuCl/Boehmite adsorbents that exhibit high CO selectivity in CO/CO2 separation,” *J. Hazard. Mater.*, vol. 344, pp. 857–864, 2018, doi: 10.1016/j.jhazmat.2017.11.037.

Chapter 4: Selective CO Adsorption separation from CO/CO_2 Gas mixture by CuCl based adsorbents

4.1 Abstract

Separation of carbon monoxide from a gaseous mixture containing carbon dioxide (CO_2) by adsorption process has captured great attention. However, the CO adsorption capacity and selectivity over some porous materials is not sufficient. For most adsorbents studied in the literature, CO_2 is adsorbed more than CO. In this study, we wanted to reverse this selectivity by modifying existing adsorbents. Copper (I) chloride (CuCl) based adsorbents were developed using coper (II) chloride ($CuCl_2$) as precursor into six different adsorbents; four activated carbons, a metal organic framework CALF20, and ordered mesoporous silica SBA 15. The adsorbents were prepared using two different methods, the impregnation using a modified polyol technique and auto dispersion method. The π complexation between Cu^{2+} ions and CO enhanced the CO adsorption uptake and selectivity while reducing the CO_2 uptake. The highest CO uptake was observed by modified activated carbon CuCl/xtrusorb (1.62 mmol/g) at 100 KPa and 298 K. The CO/CO_2 selectivity increased to 4.37 compared to 0.2 before copper incorporation. Moreover, different loading of copper was tested to determine the monolayer dispersion capacity of $CuCl_2$ on the support.

Sample characterization was performed by N_2 adsorption at 77 K for BET surface area analysis and X-Ray diffraction (XRD). The characterization results suggest that $CuCl_2$ salt is completely reduced to CuCl dispersed on the surface. CO and CO_2 equilibrium isotherms were measured using a gravimetric system at pressures ranging from 0 to 20 bar at 298 K.

4.2 Introduction

Carbon monoxide (CO) is a significant feedstock in chemical industry and a starting material for the synthesis of various components in C1 chemistry [1], [2], including methanol, acetic acid, formic acid, phosgene and liquid fuels through Fisher Tropch process [3], [4]. CO is mainly produced in gaseous mixtures along with other components such as N_2, CO_2, CH_4, H_2 and H_2O through different processes including steam and methane reforming, partial oxidation of hydrocarbons, coal gasification and CO_2 conversion processes. In steel industry, the off- gas from

blast furnace, coke oven and converter gas are very rich in CO (8-89%) [5], [6]. Therefore, CO separation and purification from other product mixtures are important to recover CO and benefit from its recycling and utilization. Furthermore, trace levels of CO should be removed from catalytic reactions as it poisons some catalyst, which is the case in hydrogen fuel cell catalyst [7], [8]. Hence, CO separation and purification from other gaseous mixtures are crucial.

Among different CO separation technologies, cryogenic distillation is used in industry. In this process the gas mixture is liquefied and CO is separated at low temperatures of -165 to -210 °C, which make this process very energy intensive. Furthermore, in the presence of N_2, CO separation from N_2 is not feasible as their boiling points are very close, with -191.5 °C for CO_2 and -195.8 °C for N_2. Adsorption separation is an alternative technology for CO recovery. It has been successfully used for CO separation using different porous materials, including activated carbons, zeolites, and metal organic frameworks (MOFs). However, the implementation of adsorption separation is challenging mostly from a mixture containing CO_2. The majority of adsorbents exhibit higher adsorption capacity toward CO_2. In addition, CO_2 molecules has larger polarizability compared to CO with very similar kinetic diameters (0.33 nm and 0.37 nm for CO_2 and CO respectively), which make kinetic separation of CO and CO_2 a difficult one [9].

To further improve the CO uptake and selectivity toward CO, several researches focussed on development of new adsorbents with incorporation of transition metal ions such as Cu^+, Ag^+, Pd^+ and Ni^+ ions [10], [11] into the pores of the adsorbent materials. The metal ions form π complex with π-orbital of gas or liquid [12]. Moreover, the σ bonds form between the s orbital of metal ions and CO molecules, and π back-donation is formed between the d-orbital of metal ion with CO molecule [13]. The schematic in Figure 4-1 represent π complex formation between metal ion and CO [14].

Different approaches were investigated to modify porous adsorbents with metal salts for CO purification, the most common and simplest method being monolayer dispersion. Fei et al. [15], Xue et al. [16] and Huang et al. [17] prepared Cu based activated carbons using solid state auto-dispersion method. Similar method was applied by Xie et al. [18], Fei et al. [19] and Ma et al. [20] to modify zeolite material by introduction of copper metallic salts. Another technique of incorporation of metal ions consists of wet impregnation by dispersing metal salts using reagents

such as hydrochloric acid, toluene and methanol in different solid adsorbents including MOF materials [21], [22]

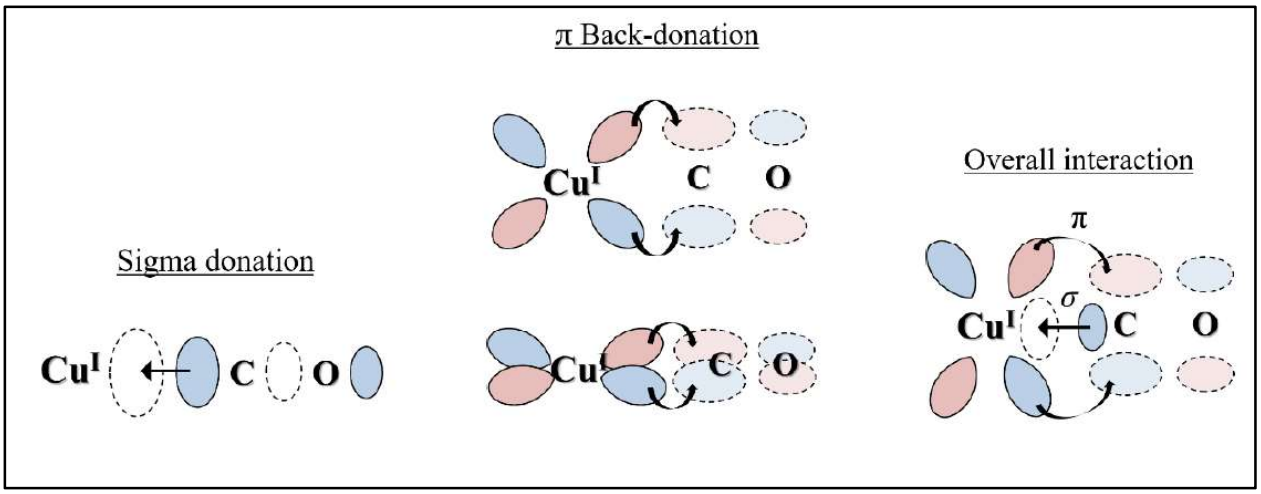

Figure 4-1. π-complexation between CO and Cu (I) ions [14].

4.3 Experimental

4.3.1 Materials

Four different samples of activated carbons (AC F300, AC F400, Xtrusorb A754, and OVC 4x10) were purchased from Calgon Carbon (Moon Township Pennsylvania, United States). Cupric chloride dihydrate ($CuCl_2.2H_2O$. 99.999 %) from Alfa Aesar (Ward Hill, MA, United States), ethylene glycol $(CH_2OH)_2$ and sodium hydroxide (NaOH), were purchased from Fisher Scientific Inc. (Ottawa, ON, Canada). CO, CO_2 and helium gases were obtained from Linde Canada Ltd. (Burlington, On, Canada). All the gases had purities of 99.99% or above.

Ordered mesoporous silica SBA15 was prepared in the lab following the method described by Zhao et al.[23]. Metal organic framework sample CALF 20 was acquired from University of Calgary.

4.3.2 Adsorbent preparation

The Cu-based adsorbents were prepared by two different methods: 1) the polyol method [24] for reduction and deposition of Cu(I), 2) thermal monolayer auto-dispersion method [25].

Polyol method

A calculated amount (0.5 g) of adsorbent was first grounded and sieved into powder. In a round-bottom flask inside a fume hood, 50 ml of a 0.08 M prepared solution of NaOH (0.16 g) and ethylene glycol (50 ml) was mixed with a fixed amount (0.59 g) of copper (II) chloride salt using magnetic stirrer at ambient temperature for one hour. The solution was then attached to a reflux column connected to a cooling water and suspended in silicon oil bath sitting at the top of a hotplate (IKA® C-MAG HS7). The temperature was controlled with an electronic contact thermometer (IKA ETS D5). The solution was gradually heated to 160 °C while continuously stirring with the magnetic stirrer and kept at this temperature while stirring for 2 hours. After this step the heat is turned off and the solution was cooled down naturally to room temperature while being stirred until it is cooled. Afterward, the solution is transferred to two flacon tubes, then centrifuged at 4000 rpm for 10min three times to separate the liquid from the solid. The supernatant was decanted, and the solids were washed between each run with deionized water. The obtained mixture was subsequently dried at room temperature in a fume hood for about three days. Schematic diagram of the procedure is shown in Figure 4-2.

Monolayer auto-dispersion method

A calculated amount (0.5g) of different porous material in a powder form and $CuCl_2.2H_2O$ (0.59 g) were mixed in an ultrasonic bath for an hour at room temperature. The sample was then dried at 120 °C under vacuum for five hours to remove moisture. It was then further activated in situ by raising the heater temperature to 450 °C under CO gas environment at a pressure of 1.5 bar as a reducing agent for four hours. For activated carbon Xtrusorb A754, different copper loadings were prepared. 3, 5 and 7mmol/g denoted as X-Cu@xtrusorb where X indicates the copper loading. Table 4.1 shows the list of adsorbents used and their notation after copper addition.

Table 4-1. List of adsorbents before and after modification.

Adsorbents	Modified adsorbents	Copper loading (mmol/g)
Activated carbon F300	X-Cu@F300	X=7
Activated carbon F400	X-Cu@F400	X=7
Activated carbon Xtrusorb A754	X-Cu@xtrusorb	X=3,5,and 7
Activated carbon OVC 4x10	X-Cu@OVC	X=7
MOF CALF20	X-Cu@CALF20	X=7
Ordered mesoporous silica SBA 15	X-Cu@SBA15	X=7

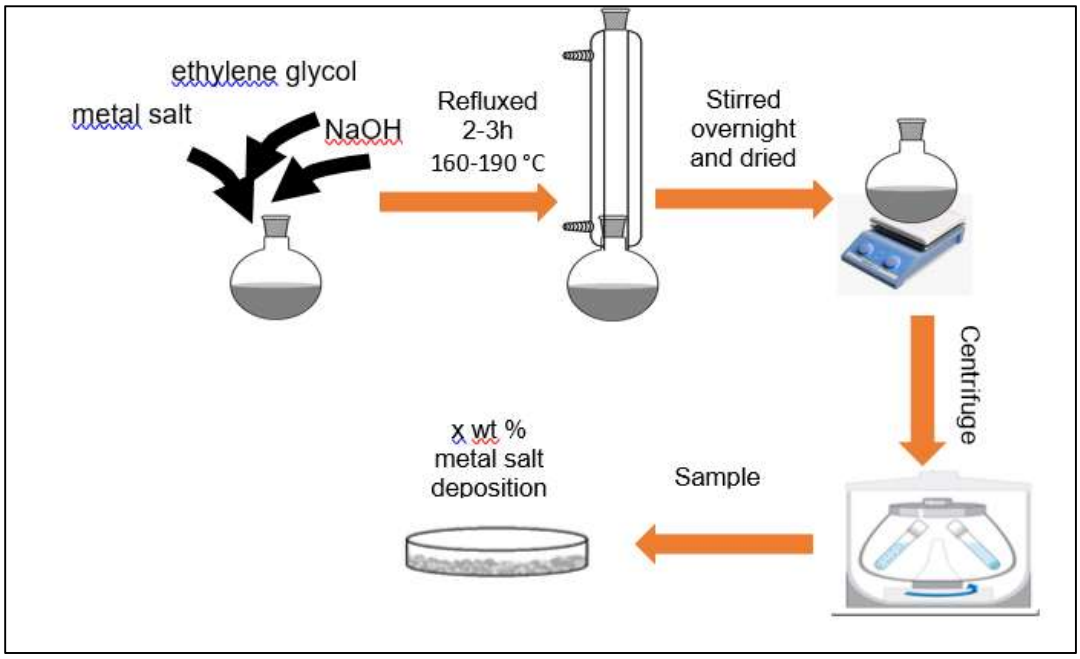

Figure 4-2. Modified Polyol method for copper nanoparticle deposition.

4.3.3 Adsorbent characterizations

BET surface area

Nitrogen adsorption/desorption equilibrium isotherms of the samples were determined using liquid Nitrogen at 77K in a Micrometrics ASAP 2020 analyser. Prior the measurements, the samples were degassed overnight at 300 ºC. The samples' specific surface areas were determined from the equilibrium isotherms using Brunauer-Emmett-Teller (BET) method. The total pore volumes were calculated based on the equilibrium isotherms at the relative pressures, $P/P_{0,}$ near to 1.

X-Ray Powder Diffraction

To identify the crystalline material of the samples, Powder X-ray diffraction (XRD) is used. The XRD scans of the samples were collected on the Rigaku Ultima IV X-ray diffractometer over the angular range of 10 to 58° (2theta). The XRD system operates in the theta:theta geometry using CuKα radiation, 1.5405981 Å, and is equipped with a D/teX high speed detector. The generator voltage and current settings were 40 kV and 44 mA, respectively.

4.3.4 Equilibrium isotherm measurements

Adsorption equilibrium isotherms of CO and CO_2 were measured using a gravimetric system (Intelligent gravimetric analyser: IGA) from Hiden Isochema Limited (Warrington, UK). The isotherms were measured at 25 °C for a pressure range of 0-20 bar. The IGA microbalance has a mass resolution of 0.1 μg. To control the sample temperature, a thermostatic water bath is used for a temperature range of 5 to 80 °C. For higher temperature applications, a high temperature furnace is used (1000 °C with quartz reactor).

Before isotherm measurements, the adsorbents were degassed at vacuum at 300 °C overnight to remove humidity and impurities that may be adsorbed in the sample. The sample temperature is measured by an in situ RTD temperature probe which is accurate to ± 0.1 °C. To correct for the buoyancy forces acting on the microbalance components, the buoyancy force correction (F_b) in equation (4.1) is considered

$$F_b = gr^2 V_i \rho_g = g \frac{m_i}{\rho_i} \ \rho_g(T, P) \quad (4.1)$$

Where g is the gravitational acceleration, V_i is the volume of the object, and ρ_g is the density of the gas surrounding the object at a known temperature and pressure (T, P).

Adsorbents' skeletal density was measured using the gravimetric system by helium displacement method. Results are shown in Table 4-2. The schematic diagram of the apparatus used for equilibrium isotherm measurements is illustrated in Figure 4-3.

Table 4-2. Textural properties and skeletal density values of the unmodified adsorbents studied.

Unmodified Adsorbent	BET surface area (m^2/g)	Langmuir surface area (m^2/g)	Total pore volume (cm^3/g)	Pore diameter (Å)	Skeletal density (g/cm^3)
AC F300	847	1147.62	0.471	22.25	2.19
AC F400	907	1228.23	0.517	22.8	2.042
OVC 4x10	1084	1454.82	0.521	19.20	2.218
Xtrusorb	1082	1451.38	0.574	21.22	1.952
SBA 15	496	677.6	0.474	38.28	2.48
CALF 20	387.036	511.14	0.205	21.27	1.834

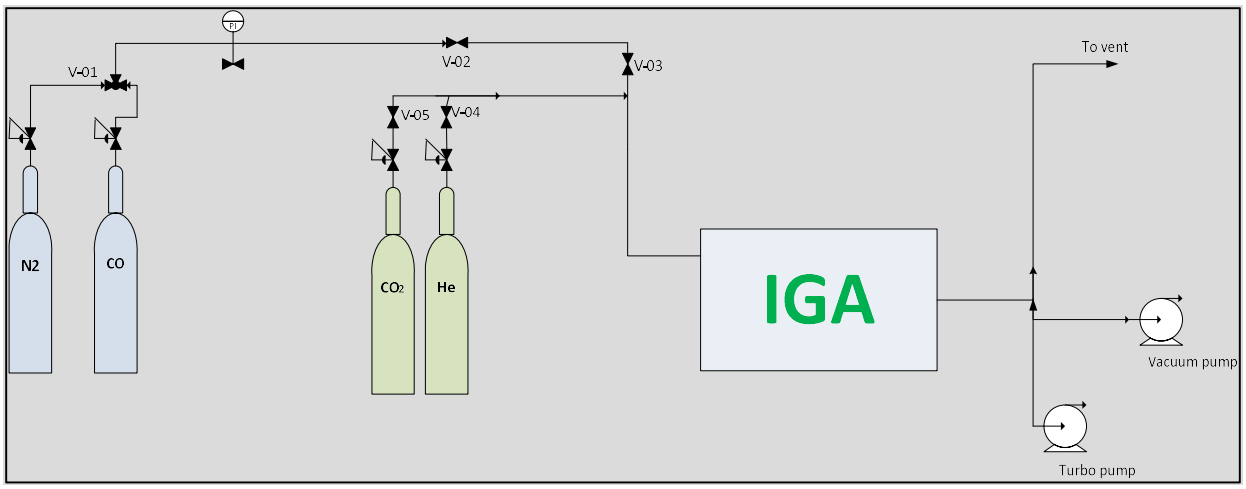

Figure 4-3. Schematic diagram of the gravimetric adsorption apparatus used in this study.

4.3.5 Adsorption Isotherm models

To correlate the adsorption isotherms of CO and CO_2 with different adsorbents, the Langmuir, dual site Langmuir and SIPS models were used.

Langmuir isotherm model describe the monolayer coverage of the adsorbate on the surface with no interactions between adsorbate molecules. The equation is written as

$$\frac{q_e}{q_s} = \frac{bP}{1+bP} \tag{4.2}$$

Where q_e is the adsorbed amount at equilibrium in mmol/g, qs, is the maximum adsorption amount at the isotherm temperature (mmol/g), P is the equilibrium pressure (bar) and b (bar^{-1}) is the Langmuir adsorption equilibrium constant.

Sips Model is a combination of Langmuir and Freundlich models to predict the behaviour of heterogeneous adsorption system [19].

$$\frac{q_e}{q_s} = \frac{(bP)^n}{1+(bP)^n} \tag{4.3}$$

where n is a dimensionless isotherm parameter describing the heterogeneity of the adsorption.

Dual site Langmuir equation is given by:

$$q_e = q_1 + q_2 = \frac{q_1 b_1 P}{1+b_1 P} + \frac{q_2 b_2 P}{1+b_2 P} \quad (4.4)$$

where the adsorption happens in two distinct sites1 and 2.

4.3.6 Selectivity

The pure component selectivity of CO over CO_2 gas is calculated by using equation (4.5)

$$S_{ads} = \frac{q_{CO}}{q_{CO_2}} \quad (4.5)$$

Where q_{CO} and q_{CO2} are the adsorbed amounts of CO and CO_2 at equilibrium, respectively, at given pressure and temperature

4.4 Results and discussions

4.4.1 Adsorption/desorption isotherms with unmodified adsorbents

The adsorption and desorption isotherms of carbon monoxide and carbon dioxide with the six unmodified porous materials at room temperature (298 K) and pressure range of 0 to 20 bar are presented in Figure 4-4. These isotherms increased steadily with increasing pressure following type I isotherm for activated carbon samples. Furthermore, the activated carbon isotherms show a marked reversible behaviour of adsorption and desorption. The MOF CALF 20 exhibited a sharp increase in CO_2 adsorption at low pressure range, implying high interaction with CO_2 molecules. For SBA 15, a marked hysteresis between adsorption and desorption isotherm is observed in CO isotherm. This could be explained by the capillary condensation which is signature for mesoporous materials.

The adsorption isotherms clearly showed that the adsorption capacity of CO_2 is much higher than those of CO. The higher uptake of CO_2 is due to its higher quadrupole moment (13.4×10^{-40} C m^2) and polarizability (26.3×10^{-25} cm^3) compared to CO (12.3×10^{-40} C m^2 and 18.44×10^{-25} cm^3).

The difference in CO_2 uptake between different adsorbents is also due to their specific surface area and pore volume, which result in higher adsorption capacity for samples with larger surface area.

The highest CO_2 and CO uptake values are observed with OVC4x10 and Xtrusorb A754 samples with the values of 8.99 mmol/g and 9.47 mmol/g for CO_2 and 3.42 mmol/g and 3.45 mmol/g for CO, respectively, at 25 °C and pressure of 20 bar. Their surface areas of 1084 m^2/g and 1082 m^2/g are the largest as seen in Table 4-2. The adsorbed amount of CO at 298 K with Xtrusorb A754 and OVC4x10 for pressures of 1 bar to 20 bar increased by 608% and 536%, respectively. Furthermore, the CO and CO_2 isotherms with SBA-15 are quite linear, suggesting weak interaction between SBA-15 and both CO and CO_2.

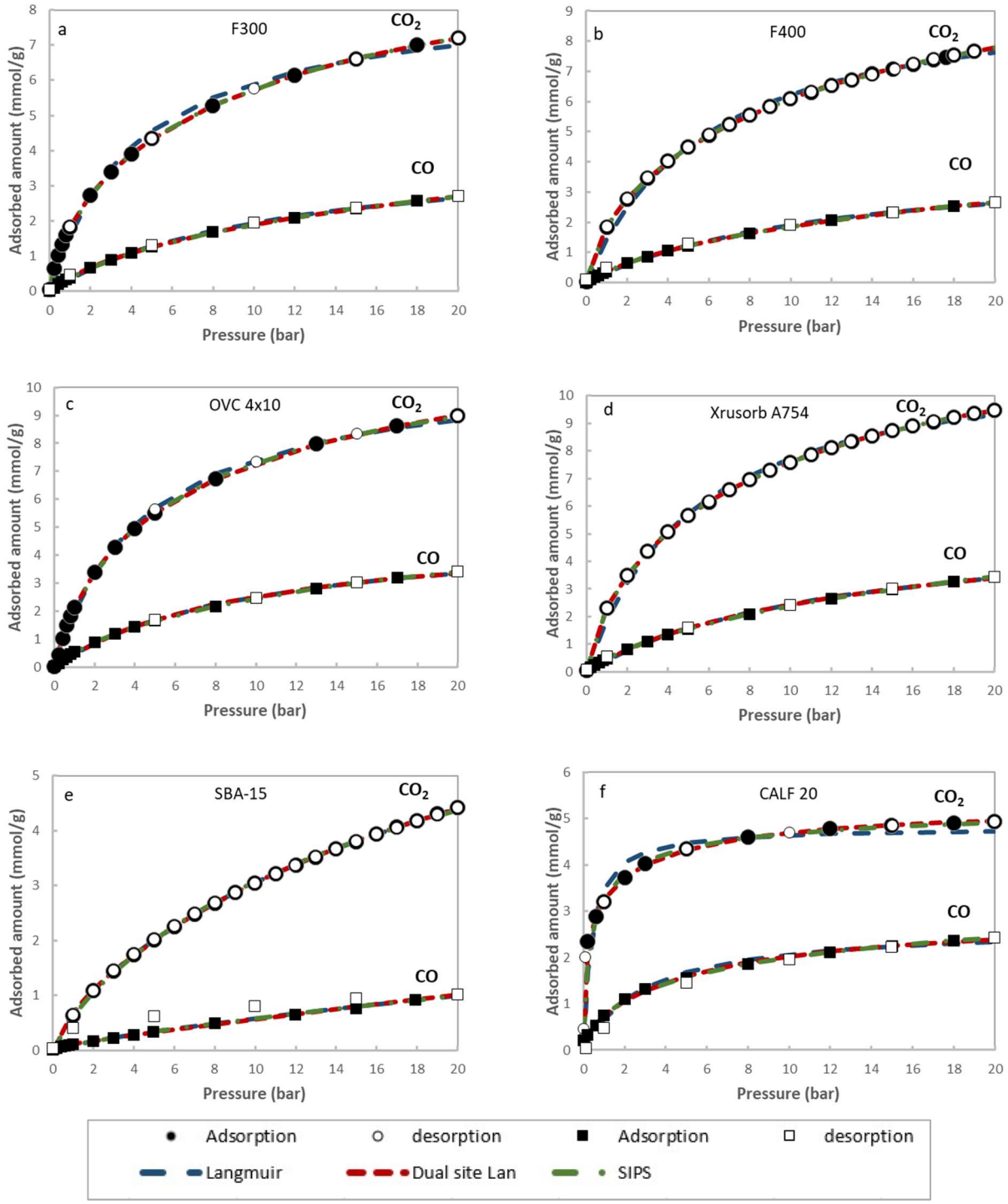

Figure 4-4. CO and CO_2 adsorption equilibrium isotherms at 298K with unmodified adsorbents (a) F300, (b) F400, (c) OVC 4x10, (d) Xtrusorb, (e) SBA 15, and (f) CALF 20

Figure 4-5 summarizes the results of the CO and CO_2 isotherms of the six studied adsorbents to compare the capacities of each gas for different unmodified adsorbents. At high pressures, the highest and the lowest adsorption capacity of CO and CO_2 are seen with activated carbon Xtrusorb and SBA 15, respectively.

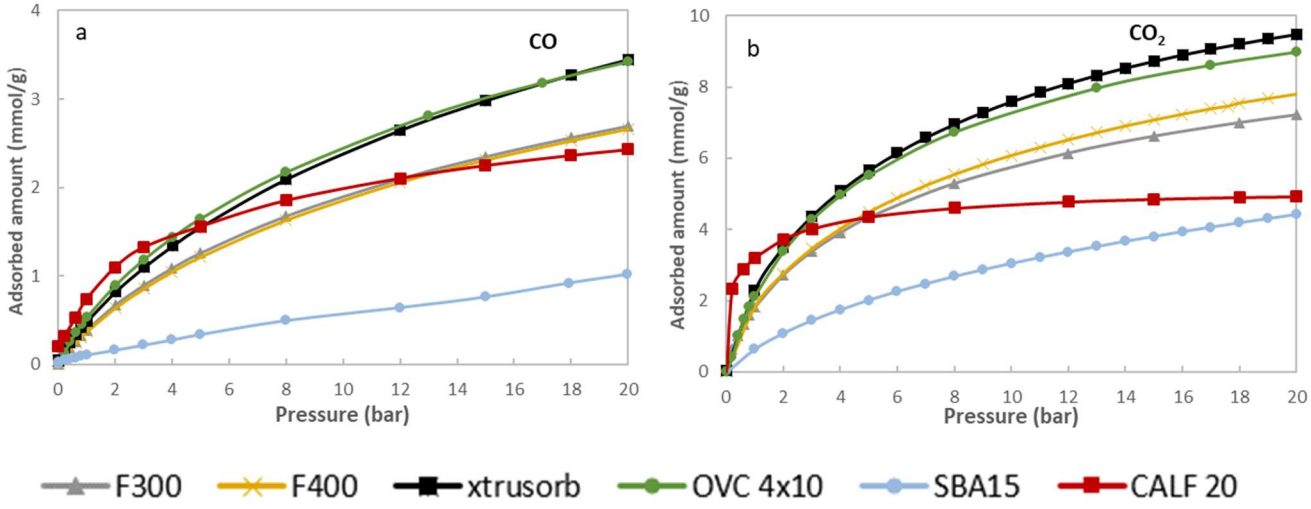

Figure 4-5. Adsorption isotherms of six unmodified adsorbents at 298K for (a) CO and (b) CO_2.

Modelling the adsorption isotherm data obtained from experimental tests is essential to predict the adsorption performance and for design, prediction and optimization of adsorption processes.

To define an adsorption isotherm model that best represent the experimental data of adsorption isotherms, several models are applied. In this work, we considered three models: Langmuir, dual site Langmuir and Sips models. To find the best fitting adsorption model, nonlinear regression analysis was applied to fit the three models. As observed in Figure 4-4, the three models fit the experimental data well, however the dual site Langmuir model showed the lowest residual sum of square (RSS) value which indicate that this model is the best to represent the experimental data. Table 4-3 lists the values of corresponding isotherm parameters for Langmuir, Sips and dual site Langmuir models.

Table 4-3. Langmuir, Sips and dual site Langmuir model parameters for CO and CO_2 adsorption isotherms for the unmodified adsorbents in this study.

Unmodified Adsorbent	Gas	Langmuir		Dual site Langmuir				Sips		
		q_s	B	q_1	b_1	q_2	b_2	q_s	b	n
		mmol/g	bar^{-1}	mmol/g	bar^{-1}	mmol/g	bar^{-1}	mmol/g	bar^{1}	-
AC F300	CO_2	8.49	0.23	8.10	0.09	1.90	1.40	11.64	0.09	1.37
	CO	4.10	0.09	0.60	0.48	4.58	0.04	5.57	0.04	1.19
AC F400	CO_2	9.87	0.17	9.51	0.08	1.92	1.48	13.80	0.07	1.41
	CO	4.17	0.08	4.62	0.05	0.48	0.53	5.61	0.04	1.18
OVC 4x10	CO_2	10.83	0.22	4.52	0.10	0.49	0.10	12.11	0.16	1.15
	CO	5.01	0.10	5.26	0.45	7.38	0.07	6.74	0.05	1.20
Xtrusorb	CO_2	11.77	0.19	10.89	0.10	2.19	1.43	14.90	0.10	1.32
	CO	5.43	0.08	3.96	0.02	3.21	0.13	8.60	0.03	1.25
SBA 15	CO_2	0.02	12.01	8.09	0.04	0.60	1.24	9.42	0.04	1.19
	CO	0.01	36.24	10.49	0.00	0.09	2.38	35.80	0.00	1.27
CALF20	CO_2	4.82	2.63	2.29	0.30	3.00	10.40	5.35	2.01	1.57
	CO	2.69	0.33	2.48	0.17	0.49	4.17	3.99	0.10	1.59

To evaluate the studied adsorbents for CO/CO_2 separation, the CO/CO_2 selectivity is calculated from dual site Langmuir model by using equation 4.5. The results are summarized in Figure 4-6. The CO/CO_2 selectivity is very low, and increase as the pressure increases, with the highest value of 0.48 observed in MOF CALF 20.

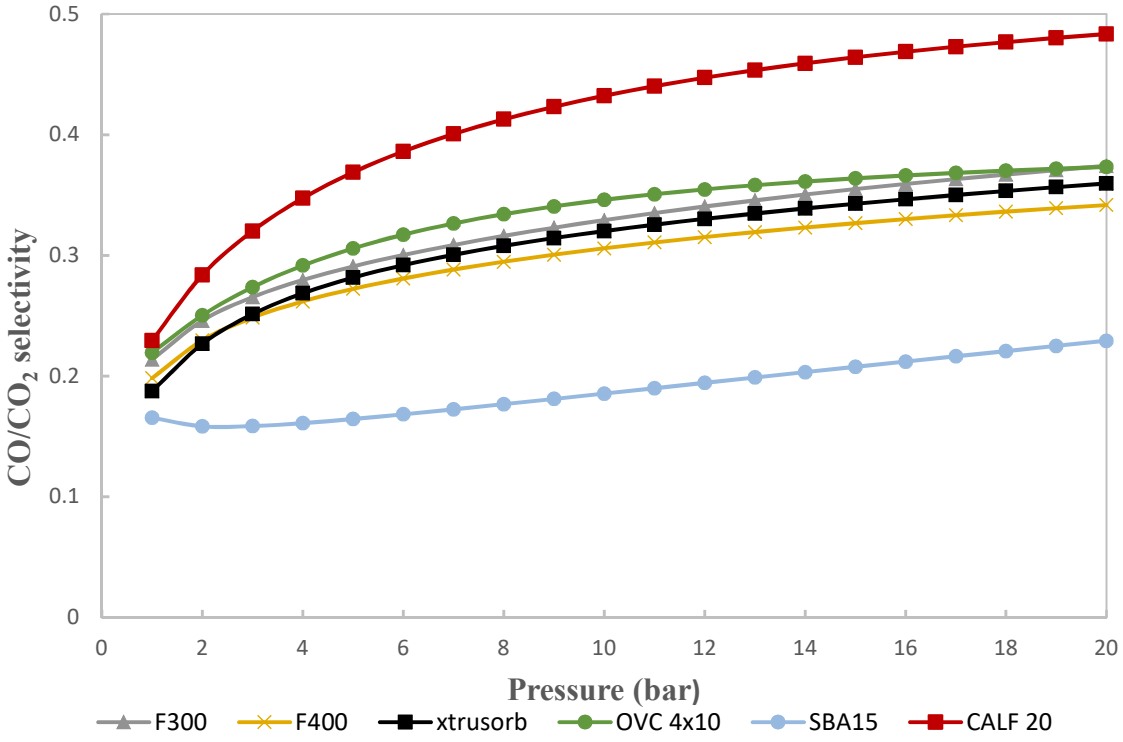

Figure 4-6. CO/CO_2 adsorption selectivity at 298K for studied unmodified adsorbents.

As seen from previous pure equilibrium isotherms and selectivity calculation results, it is difficult to separate and recover CO from a gaseous mixture. It is challenging to find porous material with high affinity toward CO in a mixture containing CO_2 since CO_2 has a high polarizability and higher quadrupole moment, thus most adsorbents exhibit higher CO_2 uptake than CO. Therefore, to separate and recover CO from gaseous mixture containing CO_2, and obtain high purity CO gas, development of new adsorbent materials featuring high affinity and interaction with CO molecules, thus increasing the CO adsorption capacity and selectivity is necessary. Furthermore, this interaction should be weak enough, so adsorbents' regeneration does not necessitate high energy during desorption process, so that change in pressure or temperature using either pressure swing adsorption (PSA) or temperature swing (TSA) between consecutive cycles is sufficient for a continuous process.

π complexation adsorption is a promising method for CO recovery and purification. Transition metal ions such as Cu(I), Ag(I) and Pd(II) has been used for π complexation interaction with CO molecules and many studies had proved their efficiency for CO recovery.

In this study, copper chloride (II) is incorporated into the adsorbents studied following the two methods described above, polyol and auto-dispersion method. For Xtrusorb sample, different copper loadings are tested to determine the threshold of the copper required to cover the sample surface. The adsorption isotherm results obtained with these modified adsorbents are given in section 3.3.

4.5 Characterization of adsorbent samples

4.5.1 XRD results

The XRD diffraction patterns of the activated carbon Xtrusorb and the loaded samples with $CuCl_2$ are presented in Figure 4-7. The results show the diffraction peaks of $CuCl_2$ appear at 2 Θ values of 16.3^0, 22°, 33.4° and 54°. The $CuCl_2$ peaks disappeared after sample activation suggesting that $CuCl_2$ is well reduced to CuCl. The diffraction peaks of CuCl at 2 Θ values of 28.5°, 47.5° and 56° are seen in 3-Cu@xtrusorb, 5-Cu@xtrusorb and 7-Cu@xtrusorb, with less intensity in 3-Cu@xtrusorb which might de due to well dispersed CuCl on the surface. Furthermore, the reflection intensity of CuCl peaks increases with increasing CuCl loading in the samples. However at $28.5^{0,}$ the intensity in 5-Cu@xtrusorb is higher than 7-Cu@xtrusorb. This could be explained by small crystals of CuCl with higher Cu (I) dispersion in 7-Cu@xtrusorb sample so XRD did not detect it. Another speculation could be the excessive loading of copper into the support, leading to appearance of smaller diffraction.

4.5.2 BET surface area analysis

Table 4.4 represents the data obtained for activated carbon Xtrusorb and the three modified ones with different copper loading (3, 5, and 7 mmol/g). The activated carbon Xtrusorb's surface area and total volume are 1082 m^2/g and 0.574 cm^3/g respectively. The samples with cooper loading exhibit a gradual decrease in surface area and pore volume as the $CuCl_2$ loading increase. This indicate the dispersion of the copper into the pores of the support reducing the number of open pores. Likewise, increasing copper loading lead to further decrease in the surface area as more

copper occupy the surface. In addition, it is observed that the average pore diameter increases as the copper loading in the adsorbent increase from 3 to 7 mmol/g. As the copper loading increases, more microspores are occupied with copper, thus the average pore diameter represent more of the mesopores in the adsorbent.

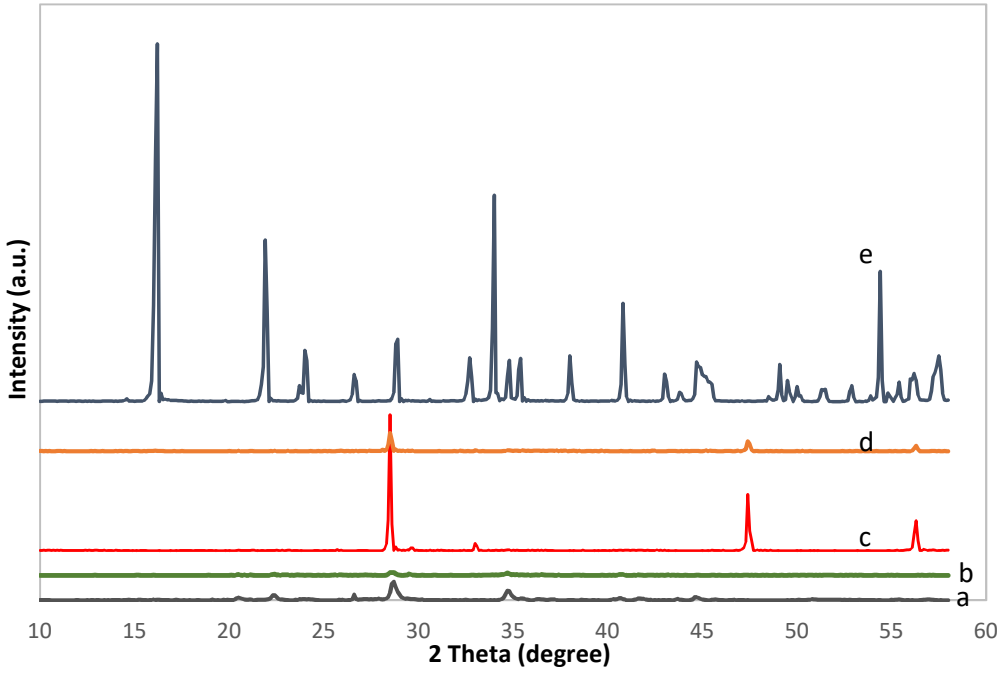

Figure 4-7. X-Ray diffraction patterns of Xtrusorb and $CuCl_2$ before and after activation: (a)Xtrusorb, (b) 3-Cu@xtrusorb, (c) 5-Cu@xtrusorb, (d) 7-Cu@xtrusorb, and (e) $CuCl_2$

Table 4-4. Textural properties of activated carbon Xtrusorb A754 loaded with $CuCl_2$

Samples	Cu content (wt%)	BET surface area (m^2/g)	Total pore volume (cm^3/g)	Average pore diameter (Å)
Xtrusorb A754	-	1082.41	0.574	21.22
3-Cu@xtrusorb	19	497.94	0.27	22.19
5-Cu@xtrusorb	31.7	192.65	0.12	25.29
7-Cu@xtrusorb	44	106.46	0.07	26.28

4.6 Equilibrium adsorption isotherms of modified adsorbents

4.6.1 Results obtained with Polyol method

Figure 4-8 represent the equilibrium isotherms of pure CO and CO_2 in adsorbents impregnated with $CuCl_2$ at 298 K. The adsorbent samples were loaded with 7mmol/g of $CuCl_2.2H_2O$ using polyol method as described before. A very small increase of CO uptake in impregnated activated carbon Xtrusorb F400, OVC4x10, SBA 15 and CALF 20 at low pressures compared to the non modified adsorbents was observed from the results. On the other hand, the CO_2 adsorption capacity in these modified adsorbents had decreased compared to the previous results obtained before sample impregnation. These results suggest that there was a weak interaction between CO and Cu (I) in modified adsorbents. Furthermore, the CO_2 uptake decreased due to reduction of open site available for interaction with CO_2, which are occupied by impregnated copper.

For Cu based F300, there was an interesting increase in CO uptake at low pressures, suggesting a strong interaction with Cu (I). At higher pressures, a smaller amount of CO is adsorbed, this may be caused by the absence of Cu (I) in micropores.

In general, the polyol method for Cu nanoparticle deposition into the surface of the adsorbent did not show a significant change in CO adsorption capacity, suggesting a weak interaction of Cu with this adsorbent, thus the π complexation did not happen. Further investigation and testing is required to improve the employment of this method for Cu impregnation into porous materials.

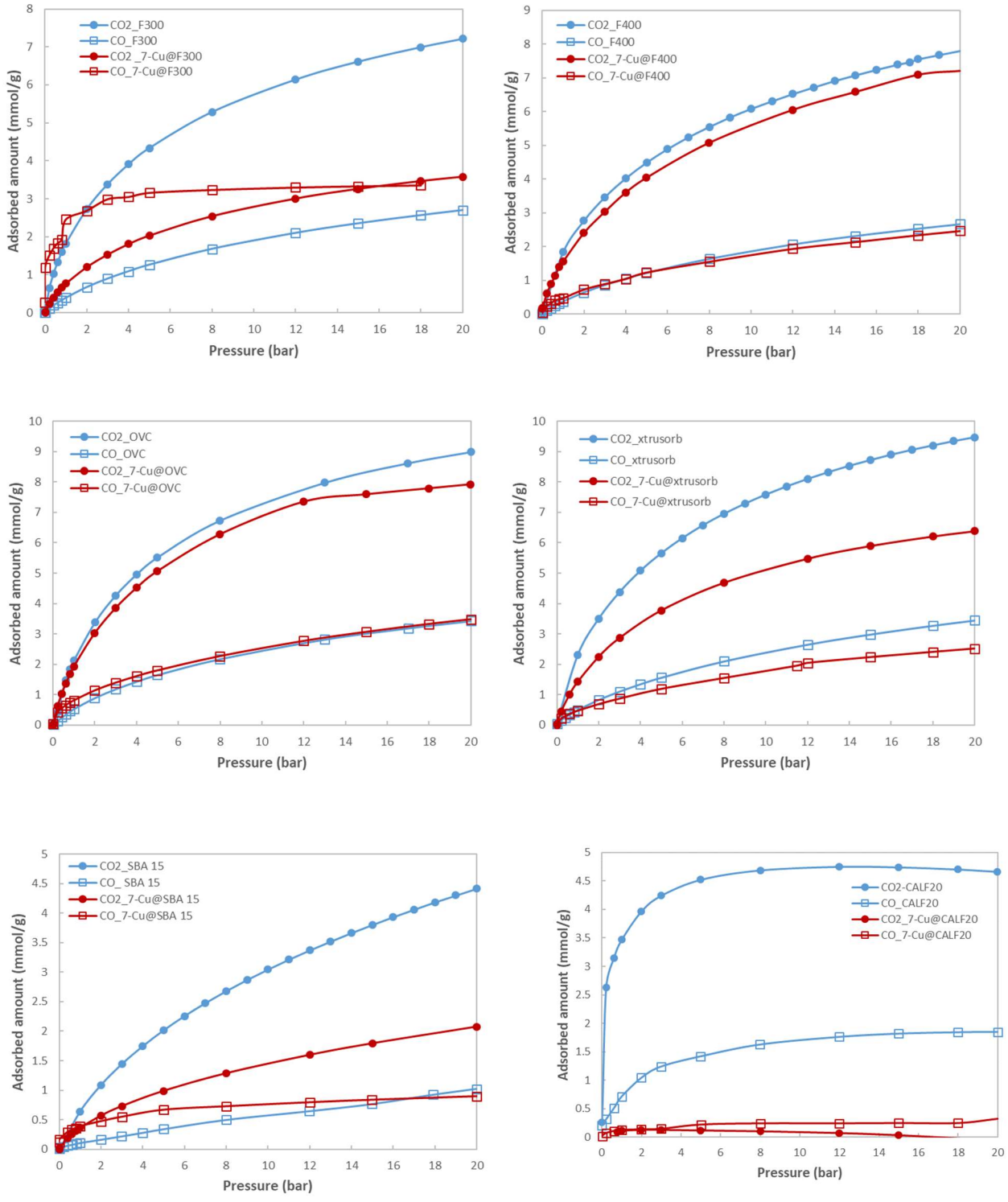

Figure 4-8. Equilibrium adsorption isotherms for CO and CO_2 in different adsorbents impregnated with $CuCl_2$ via polyol method.

A different method was then investigated through the employment of solid state auto-dispersion method for adsorbent modification using $CuCl_2$ as precursor.

4.6.2 Results obtained with monolayer auto-dispersion method

Samples were prepared by dispersion of $CuCl_2$ as precursor by a monolayer auto-dispersion method as described before. Pure CO and CO_2 equilibrium isotherms were measured at 298K and the results are shown in Figure 4-9 for all the samples.

To avoid sample oxidation and hydrolysis of Cu (I) if exposed to air, sample preparation and reduction was performed in situ (inside IGA reactor) . Sample degassing under vacuum was performed to desorb any CO gas used as reducing reagent. CO adsorption/desorption isotherms were measured at constant temperature using a thermostatic water bath.

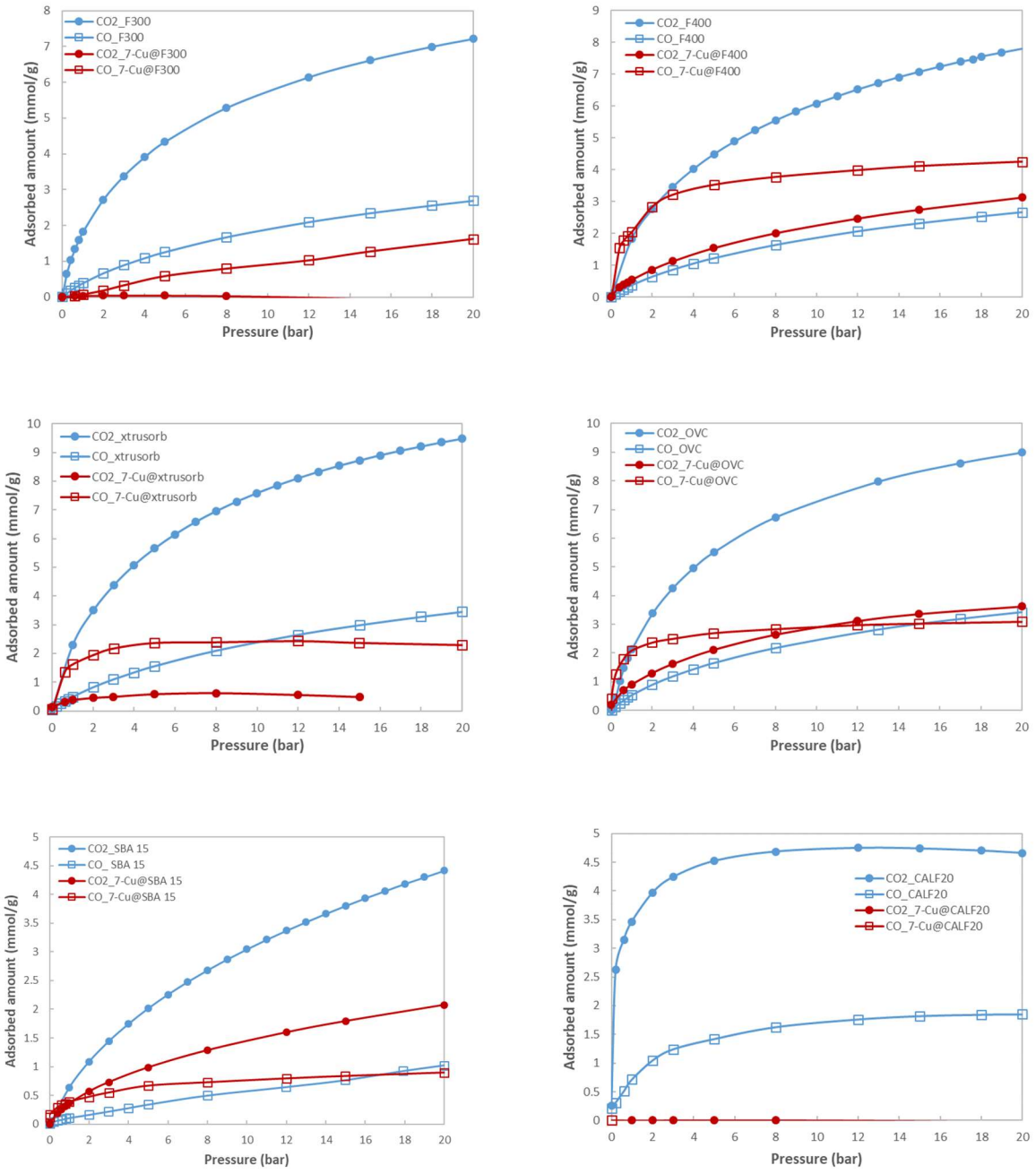

Figure 4-9. Equilibrium adsorption isotherms for CO and CO_2 in different $CuCl_2$ modified adsorbent by monolayer dispersion

From Figure 4-9, it is observed that CO adsorption capacity increased significantly in Cu modified adsorbents compared to non modified adsorbents. In contrast, CO_2 adsorption had decreased substantially. This clearly shows that the monolayer dispersion of Cu on the surface of the adsorbents can effectively adsorb more of CO molecules compared to non modified adsorbents. This is attributed to the formation of π-complex between CO molecule and Cu (I) ions. These results had confirmed that Cu (I) ions were successfully dispersed into the pores of the adsorbents. Moreover, the CO_2 adsorption capacity decreased substantially in Cu-based adsorbents, which is attributed to the reduction of accessible sites for CO_2 as they are occupied by incorporated Cu (I) ions, thus decreasing the adsorption capacity of CO_2. This is also confirmed by the results observed with a decrease in BET surface area as shown in Table 4-4. Consequently, the CO/CO_2 selectivity in Cu-based adsorbents increased significantly as illustrated in Figure 4-10 for all the adsorbents, reversing the previous results obtained before for the non modified adsorbents. The highest selectivity is observed in activated carbon 7-Cu@Xtrusorb with the value of 4.9 at 15 bar.

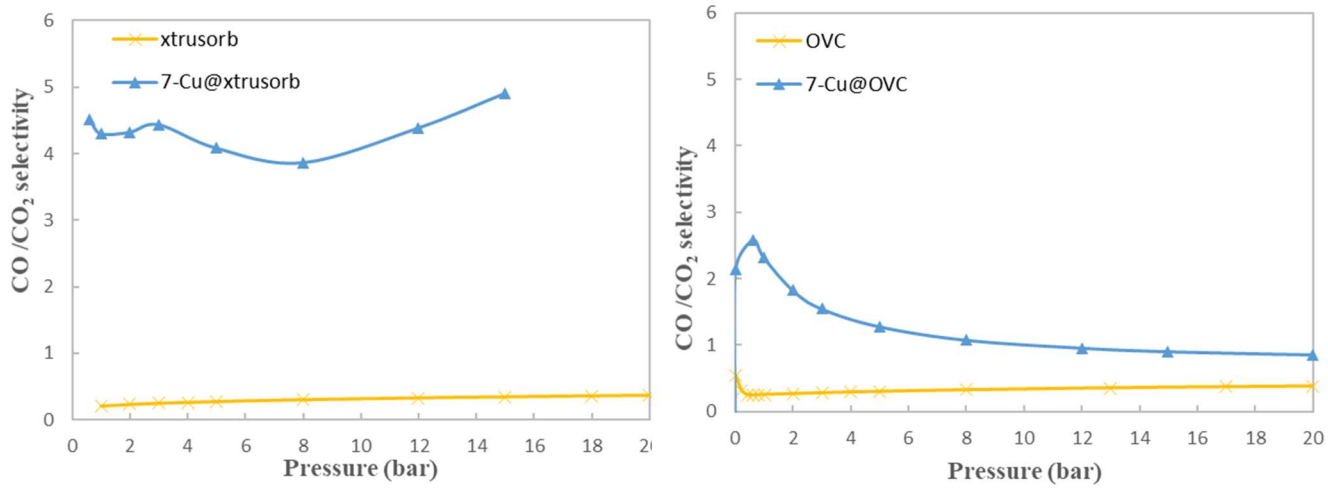

Figure 4-10. CO/CO_2 adsorption selectivity values with activated carbon Xtrusorb and OVC 4x10 before and after Cu (I) dispersion.

4.6.3 Optimal copper loading for CO/CO_2 separation

Figure 4-11 represents the adsorption equilibrium isotherms of CO and CO_2 in activated carbon Xtrusorb with different copper loadings at 25 °C. The adsorption capacity of CO on modified

adsorbents significantly increased as more copper is loaded into the sample compared to the parent adsorbent Xtrusorb. At 1 bar, the CO uptake in Xtrusorb was 0.48 mmol/g and increased to 1.99 mmol/g in Xtrusorb loaded with 7mmolg of $CuCl_2$, an increase of 314%. Increasing copper loading imply that more copper occupy the pores of the support as it was seen from BET surface area results. Consequently, there is less available open site for CO_2 interaction. Therefore less CO_2 uptake as seen in the Figure 4-11. The highest CO uptake of 4.43 mmol/g was marked at 20 bar in 7-Cu@Xtrusorb adsorbent. Furthermore, increasing the copper loading to 7mmol/g does not seem to be the threshold limit for copper loading in Xtrusorb since the CO uptake keep increasing, therefore the optimal copper loading may be higher than 7mmolg.

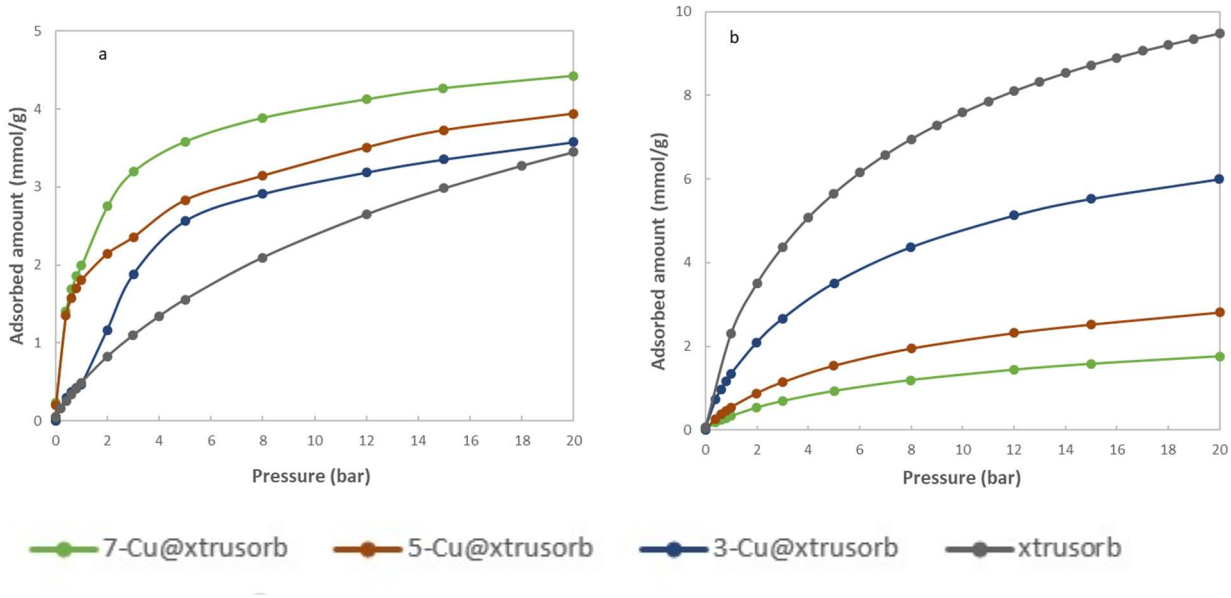

Figure 4-11. Adsorption isotherms in X-Cu@Xtrusorb at 298 K for CO (a) and CO_2 (b)

For gas separations, adsorption selectivity is an important factor. To predict the behaviour of CO and CO_2 in a gaseous mixture, the pure isotherm measurements of CO and CO_2 are used to calculate the adsorption selectivity of CO using equation 4.5. Figure 4-12 illustrates the results

obtained for selectivity values for Xtrusorb adsorbents with different copper loadings. The obtained results are compared with other adsorbents from the literature as shown in Table 4-5.

The CO/CO_2 adsorption selectivity at 1 bar with 7-Cu@Xtrusorb is 5.89 mmol/g, and further increase in Cu loading may further improve this selectivity.

The incorporation of Cu (I) into activated carbons had significantly enhanced the separation performance of CO which allows them to be attractive materials for separation and purification of gaseous mixtures of CO and CO_2.

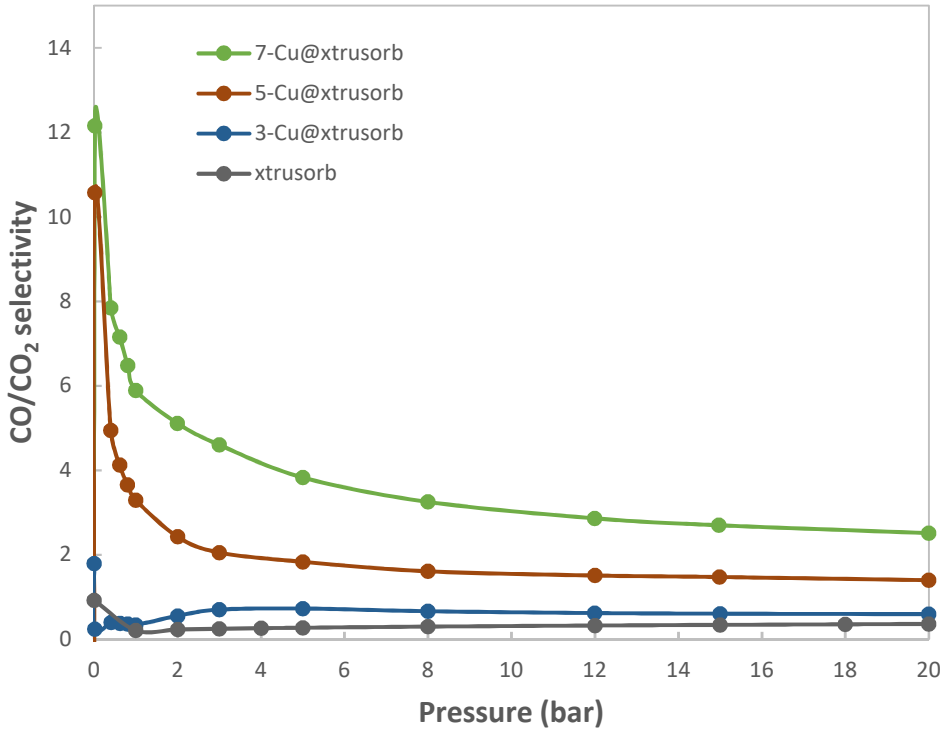

Figure 4-12. CO/CO_2 adsorption selectivity values with X-Cu@xtrusorb at 298 K

Table 4-5. Comparison of adsorbent uptakes and selectivity values at 1 bar with literature.

Adsorbents	Adsorbed amount (mmol/g)		Temperature (K)	Selectivity (CO/CO_2)	Refs.
	CO	CO_2			
CuCl/Zeolite NaY	2.4	1.3	303	1.84	[3]
Zeolite 13X	0.7	4	298	0.175	[23]
Zeolite HY	2.67	0.96	303	2.83	[19]
MIL101(Cr)	1.13	3.8	288	0.29	[24]
CuCl/Boehmite	1.55	0.14		11.1	[25]
0.9Cu@MIL-100	3.52	0.49	303	7.2	[11]
7Cu@AC	1.62	0.37	298	4.37	This work

4.7 Conclusions

Overall, this study had confirmed the strong interaction between Cu (I) ions and CO molecules through π complexation leading to high CO uptake and selectivity. Thus, the application of Cu (I) incorporated adsorbent is very promising for CO/CO_2 separation as well as in other gas mixtures containing CO gas.

The impregnation of copper ions using polyol method did not show a significant change in CO and CO_2 adsorption capacity values except for activated carbon F300. This could be explained by low reduction of Cu (II) to Cu (I) ions, thus the number of active copper sites to interact with CO was very low. Sample characterisation using XRD or X-ray photoelectron spectroscopy (XPS) to confirm the oxidation state of copper on the surface will help identify the problem.

Copper based adsorbents for selective separation of CO has been successfully obtained using a monolayer dispersion of $CuCl_2$ as precursor on six different adsorbents. The Cu (II) ions were reduced to Cu (I) with activation at 450°C and under CO environment. As a result, a highly

dispersed Cu (I) ions on the surface of the adsorbents was observed as revealed by the characterization of XRD and N_2 adsorption for BET surface area determination. The results confirmed the preferential interaction between CO molecules and Cu (I) ions site rather than CO_2 leading to higher CO adsorption uptake and selectivity. The CO capacity and CO/CO_2 selectivity in 7-Cu@xtrusorb adsorbent at 25°C and 20 bar increased by 28.4% and 597% respectively. Furthermore, higher CO adsorption was obtained as the Cu (II) loading in the sample increased from 3 to 7 mmol/g, with the highest CO/CO_2 selectivity obtained with 7mmol/g $CuCl_2$ loading.

4.8 Abbreviation

ρ_g	Density of the gas
$(CH2OH)_2$	Ethylene glycol
Å	Angstrom
CuCl	Copper (I) Chloride
CuCl2	Copper (II) Chloride
g	Gravitational acceleration
M	Molarity
NaOH	Sodium hydroxide (NaOH
V	Volume

4.9 References

[1] N. N. Dutta and G. S. Patil, "Developments in CO separation," *Gas Sep. Purif.*, vol. 9, no. 4, pp. 277–283, 1995, doi: 10.1016/0950-4214(95)00011-Y.

[2] E. Drent, "Chemical Synthesis from C1 Compounds," *Microb. Growth C1 Compd.*, pp. 272–281, 1987, doi: 10.1007/978-94-009-3539-6_33.

[3] Y. Xie *et al.*, "Zeolite Modified by CuCl for Separating CO from Gas Mixtures Containing CO2," *Adsorpt. J. Int. Adsorpt. Soc.*, vol. 32, pp. 27–32, 1996.

[4] D. Saha and S. Deng, "Adsorption equilibria and kinetics of carbon monoxide on zeolite 5A, 13X, MOF-5, and MOF-177," *J. Chem. Eng. Data*, vol. 54, no. 8, pp. 2245–2250, 2009, doi: 10.1021/je9000087.

[5] H. Tamon, K. Kitamura, and M. Okazaki, "Adsorption of carbon monoxide on activated carbon impregnated with metal halide," *AIChE J.*, vol. 42, no. 2, pp. 422–430, 1996, doi: 10.1002/aic.690420212.

[6] G. Sethia, R. S. Somani, and H. Chand Bajaj, "Adsorption of carbon monoxide, methane and nitrogen on alkaline earth metal ion exchanged zeolite-X: Structure, cation position and adsorption relationship," *RSC Adv.*, vol. 5, no. 17, pp. 12773–12781, 2015, doi: 10.1039/c4ra11511b.

[7] B. Singh, A. Saxena, A. K. Srivastava, and R. Vijayaraghavan, "Impregnated carbon based catalyst for protection against carbon monoxide gas," *Appl. Catal. B Environ.*, vol. 88, no. 3–4, pp. 257–262, 2009, doi: 10.1016/j.apcatb.2008.11.016.

[8] H. Igarashi, H. Uchida, M. Suzuki, Y. Sasaki, and M. Watanabe, "Removal of carbon monoxide from hydrogen-rich fuels by selective oxidation over platinum catalyst supported on zeolite," *Appl. Catal. A Gen.*, vol. 159, no. 1–2, pp. 159–169, 1997, doi: 10.1016/S0926-860X(97)00075-6.

[9] O. Cheung and N. Hedin, "Zeolites and related sorbents with narrow pores for CO2 separation from flue gas," *RSC Adv.*, vol. 4, no. 28, pp. 14480–14494, 2014, doi: 10.1039/c3ra48052f.

[10] Q. Zhu *et al.*, "Highly Porous Carbon Xerogels Doped with Cuprous Chloride for Effective CO Adsorption," *ACS Omega*, vol. 4, no. 4, pp. 6138–6143, 2019, doi: 10.1021/acsomega.8b03647.

[11] A. R. Kim, T. U. Yoon, S. I. Kim, K. Cho, S. S. Han, and Y. S. Bae, "Creating high CO/CO2 selectivity and large CO working capacity through facile loading of Cu(I) species into an iron-based mesoporous metal-organic framework," *Chem. Eng. J.*, vol. 348, no. April, pp. 135–142, 2018, doi: 10.1016/j.cej.2018.04.177.

[12] N. A. Khan and S. H. Jhung, "Adsorptive removal and separation of chemicals with metal-organic frameworks: Contribution of π-complexation," *J. Hazard. Mater.*, vol. 325, pp. 198–213, 2017, doi: 10.1016/j.jhazmat.2016.11.070.

[13] R. T. Y. Adsorbents, *Fundamentals and Applications*. New York: Wiley, 2003.

[14] A. R. Kim, T. U. Yoon, S. I. Kim, K. Cho, S. S. Han, and Y. S. Bae, "Creating high CO/CO2 selectivity and large CO working capacity through facile loading of Cu(I) species into an iron-based mesoporous metal-organic framework," *Chem. Eng. J.*, vol. 348, no. I, pp. 135–142, 2018, doi: 10.1016/j.cej.2018.04.177.

[15] F. Gao, Y. Wang, X. Wang, and S. Wang, "Selective CO adsorbent CuCl/AC prepared using CuCl2 as a precursor by a facile method," *RSC Adv.*, vol. 6, no. 41, pp. 34439–34446, 2016, doi: 10.1039/c6ra03116a.

[16] C. Xue, W. Hao, W. Cheng, J. Ma, and R. Li, "CO adsorption performance of CuCl/activated carbon by simultaneous reduction-dispersion of mixed Cu(II) salts," *Materials (Basel).*, vol. 12, no. 10, 2019, doi: 10.3390/ma12101605.

[17] Y. Huang, Y. Tao, L. He, Y. Duan, J. Xiao, and Z. Li, "Preparation of CuCl@AC with high CO adsorption capacity and selectivity from CO/N2 binary mixture," *Adsorption*, vol. 21, no. 5, pp. 373–381, 2015, doi: 10.1007/s10450-015-9677-5.

[18] Y. Xie *et al.*, "from Gas Mixtures Containing C02," *Adsorpt. J. Int. Adsorpt. Soc.*, vol. 32, pp. 27–32, 1996.

[19] F. Gao, Y. Wang, and S. Wang, “Selective adsorption of CO on CuCl/Y adsorbent prepared using CuCl2 as precursor: Equilibrium and thermodynamics,” *Chem. Eng. J.*, vol. 290, pp. 418–427, 2016, doi: 10.1016/j.cej.2016.01.054.

[20] J. Ma, L. Li, J. Ren, and R. Li, “CO adsorption on activated carbon-supported Cu-based adsorbent prepared by a facile route,” *Sep. Purif. Technol.*, vol. 76, no. 1, pp. 89–93, 2010, doi: 10.1016/j.seppur.2010.09.022.

[21] A. Evans, R. Luebke, and C. Petit, “The use of metal-organic frameworks for CO purification,” *J. Mater. Chem. A*, vol. 6, no. 23, pp. 10570–10594, 2018, doi: 10.1039/c8ta02059k.

[22] H. Hirai, K. Wada, and K. Makoto, “Active Carbon-Supported Aluminium Copper(I) Chloride as Solid Carbon Monoxide Adsorbent,” *Bull. Chem. Soc. Jpn.*, vol. 59, no. 4, pp. 1043–1049, 1986.

[23] J. A. Delgado, V. I. Águeda, M. A. Uguina, J. L. Sotelo, P. Brea, and C. A. Grande, “Adsorption and Diffusion of H2, CO, CH4, and CO2 in BPL Activated Carbon and 13X Zeolite: Evaluation of Performance in Pressure Swing Adsorption Hydrogen Purification by Simulation,” Industrial & Engineering Chemistry Research, vol. 53, no. 40, pp. 15414–15426, 2014. K. Munusamy, G. Sethia, D. V. Patil, P. B. Somayajulu Rallapalli, R. S. Somani, and H. C. Bajaj, “Sorption of carbon dioxide, methane, nitrogen and carbon monoxide on MIL-101(Cr): Volumetric measurements and dynamic adsorption studies,” *Chem. Eng. J.*, vol. 195–196, pp. 359–368, 2012, doi: 10.1016/j.cej.2012.04.071.

[25]

K. Cho, J. Kim, H. T. Beum, T. Jung, and S. S. Han, “Synthesis of CuCl/Boehmite adsorbents that exhibit high CO selectivity in CO/CO2 separation,” *J. Hazard. Mater.*, vol. 344, pp. 857–864, 2018, doi: 10.1016/j.jhazmat.2017.11.037.

Chapter 5: **Conclusions and Recommendations**

5.1 Conclusions

CO_2 capture and conversion has been the focus of significant research activities. After its capture, CO_2 can be converted to liquid fuels and value added chemicals through different processes. In this work, Reverse Water Gas Sift reaction for syngas production has been considered. It was found from HYSYS process simulation that increasing the reaction temperature and hydrogen to CO_2 ratio increases the reaction conversion. Furthermore, recycling unreacted CO_2 have the advantage of improving the overall conversion of the reaction, in addition of avoiding side reactions that may happen if CO_2 remain in the product stream when sent to next step of syngas processing. To recover and recycle CO_2 from the gaseous mixture containing CO and H_2, adsorption separation has been considered as a promising technology for CO separation and purification. In this research, six porous materials were studied, including activated carbons, metal organic frameworks and ordered mesoporous silica. Pure equilibrium isotherm results obtained by using a gravimetric system at ambient temperature and pressures up to 20 bar indicated that the CO uptake and selectivity is not significant compared to CO_2 adsorption.

In order to improve the adsorbent uptake of carbon monoxide gas, six porous materials were modified by incorporation of metallic salt. In this work, copper (II) chloride was chosen as the salt. Adsorbents' synthesis was performed via two different techniques: polyol method and thermal monolayer auto-dispersion of copper (II) chloride. The highest CO and CO_2 adsorption capacity was observed in activated carbon Xtrusorb A754 with values of 3.45 mmol/g and 9.47 mmol/g respectively, at 20 bar and 298 K. However, after adsorbents' modifications with incorporation of copper (II) chloride, the selectivity and CO capacity reversed compared to the parent adsorbent, suggesting high interaction between copper (I) and CO molecules via π complexation. The highest CO/CO_2 selectivity of 4.9 at 15 bar was observed in activated carbon 7-Cu@Xtrusorb compared to 0.34 in the parent adsorbent Xtrusorb. Furthermore, different copper loadings were tested in Xtrusorb sample. Adsorption performance of CO increased as the copper loading increased from 3 mmol/g to 7 mmol/g, while CO_2 adsorption capacity gradually decreased. This was ascribed to the monolayer dispersion of copper in the pores of the support (Xtrusorb) with less open site to

interact with CO_2 gas. The results were confirmed by BET surface area measurements, pore size and XRD characterizations.

In general, the results obtained from this study is promising for CO recovery using copper based adsorbents featuring large surface area, thus more copper can be incorporated, resulting in more CO adsorption.

5.2 Recommendations and Future work

To further enhance CO adsorption capacity and selectivity using different porous materials by monolayer auto-dispersion method, few other parameters could be explored:

- Adsorbents' impregnation using other metallic salts
- Test adsorbents with higher surface area materials such as MOF
- Improve copper reduction conditions including temperature, reducing gas, reduction time
- Study adsorbents' stability through multiple cyclic adsorption/desorption

Copper impregnation using polyol method was not very successful for improving CO adsorption. Further investigation is recommended to understand the issue. For instance, sample characterization using XRD and XPS will help us understand if the copper (II) was reduced to Cu (I). STEM characterization is another technique that will help identify the copper particle size in the support, thus indicating if the copper nanoparticles were formed. From the characterization results, one can improve the synthesis method and decide which parameter to modify.

Finally, breakthrough experiments to study the kinetics and behaviour of gas mixture containing CO, CO_2 and H_2 were not completed due to COVID restrictions. These tests will be performed before testing the adsorbents in larger scale PSA system.